Dissecting the Role of the Serotonin Transporter in the Developmental and Neurobehavioral Features of Autism Spectrum Disorder

By

Christopher Louis Muller

Dissertation

Submitted to the Faculty of the

Graduate School of Vanderbilt University

in partial fulfillment of the requirements

for the degree of

DOCTOR OF PHILOSOPHY

in

Neuroscience

May, 2015

Nashville, Tennessee

Alexandre Bonnin, Ph.D.
Randy Blakely, Ph.D.
Gregg Stanwood, Ph.D.
Mark Wallace, Ph.D.
Jeremy Veenstra-VanderWeele, M.D.

DEDICATION

In memory of my grandparents, Martha and Mickey Henriquez.
I hope I have made you proud.

ACKNOWLEDGEMENTS

There are countless people who have mentored and supported me during my graduate training. First, I would like to thank my mentor, Jeremy Veenstra-VanderWeele, for giving me the opportunity to learn and develop into an independent neuroscientist. It has been a pleasure being your first graduate student, and I am forever grateful for all that you have taught me. To all the current and former members of the VVW lab, thank you for everything you have done to contribute to this work. The marathon of graduate school was that much easier working with you. To my thesis committee members, I thank you all for your tremendous expertise and for supporting me through the ups and downs of science. To the Vanderbilt Graduate Training Program and Autism Speaks, thank you for your financial support, allowing me the freedom to explore my scientific ideas. To the Vanderbilt Brain Institute, thank you for helping me navigate through all the red tape in graduate school.

I would also like to thank all of my other friends in Nashville and around the country who have supported me during my time at Vanderbilt. While graduate school has been the experience of a lifetime, it has coincided with some personally difficult times in my life. Your constant encouragement gave me the motivation to keep moving forward.

To my family, you are the reason I am here today. You instilled in me the values of hard work and compassion, and they have carried me farther than I ever dreamed. In particular, I would not be here without my mother, Natalie, who has been my biggest supporter from day one. I love you, Mom.

Finally, to my wife Sudipta, my pecha, I love you with all my heart. Life has a way of giving you the things you need most at the right time, and I am so lucky that I found you at Vanderbilt. I cannot imagine my life without you.

TABLE OF CONTENTS

Page

LIST OF FIGURES

LIST OF SUPPLEMENTARY FIGURES

LIST OF ABBREVIATIONS

5-HIAA.....5-hydroxyindoleacetic acid
5-HT 5-hydroxytryptamine
5-HTP 5-hydroxytryptophan
5-HTTLPR ..... 5-hyrdroxytryptamine transporter linked polymorphic region
AADC .....aromatic acid decarboxylase
ADI-R ..... autism diagnostic interview - revised
ADOS ..... autism diagnostic observation schedule
AGRE ..... autism genetic resource exchange
Ala .....alanine
ASD .....autism spectrum disorder
Asn ..... asparagine
Cl .....chloride
CNS..... central nervous system
E .....embryonic day
FMR1 .....fragile x mental retardation 1
fMRI.....functional magnetic resonance imaging
FMRP .....fragile x mental retardation protein
FSIQ..... full scale IQ
FXS .....fragile x syndrome
Gly.....glycine
GPCR..... g-protein coupled receptor
Grm5 ..... glutamate receptor, metabotropic 5
GWAS ..... genome wide association study
Ile .....Isoleucine
ITGB3..... integrin beta 3
KBIT .....kauffman brief intelligence test
KI.....knock-in
KO .....knockout
L ..... long

Leu ..... leucine
LOD ..... logarithm base 10 of odds
LSD ..... lysergic acid
LTD ..... long term depression
Lys ..... lysine
MAOA ..... monoamine oxidase a
MAPK ..... mitogen-activated protein kinase
mGlur ..... metabotropic glutamate receptor
MSEL ..... mullen scales of early learning
Na ..... sodium
NET ..... norepinephrine transporter
P ..... phosphorus
PET ..... positron emission tomography
Phe ..... phenylalanine
PKG ..... protein kinase G
PNS ..... peripheral nervous system
QTL ..... quantatiive trait locus
RBS-R ..... repetitive behavior scale - revised
RNA ..... ribonucleic acid
S ..... short
S1 ..... primary somatosensory cortex
SCQ ..... social communication questionnaire
SEQ ..... sensory experience questionnaire
SERT ..... serotonin transporter
SLC6A4 ..... solute carrier family 6 member 4
SNP ..... single nucleotide polymorphism
SP ..... sensory profile
SPECT ..... single-photon emission computed tomography
SSRI ..... selective serotonin reuptake inhibitors
TCA ..... thalamocortical axon
TD ..... typically developing

TPH ..... tryptophan hydroxylase
Val ..... valine
WASI ..... weschler abbreviated scale of intelligence
WT ..... wildtype

CHAPTER 1

INTRODUCTION

Introduction to the Serotonin System

For millions of years, serotonin (5-hydroxytryptamine, 5-HT) has existed as a signaling molecule across phylogeny (Hay-Schmidt, 2000), but the scientific exploration of 5-HT did not begin until the convergent discoveries of the monoamine by Erspamer and Page in the mid 20th century (Erspamer and Asero, 1952; Rapport et al., 1948). 5-HT is produced from the essential amino acid, tryptophan, via a two-step synthetic pathway. In the first step, tryptophan is converted to 5-hydroxytryptophan (5-HTP) by the rate-limiting enzyme in 5-HT synthesis, tryptophan hydroxylase. There are two isoforms of tryptophan hydroxylase, TPH1 and TPH2, which are primarily responsible for 5-HT synthesis in the periphery and central nervous system (CNS), respectively (Lovenberg et al., 1967; Walther et al., 2003). In the final step, the intermediate product, 5-HTP, is converted to 5-HT by aromatic acid decarboxylase (AADC). Degradation of 5-HT primarily occurs by the mitochondrial bound protein monoamine oxidase A (MAOA), leading to the production of the metabolite, 5-hydroxyindoleacetic acid (5-HIAA).

Though more recognized for its role as a neurotransmitter, the vast majority of 5-HT produced in the body is located in the periphery. Specifically, enterochrommafin cells that line the lumen of the gastrointestinal tract are the primary source of peripheral 5-HT, which is then taken up by platelets as they pass through enteric circulation (Anderson et al., 1987). Thus, circulating platelet 5-HT is able to biologically impact cells throughout the body. Interestingly, transient peripheral production of 5-HT during

pregnancy has also been documented (Bonnin et al., 2011; Kim et al., 2010), suggesting an additional developmental role for 5-HT which will be discussed later in this chapter.

Although gut-derived 5-HT influences numerous aspects of peripheral physiology, it is unable to cross the mature blood brain barrier and interact with neural tissue (Hardebo and Owman, 1980). Consequently, 5-HT found in the brain is produced by TPH2-expressing serotonergic neurons in the midbrain and hindbrain. Serotonergic neurons are organized into nine discrete clusters (B1-B9), collectively known as the raphe nuclei (Dahlstroem and Fuxe, 1964). The caudal raphe nuclei (B1-B5) project to the peripheral nervous system (PNS). The rostral clusters (B6-B9), the dorsal and median raphe nuclei, primarily send their projections to forebrain structures (Conrad et al., 1974; O'Hearn and Molliver, 1984). Despite their relatively small number, serotonergic neurons innervate a broad collection of brain regions (Jacobs and Azmitia, 1992), allowing 5-HT to influence neural circuitry underlying a myriad of behaviors.

Reflective of its seemingly ubiquitous presence in the brain and periphery, 5-HT exerts its effects through 14 genetically distinct receptor subtypes (Hannon and Hoyer, 2008; Millan et al., 2008). 5-HT receptors are further classified by their pharmacological properties and downstream signaling mechanisms into seven groups. Six out of the seven groups are G-protein-coupled receptors (GPCRs): 5-HT_1 (5-$HT_{1A,B,D-F}$) and 5-HT_5 (5-$HT_{5A,B}$) receptors coupled to $G_{i/o}$ proteins; 5-HT_4, 5-HT_6, and 5-HT_7 receptors coupled to G_s proteins; and 5-HT_2 receptors (5-HT_{2A-C}) coupled to G_q proteins. In contrast, 5-HT_3 receptors are ligand gated ion channels, homologous to other multi subunit Cys-loop receptors. Moreover, mRNA editing and alternative splicing adds another layer of

complexity to an already diverse signaling system (Burns et al., 1997; Kishore and Stamm, 2006). While a thorough description of 5-HT receptor function in the brain and periphery is beyond the scope of this introduction, it should be clearly noted that the unique temporal and spatial patterns of 5-HT receptor expression implicate 5-HT as a key developmental molecule (Bonnin et al., 2006; Lidow and Rakic, 1992).

Arguably the most crucial aspect of 5-HT homeostasis is the clearance of extracellular 5-HT. In addition to terminating 5-HT receptor signaling, reuptake of 5-HT back into intracellular spaces helps recycle the monoamine for future use (Blakely and Edwards, 2012). Remarkably, while neuronal 5-HT uptake could be observed and pharmacologically manipulated in synaptosomal preparations since the 1970s (Fuller et al., 1974; Snyder, 1970), the serotonin transporter (5-HTT, SERT) was not identified as the protein of interest until its gene was cloned in 1991. SERT is an integral plasma membrane protein that actively transports 5-HT in a Na^+/Cl^--coupled dependent and anti-depressant sensitive manner (Blakely et al., 1991). In addition to being found on presynaptic terminals at serotonergic synapses in the brain, SERT is expressed at numerous sites in the periphery (Qian et al., 1995). Since the discovery of SERT, there has been immense interest in understanding its role in psychiatric disorders due to the fact that selective serotonin reuptake inhibitors (SSRIs), which bind to SERT and block 5-HT uptake, are used to treat conditions such as depression, anxiety, and obsessive-compulsive disorder (Vaswani et al., 2003).

Introduction to Autism Spectrum Disorder

Autism spectrum disorder (ASD) is a heterogeneous group of neurodevelopmental disorders characterized by impaired social interaction/communication and repetitive behavior. In addition to these core diagnostic features, individuals with ASD also display a number of secondary symptoms such as epilepsy (Volkmar and Nelson, 1990), gastrointestinal dysfunction (Molloy and Manning-Courtney, 2003), and sensory abnormalities (Ben-Sasson et al., 2009) at a much higher rate than the general population. The most recent estimates given by the Centers for Disease Control and Prevention now place the prevalence of ASD in the United States to be 1 in 68 children, with the disorder five times more likely in males than females (Developmental Disabilities Monitoring Network Surveillance Year Principal et al., 2014).

Among neuropsychiatric disorders, ASD has been shown to be the most heritable (Burmeister et al., 2008). Depending on diagnostic criteria, twin studies find concordance rates of 60-90% for monozygotic twins versus 0-10% for dizygotic twins (Bailey et al., 1995). The field of psychiatric genetics has had two prevailing perspectives into the genetic architecture of ASD, the common and rare variant hypotheses (State and Levitt, 2011). The common variant hypothesis proposes that common alleles (i.e. minor allele frequency > 5%) act together to confer risk for the disorder, but alone are not sufficient to cause ASD. In contrast, the rare variant hypothesis posits that deleterious rare alleles, both inherited and *de novo*, carry the majority of the risk for ASD. Although both views attempt to reconcile the immense genetic heterogeneity of ASD, the common and rare variant hypotheses have each

encountered resistance. Due to statistically underpowered sample sizes, unbiased genome-wide association studies (GWAS) have largely been unsuccessful in identifying common alleles that contribute to ASD risk (Devlin et al., 2011). Furthermore, while next generation sequencing technology has dramatically increased our ability to detect rare polymorphisms found in individuals with idiopathic ASD, there is debate whether rare functional variants account for a sizable proportion of overall risk for the disorder (Gratten et al., 2013).

Hyperserotonemia in Autism Spectrum Disorder

To help parse the heterogeneity of ASD, researchers have tried to identify biomarkers to classify affected individuals into distinct subpopulations. A biomarker is a quantitative biological trait that is associated with a disease or risk state. One of the oldest and most replicated biomarkers documented in ASD is elevated blood 5-HT levels or hyperserotonemia. In 1961, Schain and Freedman first reported that six children in a cohort of 23 individuals with a diagnosis of infantile autism had dramatically increased blood 5-HT levels (Schain and Freedman, 1961). Although there was initial debate whether this finding was unique to autism or more generally to intellectual disability (Hanley et al., 1977; Partington et al., 1973), it has been accepted that elevated blood 5-HT levels are a distinctive biomarker found in approximately 25% of individuals with ASD (Gabriele et al., 2014). Several groups have attempted to find clinical correlates of hyperserotonemia in ASD but have had limited success. 5-HT blood measures have not shown a clear association with any of the standard behavioral measures used to diagnose autism (Kolevzon et al., 2010; McBride et al., 1998; Mulder

et al., 2004). However, the relationship between hyperserotonemia and ASD secondary traits with known biological interactions with the serotonergic system has yet to be fully explored.

Genetics of Blood Serotonin Levels

The discovery of hyperserotonemia as an ASD biomarker has spurred a great deal of interest in examining genetic influences on blood 5-HT. The first hints that blood 5-HT levels were a heritable trait came from initial studies reporting that first-degree relatives of hyperserotonemic children with ASD have increased blood 5-HT themselves (Abramson et al., 1989; Cook et al., 1990; Piven et al., 1991). Expanding upon these findings, Abney and colleagues determined that variation in whole blood 5-HT is largely under genetic control through their studies of the Hutterites, a large founder population ideally suited to examine the genetic architecture of biological traits (Abney et al., 2001). Further, quantitative trait locus (QTL) analysis of the Hutterites revealed sex-specific loci for whole blood 5-HT in males, including the genes encoding integrin beta 3 (*ITGB3*) and the serotonin transporter (*SLC6A4*) (Weiss et al., 2005).

Due to their genetic influence on blood 5-HT, *ITGB3* and *SLC6A4* have been heavily scrutinized as candidate genes harboring ASD risk variants. While *ITGB3* variants are associated with autism (Coutinho et al., 2007; Ma et al., 2010), it appears that the genetic variation in *ITGB3* that impacts ASD susceptibility is different from variation underlying 5-HT blood levels (Napolioni et al., 2011). Additional ASD candidate gene studies of *ITGB3* have also documented a genetic and expression interaction with *SLC6A4* that may contribute to autism risk (Weiss et al., 2006). Functional relationships

between ITGB3 and SERT are currently being explored to help elucidate the role this interaction may play in the etiology of hyperserotonemia and ASD (Whyte et al., 2014).

Similar to the *ITGB3* literature, genetic studies examining *SLC6A4* have encountered seemingly paradoxical results indicating distinct influences on blood 5-HT and ASD risk. The vast majority of research in this field has focused on the influence of the serotonin transporter-linked polymorphic region known as the 5-HTTLPR. This functional promoter insertion/deletion polymorphism is characterized by two common alleles, long (L) and short (S), with the long allele causing increased expression of SERT (Heils et al., 1996; Lesch et al., 1996). It has been hypothesized that increased SERT function could cause hyperserotonemia through enhanced platelet 5-HT uptake, but it appears that the 5-HTTLPR alone exerts a minimal effect on blood 5-HT (Anderson et al., 2002; Cross et al., 2008). Although controversial, there is mounting evidence that the lower SERT-expressing S allele of the 5-HTTLPR is associated with ASD (Devlin et al., 2005), again indicating there may be separate genetic determinants of 5-HT blood levels and ASD susceptibility.

Platelet Serotonin Uptake and Autism Spectrum Disorder

One potential mechanism for hyperserotonemia in ASD is abnormal platelet 5-HT uptake. In the blood, platelets contain approximately 99% of 5-HT, which is taken up via SERT as platelets pass through the enteric circulation (Anderson et al., 1987). Due to its central role in transporting 5-HT into the platelets, SERT function has been of particular interest in understanding the molecular mechanisms behind hyperserotonemia. Studies of platelet SERT function in ASD have primarily evaluated

SERT specific binding and 5-HT uptake. In the earliest SERT binding study in ASD, there were no reported differences in SERT binding using [^{3}H]imipramine, a tricyclic reuptake inhibitor that blocks both SERT and norepinenephrine transporter (NET) (Anderson et al., 1984). Later studies, using more selective radioligands for SERT, [^{3}H]paroxetine and [^{3}H]citalopram, have also noted little to no change in platelet binding site density measures in individuals with ASD or their families (Anderson et al., 2002; Cook et al., 1993).

Similar to SERT binding measures, studies examining 5-HT uptake in platelets have found modest changes in ASD. Before the heritability of blood 5-HT was conclusively demonstrated, twin studies of platelet uptake in the general population indicated that the maximal velocity (V_{max}) of platelet 5-HT uptake is a heritable trait (Meltzer and Arora, 1988). Exploring this idea further, Cook and colleagues examined platelet 5-HT uptake measures in hyperserotonemic and normoserotonemic first-degree relatives of children with autism. Although they found no mean differences in V_{max} or K_m between the two groups, they did report several V_{max} outliers in their hyperserotonemic groups as well as a significant positive correlation between V_{max} and whole blood 5-HT (Cook et al., 1993). In a more recent study of 5-HTTLPR effects on platelet function in ASD, Anderson et al. found that individuals homozygous for the long allele had significant increases in V_{max}, but no differences in blood 5-HT levels. In their sample as a whole, however, they also reported a significant positive correlation between V_{max} and blood 5-HT (Anderson et al., 2002). Collectively, these studies suggest enhanced SERT function may only play a causative role in hyperserotonemia in a subset of individuals with ASD.

Serotonin Transporter Human Neuroimaging Findings in ASD

While platelet studies have been informative about the mechanisms of hyperserotonemia in ASD, this peripheral biomarker only provides indirect evidence of 5-HT dysfunction in the brain. With the advent of neuroimaging tools such as positron emission tomography (PET) and single-photon emission computed tomography (SPECT), researchers now have the ability to explore molecular hypotheses about the pathophysiology of ASD in the living human brain. In contrast to platelet findings, neuroimaging studies have described significant differences in SERT binding in ASD, with most reports finding a decrease in binding sites. Using SPECT, Makkonen et al. initially documented decreases in [^{123}I]nor-β-CIT binding in children with autism. While the authors reported binding decreases in medial frontal cortex, midbrain, and temporal lobe in their sample, only differences in medial frontal cortex survived corrections due to sedation effects (Makkonen et al., 2008). In addition, a subsequent PET study documented global decreases in [^{11}C](+)McN-5652 binding in young adults with autism (Nakamura et al., 2010). Interestingly, decreases in [^{11}C](+)McN-5652 binding in the cingulate were correlated with measures of social cognition. However, in the most recent PET examination of cortical SERT in ASD, Girgis et al. found no changes in [^{11}C]DASB binding in adults with Asperger disorder (Girgis et al., 2011). While it is tempting to unify findings from these neuroimaging studies, significant differences in methodology and subject demographics make it difficult to form generalized conclusions about the nature of 5-HT dysfunction in ASD.

SLC6A4 Neuroimaging Genetics

In the field of neuroimaging genetics, no gene has been as heavily scrutinized for its impact on brain function than *SLC6A4*. As with most genetic studies focused on *SLC6A4,* the functional promoter polymorphism, 5-HTTLPR, has been the primary variant examined for its influence on various magnetic resonance imaging (MRI) measures of the brain (Hariri and Holmes, 2006). In the first ASD neuroimaging study to examine the 5-HTTLPR, Wassink et al. found that the short allele was significantly associated with increased cerebral cortex grey matter volume in children with autism (Wassink et al., 2007). Besides hyperserotonemia, one of the most consistent findings in ASD is an altered developmental trajectory of brain growth, with increased brain size during childhood that normalizes over time (Courchesne et al., 2001). Interestingly, a subsequent study examining 5-HTTLPR effects on cortical grey matter volume in adults with Asperger disorder reported no significant genotype associations, suggesting SERT influences on brain anatomy may be attenuated by age and ASD severity (Raznahan et al., 2009).

In addition to basic structural MRI measures, there is emerging literature that indicates SERT function may impact the connectivity and function of neural circuits in ASD. In the first study to examine 5-HT-mediated connectivity differences in ASD, Wiggins et al. reported that affected children and adolescents with high-expressing SERT 5-HTTLPR genotypes had stronger connectivity of the default mode network, a broadly distributed, interconnected group of brain regions that are active during wakeful rest. In contrast, typically developing children showed the opposite trend, with low-expressing SERT genotypes being associated with stronger default mode connectivity

(Wiggins et al., 2012). The Monk laboratory has also explored 5-HTTLPR genotype effects on amygdala responsiveness in ASD. In a pioneering genetic neuroimaging study, Hariri et al. found that 5-HTTLPR short allele carriers demonstrated increased amygdala activation in response to fearful stimuli as measured by functional MRI (fMRI) (Hariri et al., 2002). While this study focused on emotional stimuli, it suggests that genetic variation in SERT function could modulate responses to other information processed by the amygdala, such as social stimuli (Adolphs et al., 1998). Exploring this idea, Wiggins et al. used fMRI to examine potential SERT genotype differences in amygdala habituation to face stimuli in children and adolescents with ASD. The authors found that affected individuals with low SERT expressing genotypes had decreased amygdala habituation upon repeated exposure to faces (Wiggins et al., 2014). Collectively, the Monk neuroimaging studies provide additional evidence that altered SERT function plays a role in modulating specific ASD symptomatology.

In one of the most cited studies of central 5-HT function in ASD, Chugani et al. examined the developmental trajectory of 5-HT synthesis rates in children with autism, their unaffected siblings, and epileptic children without developmental disabilities (Chugani et al., 1999). Using the PET tracer [^{11}C]methyl-L-tryptophan to measure 5-HT synthesis, cross-sectional data from participants without autism indicated that children undergo a period of increased 5-HT production in the brain until the age of five, which decreases towards stable values in adulthood. In contrast, children with autism exhibit a blunted developmental increase in 5-HT synthesis capacity that plateaus to values significantly greater than those seen in typically developing adults. Furthermore, the authors noted in the control groups that 5-HT production declined at an earlier age in

girls compared to boys, a gender effect not found in study participants with autism. While there are concerns raised with the PET methodology used by Chugani et al. (Shoaf et al., 2000), their findings nonetheless suggest that the 5-HT system is dynamically regulated during early development.

Serotonin and Sensory Neurodevelopment

In addition to its well-known role as a modulatory neurotransmitter in the adult brain, 5-HT has more recently been appreciated as a critical signaling molecule during neurodevelopment (Gaspar et al., 2003). While 5-HT has been linked to developmental processes such as cell proliferation, migration and differentiation (Lauder, 1993), the most definitive evidence of a developmental role for 5-HT emerged from studies of rodent whisker barrel cortex. Barrel field architecture is formed by thalamocortical axons (TCAs) from the ventral posteromedial (VPM) nucleus that project to layer IV of primary somatosensory cortex (S1) (Woolsey and Van der Loos, 1970). Each barrel is a cortical representation of a peripheral snout whisker, where densely packed layer IV neurons surrounding the TCAs will fire in response to tactile whisker stimulation (Welker, 1971). The somatopic map present in barrel cortex is also present as ‘barreloids’ in the VPM nucleus and ‘barrelettes’ in the principal sensory nucleus of the trigeminal nerve, the two primary subcortical nuclei that relay whisker sensory information (Ma and Woolsey, 1984; Van Der Loos, 1976). Due to its stereotyped patterning, rodent barrel cortex has been extensively studied to evaluate the molecular mechanisms involved in sensory neurodevelopment (Erzurumlu and Gaspar, 2012).

Initial evidence that 5-HT may play a role in sensory neurodevelopment came from 5-HT immunohistochemistry and [^{3}H]citalopram autoradiography studies of rodent barrel cortex. Expanding on prior data in mice (Fujimiya et al., 1986), D'Amato and colleagues first reported a dense, transient source of serotonergic innervation in multiple primary sensory areas of the developing rat brain (D'Amato et al., 1987). Both 5-HT immunostaining and [^{3}H]citalopram binding indicated that the transient serotonergic innervation of primary sensory areas peaked during the first postnatal week of life and disappeared by postnatal day (P)21. While it was initially thought that the transient 5-HT innervation of sensory brain areas originated from the midbrain raphe nuclei, Lebrand et al. demonstrated that 5-HT detected in barrel cortex was actually contained in glutamatergic TCAs (Lebrand et al., 1996). Although TCAs do not have the capacity to synthesize 5-HT, extracellular 5-HT can be taken up through SERT and packaged into vesicles via VMAT2. However, it remains unclear if 5-HT captured by TCAs plays a functional role during neurodevelopment.

As the importance of 5-HT in sensory system development became appreciated, several groups have pharmacologically or genetically manipulated 5-HT levels in the developing brain to elucidate 5-HT-mediated mechanisms of sensory map formation. Pharmacological studies of barrel cortex focused on reducing extracellular 5-HT levels in the developing brain through a variety of methods; including inhibiting 5-HT synthesis (Persico et al., 2000), eliminating 5-HT neurons with specific serotonergic toxins (Bennett-Clarke et al., 1994), or depleting vesicular 5-HT stores (Bennett-Clarke et al., 1995). These studies have only noted subtle changes in barrel cortex formation, most notably decreased area of individual barrels and delayed sensory map maturation.

However, there is considerable debate whether these noted alterations are specifically due to 5-HT or to overall reductions in brain growth (Persico et al., 2000). Similarly, recent targeted genetic manipulations in mice have also shown that the topographical organization of barrel field architecture is largely unaffected by dramatic 5-HT depletion (van Kleef et al., 2012).

In contrast to models that deplete 5-HT, manipulations that increase 5-HT levels in the developing brain have significant effects on barrel cortex formation. In a landmark study, Cases et al. reported that mice that lack the 5-HT degrading enzyme, MAOA, do not possess barrel field architecture in S1 despite the presence of somatopic maps in subcortical sensory relay nuclei (Cases et al., 1996). While TCAs manage to reach the proper layer IV target, they do not segregate into discrete barrels. This phenotype is a direct result of the excessive 5-HT levels in the developing brain of MAOA KOs, as normalizing 5-HT levels during the early postnatal period rescued alterations in barrel cortex. Interestingly, the authors also noted that pharmacological inhibition of MAOA from P0 to P6 prevents barrel cortex formation to a similar extent as seen in the genetic model. As a result, it has been hypothesized that there is a critical period during the first postnatal week of life when 5-HT exerts its effects on developing TCAs.

While it is clear that excessive 5-HT levels during neurodevelopment disrupt normal patterning of sensory maps in the brain, the 5-HT-mediated molecular mechanisms that affect TCA development remain unclear. In a seminal work, Salichon et al. examined the mechanisms behind abnormal somatosensory and visual TCA development in MAOA knockout mice (Salichon et al., 2001). Focusing on the 5-HT_{1B} receptor and SERT, two proteins transiently expressed on TCAs during development

(Bennett-Clarke et al., 1996; Bennett-Clarke et al., 1993), the authors found that altered sensory map patterning in MAOA knockouts were a direct result of overactivation of TCA 5-HT_{1B} receptors by excessive extracellular 5-HT levels. However, while MAOA/5-HT_{1B} double knockout mutants had grossly normal TCA patterning, subtle postsynaptic cytoarchitecture differences were reported, indicating that 5-HT may have multiple roles in TCA development. Interestingly, 5-HT_{1B} knockout mice have normal TCA patterning, which some have attributed to the compensatory activity of 5-HT_{1D} receptors also expressed on developing TCAs (van Kleef et al., 2012). As a whole, these results indicate that 5-HT signaling appears to play only a modulatory role in TCA patterning and is not a necessary instructive cue for sensory map formation.

Following up on the aforementioned findings, several studies have sought to understand how 5-HT_{1B} receptor signaling influences developing TCAs and barrel field architecture. Using a slice preparation that maintains thalamic connectivity with somatosensory cortex (Agmon and Connors, 1991), Rhoades et al. first demonstrated that 5-HT_{1B} activation inhibits presynaptic release of glutamate from TCAs (Rhoades et al., 1994). This inhibitory effect was only noted in thalamocortical slices prepared from rats younger than two weeks of age, during the time period that 5-HT_{1B} receptors are transiently expressed on TCAs. In a subsequent study in neonatal mice, Laurent et al. confirmed that 5-HT was able to inhibit TCA glutamatergic neurotransmission in a dose-dependent manner, and that this effect was absent in 5-HT_{1B} receptor KO mice (Laurent et al., 2002). In addition to its role modulating TCA neurotransmission, thalamocortical 5-HT_{1B} signaling also modulates responsiveness to axon guidance cues (Bonnin et al., 2007). Bonnin et al. demonstrated that attractive netrin-1 cues exerted on posterior

TCAs are converted to repulsive by 5-$HT_{1B/1D}$ signaling. Furthermore, *in utero* manipulations of this signaling pathway alter the trajectory of developing TCAs as they migrate towards their cortical targets.

The aforementioned studies of barrel cortex and TCAs have provided strong evidence of the developmental role of 5-HT, but the long-term consequences of 5-HT-mediated changes in sensory development remain unclear. Sensory-related behavioral studies in mouse models with barrel cortex abnormalities are conspicuously lacking, most likely due to the difficulty in performing assays that gauge whisker-specific function. Indirect measures of somatosensory function in various SERT mouse models indicate altered processing of whisker stimulation (Dawson et al., 2009; Esaki et al., 2005). Another significant question that remains is whether 5-HT-mediated mechanisms of sensory development are affected in ASD, specifically in individuals with hyperserotonemia. Despite the epidemiological evidence of sensory dysfunction in ASD, the molecular mechanisms and neuroanatomical substrates that underlie abnormal sensory-related behavior in ASD remain poorly understood. To begin to answer these questions, developmental 5-HT function needs to be assessed in mouse models that accurately reflect the genetic risk factors of ASD.

Modeling Autism Spectrum Disorder in Mouse Models

Mouse models of human disease have been instrumental in understanding pathophysiology. An impressive array of biochemical and molecular tools currently exists to dissect the mechanisms behind a particular disease to refine treatment options. However, the underlying causes of many human diseases are unknown,

making it difficult to model in animals. For example, psychiatric disorders, such as ASD, are diagnostically defined by behavioral symptoms and not specific brain abnormalities. When confronted with such challenges, it is crucial to evaluate how an animal model accurately reproduces the disease in question. First, animal models should reflect a known cause or risk factor of a disease, termed construct validity. In addition, models should exhibit symptoms and pathophysiology associated with a disease, labeled as face validity. Finally, an animal model should possess predictive validity, the ability to respond to known treatments of a disease. Although it seems intuitive that all animal models of disease should pass validity tests, the relative lack of understanding of ASD has made it difficult to adhere to these basic tenets.

Due to the significant heritably of ASD, the majority of potential mouse models of the disorder have been the result of manipulations of the mouse genome at analogous risk loci discovered by human genetic studies. Consequently, as our understanding of the complex genetics underlying ASD has grown, so has the number and variety of mouse models generated by researchers. Initial mouse models were generated based on Mendelian, monogenic causes of intellectual disability. For example, mouse lines genetically modeled after disorders such as Fragile X syndrome (FXS) (Consortium, 1994), Rett syndrome (Guy et al., 2001), and Tuberous Sclerosis (Kobayashi et al., 2001) have provided a framework to examine the pathophysiology underlying these syndromes *in vivo*. As investigators are eager to test specific hypotheses about ASD in these models, it should be carefully noted that ASD is only present in a subset of individuals with the aforementioned genetic syndromes (Abrahams and Geschwind, 2008).

Learning by Example: History of *Fmr1* Knockout

The history of the *Fmr1* knockout (KO) mouse provides an excellent example of the utility of modeling human disorders in mice and the caveats involved in translating mouse findings to ASD. FXS is the most common cause of inherited intellectual disability, with an estimated incidence in males of 1 in 5000 (Coffee et al., 2009). This X-linked syndrome is primarily caused by a large expansion of a CGG trinucleotide repeat in the 5' untranslated region of the *FMR1* gene, which leads to transcriptional silencing and loss of fragile X mental retardation protein, FMRP (Oberle et al., 1991; Verkerk et al., 1991). Individuals with FXS exhibit a range of clinical symptoms, including craniofacial abnormalities, macroorchidism, hyperactivity, epilepsy, and cognitive impairment (Bernardet and Crusio, 2006). Interestingly, approximately 30-60% of affected individuals also meet diagnostic criteria for ASD, depending upon the criteria applied, currently making FXS one of the most common genetic findings in the disorder (Harris et al., 2008; Philofsky et al., 2004).

At the time of the discovery of the genetic cause of FXS, the function of FMRP was unknown. The first clues of its function emerged from amino acid sequence homology studies that indicated FMRP is an RNA binding protein (Ashley et al., 1993a). In addition, the murine gene homolog, *Fmr1*, is highly conserved and exhibits similar overall patterns of tissue expression compared to humans (Ashley et al., 1993b). To fully evaluate the function of FMRP and the molecular mechanisms underlying FXS, the *Fmr1* knockout (KO) mouse was generated via homologous recombination, where exon 5 of the *Fmr1* gene was disrupted by a neomycin cassette sequence (Consortium, 1994). While this genetic approach causes a loss of FMRP, this model lacks full

construct validity to FXS, as it does not reproduce the deleterious CCG repeat expansion documented in the human condition. In addition, there are reports that the mouse 'knockout' allele is molecularly active at the RNA level, with aberrantly spliced *Fmr1* transcripts present in KO brain tissue (Yan et al., 2004).

Despite possessing only partial construct validity, the *Fmr1* KO mouse demonstrates a number of phenotypes with face validity to FXS. In terms of morphological and neurological features, male KO mice exhibit macroorchidism (Consortium, 1994), dendritic spine abnormalities (Weiler and Greenough, 1999), and increased seizure susceptibility (Yan et al., 2004), all characteristics documented in FXS. However, while behavior has been extensively studied in *Fmr1* KO mice, the reported behavioral and cognitive phenotypes have been surprisingly subtle and dependent on inbred strain background (Bernardet and Crusio, 2006; Spencer et al., 2011). *Fmr1* KO mice are generally found to be hyperactive, with increased exploratory activity in the open field (Mineur et al., 2002; Spencer et al., 2005). Performance in basic spatial memory and learning tasks is remarkably unaffected in *Fmr1* KOs, indicating no dramatic deficits in cognitive function (Consortium, 1994; Yan et al., 2004).

Since a significant proportion of individuals with FXS also meet criteria for ASD, investigators have also evaluated *Fmr1* KO mice for behaviors relevant to the disorder. Behavioral neuroscientists have spent considerable effort in developing assays that examine communication, repetitive behavior, and social interaction in mouse models of ASD. For the sake of clarity, this overview will focus on current 'gold standard' behavioral tasks relevant to each core ASD diagnostic domain.

As mice are a highly social species, they are an ideal model system to evaluate the impact of ASD risk factors on social behavior. While there are numerous paradigms to evaluate social behavior in mice (Silverman et al., 2010), most assay readouts simply measure the time a mouse spends in close proximity to a social stimulus, ignoring more nuanced features of social interactions. Despite these limitations, the Crawley three-chamber task has become the social assay of choice in ASD mouse model research due to its reproducibility and automated design (Nadler et al., 2004). This task is composed of two separate phases, the test for sociability and test for social novelty. In the initial phase, the test for sociability, mice are placed in the center of a partitioned apparatus and allowed to explore two adjacent side chambers containing either an inanimate object or unfamiliar mouse. Typical mice spend more time investigating a social stimulus over an inanimate object, indicating a preference for social interaction. There have been conflicting reports of *Fmr1* KO performance on this task. Although C57Bl/6 *Fmr1* KOs display levels of sociability equal to littermate controls (Moy et al., 2009; Pietropaolo et al., 2011; Spencer et al., 2005), some studies note that hybrid and pure FVB *Fmr1* strains do not have a significant preference for social stimuli (McNaughton et al., 2008; Moy et al., 2009).

In the second phase, the test for social novelty, an unfamiliar mouse replaces the inanimate object in the three-chambered apparatus, and the test mouse is now given the choice to interact with the novel mouse or the ‘familiar’ mouse from the first phase of the assay. Mice typically show greater interest interacting with novel social stimuli, demonstrating social memory and recognition. Paralleling previous findings in the test for sociability, there have been inconsistent *Fmr1* phenotypes noted for preference for

social novelty (McNaughton et al., 2008; Moy et al., 2009), with one group finding both C57Bl/6 and FVB *Fmr1* KO mice have atypical decreases in exploration of an unfamiliar mouse (Pietropaolo et al., 2011). Interestingly, these findings converge with other observations of social behavior in *Fmr1* KOs that indicate a phenotype reminiscent of social anxiety commonly seen in FXS (McNaughton et al., 2008; Spencer et al., 2005).

Communication, though poorly understood in mice, is primarily evaluated in mouse models by recording ultrasonic vocalizations (USVs) in pups temporarily separated from dams (Jiang et al., 2010). Interestingly, *Fmr1* KOs exhibit increased USVs throughout early postnatal development (Spencer et al., 2011). While similar phenotypes have been documented in some other mouse models of ASD (Jiang et al., 2010), opposing findings of decreased vocalizations are also present in the literature (Chadman et al., 2008; Winslow et al., 2000). These inconsistent phenotypes suggest that neonate vocalization behavior may be influenced by factors, such as maternal care, not directly related to communication (Young et al., 2010).

Similar to measures of communication, assays that capture repetitive behavior in mice have been difficult to develop. However, with the notable discovery of compulsive grooming in the SAPAP3 KO mouse (Welch et al., 2007), patterns of self-grooming have been scrutinized in mouse models of ASD. Increased self-grooming in mice is interpreted as a type of motor stereotypy, relevant to the repetitive motor behavior seen in individuals with ASD. While there are limited reports of *Fmr1* grooming behavior, McNaughten et al. noted that *Fmr1* KOs spend more time grooming when confronted with a social stimulus (McNaughton et al., 2008), indicating that the manifestation of repetitive behaviors may be sensitive to perceived stressors.

Although the aforementioned descriptions of behavior in *Fmr1* KO mice are by no means exhaustive, they provide a poignant example of the general difficulties encountered by investigators. Critics of mouse models of ASD are quick to assert that many of the behavioral features in the disorder, such as abnormal verbal communication, are uniquely human and can never be fully recapitulated in a mouse. While this concern is certainly warranted, this viewpoint neglects to consider that our current understanding of mouse behavior is greatly lacking. The general inconsistency of behavior studies in mice indicates that there are several unknown factors that drive complex behaviors. Our ability to characterize behavior in mouse models of ASD is further complicated by the fact that numerous phenotypes are dependent on inbred strain background, which may parallel the variability in ASD diagnosis across individuals with fragile X syndrome. In fact, strain dependent phenotypes are now being leveraged to identify genetic loci that may play a role in the variable presentation of behavioral features in ASD (Carneiro et al., 2009; Ye et al., 2014). In the end, the behavioral characterization of mouse models of ASD should not be done solely to describe features that may externally parallel human symptoms. Rather, the power of animal models of ASD is to examine how risk factors impact neurobiological mechanisms conserved across phylogeny.

Another major challenge faced by ASD research is the lack of clear molecular targets to test the predictive validity of a given animal model. Currently available therapeutic options for ASD treat co-occuring symptoms and not the underlying pathophysiology of the disorder (Veenstra-VanderWeele and Warren, 2014), making their use in mouse studies a debatable pursuit. Instead, investigators have focused on

understanding how ASD risk variants impact neurobiological mechanisms that may relate to the overall phenotype observed in a model and the human disorder. From these basic science studies, refined hypotheses can be made about novel treatment options that can be further tested in the mouse.

The utility of this approach is again best illustrated by the *Fmr1* KO literature and the development of the mGlu5 receptor theory of FXS (Bear et al., 2004). Since the development of the *Fmr1* KO mouse in 1994, our basic understanding of the role of FMRP in the brain has dramatically improved. In short, studies have indicated that FMRP is a postsynaptic protein that regulates mRNA translation at glutamatergic synapses (Dolen et al., 2010). Although the impact of FMRP absence on synaptic function was initially elusive, Huber et al. discovered that a form of synaptic plasticity in the hippocampus of *Fmr1* KOs was selectively impaired. Specifically, the authors found that activation of group 1 metabotropic glutamate receptors (mGluRs) led to enhanced protein-synthesis-dependent long term depression (LTD) (Huber et al., 2002). This basic finding prompted subsequent work examining the hypothesis that dysregulated mGlu5 receptor signaling is a central cause of FXS. In a straightforward but powerful study, Dölen et al. reported that several phenotypes documented in C57Bl/6 *Fmr1* KO mice were rescued in *Fmr1/Grm5* double mutants. By genetically reducing mGlu5 expression by 50% in mice lacking FMRP, the authors found that dendritic spine abnormalities, audiogenic seizures, enhanced protein synthesis, and specific learning and memory impairments were all normalized (Dolen et al., 2007). While the results of this study were remarkable, it remained unclear whether pharmacological mGlu5 inhibition could reverse established *Fmr1* KO phenotypes in adulthood. To address this

issue, Michalon et al. chronically administered a long-acting mGlu5 inhibitor, CTEP, to young adult *Fmr1* KOs (Michalon et al., 2012). Similar to results seen when genetically reducing mGlu5 expression, pharmacological inhibition of mGlu5 in *Fmr1* KOs was able to correct several phenotypes relevant to FXS, supporting the notion that pharmacological intervention in FXS could have therapeutic value.

The collective basic science findings in *Fmr1* KOs were the driving force that led to clinical trials of mGlu5 inhibitors in FXS. While the appropriate readouts of drug efficacy are currently unclear in human studies (Berry-Kravis et al., 2013), results from a number of mGlu5 Phase II trials suggest no significant improvement in behavioral outcomes compared to placebo in adults and adolescents with FXS. Studies have not yet been carried out in children with FXS, raising the possibility that treatment will only be effective earlier in development. Unfortunately, there is no guarantee that the insights gained from studying mouse neurobiology and behavior will translate to analogous findings in humans; however mouse models of ASD currently provide the best option to explore hypotheses regarding the mechanistic causes of the disorder. Translational success will ultimately be linked to our understanding of the complex set of ASD risk factors and our ability to accurately model these causes in mice.

Common and Rare *SLC6A4* Variation and ASD

Initial genetic evidence implicating *SLC6A4* as an ASD risk gene emerged from family-based association and linkage studies. Family-based ASD association studies involving common *SLC6A4* variation have primarily focused on the well-documented SERT promoter polymorphism, 5-HTTLPR. Collectively, the findings have been

inconsistent, with groups reporting no association or associations with either the long or short allele (Devlin et al., 2005). However, the studies with the greatest statistical power to detect excess 5-HTTLPR allele transmission have both reported an association with the short allele (Devlin et al., 2005; McCauley et al., 2004).

Similar to 5-HTTLPR association studies, genome-wide linkage scans have largely been unable to identify consistent ASD risk loci, further demonstrating the extreme genetic heterogeneity in the disorder (Werling et al., 2014). Nonetheless, out of the seven largest ASD linkage studies to date, two groups have reported significant evidence of linkage at the chromosome 17q11 region harboring *SLC6A4*. In the first study, which examined 345 multiplex families from the Autism Genetic Resource Exchange (AGRE), Yonan et al. found the strongest evidence of linkage to ASD on chromosome 17q (Yonan et al., 2003). In a subsequent analysis using the same sample set, Stone et al. demonstrated that the linkage signal at chromosome 17q increased when stratifying families by the sex of affected children. Specifically, when analyzing families with only male affected children, the linkage increased to reach genome-wide significance (Stone et al., 2004), suggesting *SLC6A4* or other genes at this locus harbor variants that contribute towards the male gender bias documented in ASD.

In addition to the complementary Yonan and Stone linkage studies, McCauley et al. also reported evidence of linkage near *SLC6A4.* While the 17q linkage signal emerged from a partially overlapping AGRE sample used in the Yonan study, the authors reported that evidence of linkage significantly increased when only examining families with high ADI-R measures of rigid-compulsive behavior (McCauley et al., 2004). Furthermore, McCauley et al. noted that common genetic variation in SERT, including

5-HTTLPR, failed to explain the suggestive linkage in both the overall multiplex sample and the rigid-compulsive behavior family subset. Due to these findings, it was hypothesized that the linkage signal near *SLC6A4* was caused by distantly located polymorphisms that modify gene expression or a heterogeneous collection of rare coding variants that account for the majority of ASD risk at this locus.

To explore this hypothesis, Sutcliffe et al. subsequently performed a genetic screen for rare ASD-associated SERT variants in families that exhibited strong evidence of linkage near *SLC6A4* (Sutcliffe et al., 2005). Replicating previous findings of sex-biased linkage near *SLC6A4*, the authors noted that families with only male affected children were primarily driving the linkage signal observed at chromosome 17q11. From the 120 families with the highest LOD scores at 17q11, unrelated probands were screened for exon and promoter SERT variants that could potentially account for the observed linkage. Interestingly, novel SERT variants, Ile425Leu, Phe465Leu, and Leu550Val, located in highly conserved transporter transmembrane domains were discovered in the initial. While the Ile425Leu and Leu550Val variants were found to segregate with autism, one affected male child from the Phe465Leu pedigree did not inherit the paternally transmitted allele, suggesting additional genetic or environmental ASD risk factors are present in this family. The Ile425Leu variant displayed a unique segregation pattern indicative of the male-biased linkage signal, with the maternally transmitted Leu425 allele present in two affected sons as well as three unaffected daughters. Furthermore, another rare SERT mutation located at the same protein residue, Ile425Val, was found in two unrelated families with a history of OCD and other psychiatric comorbidities, including ASD (Ozaki et al., 2003). The discovery of two

disease-associated mutations at an identical, highly conserved protein residue strongly implicates that these variants have a functional effect on SERT function and impact human behavior.

Beyond the discovery of three novel SERT variants, Sutcliffe et al. also screened their entire 384 family data-set for known rare coding SERT variants, Gly56Ala and Lys605Asn. While only one subject was found to carry the Asn605 allele, multiple individuals were identified carrying one or two copies of the Ala56 variant. In multiplex families with strong evidence of linkage near *SLC6A4*, the Ala56 variant was found at an elevated frequency (2.3%) than previously described in non-clinical populations (Glatt et al., 2001). Specifically, the Ala56 variant was present in seven 'linked' families, with the allele exhibiting a 15:5 transmission to nontransmission ratio. In contrast, the Ala56 allele frequency (1.1%) was not significantly elevated in families without evidence of linkage at 17q11, a finding corroborated by a subsequent screen of *SLC6A4* in a case-control association study (Sakurai et al., 2008).

Interestingly, affected carriers of the Gly56Ala, Ile425Leu, Phe465Leu, and Leu550Val variants exhibited increased rigid-compulsive behaviors as measured by the Autism Diagnostic Interview (ADI-R). In contrast to the novel transmembrane SERT alleles, the Gly56Ala variant had a unique association with ADI-R ratings of sensory aversion in affected individuals. While the limited number of Gly56Ala carrier families makes it difficult to draw strong conclusions about behavioral correlates, aberrant sensory behavior could be related to the reported role of SERT in the establishment of sensory-related circuits during neurodevelopment.

In addition to their genetic and behavioral analyses, Sutcliffe et al. also examined the impact of the Ala56 variant on SERT function in lymphocytes taken from genotyped study participants. Strikingly, lymphocytes expressing the Ala56 variant displayed significantly increased 5-HT transport at basal conditions, with homozygous Ala56 lymphocytes exhibiting an approximately 75% increase in 5-HT uptake. 5-HT transport in Ala56 lymphocytes was also insensitive to regulation by p38 mitogen-activated protein kinase (MAPK) and protein kinase G (PKG) activators, which normally enhance SERT function (Blakely et al., 2005). Moreover, these findings were subsequently confirmed in heterologous cell systems devoid of potential genetic modifiers of SERT (Prasad et al., 2009). Although it is clear that Gly56Ala is not a deterministic ASD variant, the allele's increased frequency in families with male-biased linkage near *SLC6A4* and its stark effect on SERT function implicate the Ala56 variant as an ASD risk factor.

Finding 'Missing Heritability' in ASD: Maternal-Fetal Interactions

Our current understanding of the genetic architecture of ASD does not sufficiently explain the significant heritability documented in the disorder. While advances in genome sequencing technologies are poised to close this gap, investigators are now exploring other potential sources of "missing heritability" found in ASD (Manolio et al., 2009). One proposed hypothesis is that risk alleles may also exert their effects by negatively impacting the prenatal environment in maternal carriers. Obstetric complications, such as gestational diabetes (Xu et al., 2014) and pre-term birth (Lyall et al., 2012), have been found to be significant risk factors for ASD. Consequently, ASD-

associated variants that also disrupt maternal physiology during pregnancy may have a larger impact on fetal development than originally estimated.

Whereas examples of genetic parent-of-origin effects have been clearly documented in developmental disorders (Buiting et al., 1995), there has been a dearth of research that has examined maternal effects in ASD. In contrast to parent-of-origin effects, maternal effects are independent of offspring genotype. Thus, maternal effects on neurodevelopment are thought to occur by impacting the maternal prenatal environment and/or maternal behavior. To explore the hypothesis that maternal genetic variation may account for a proportion of ASD risk, two groups recently performed genome wide association studies in mothers of affected children (Tsang et al., 2013; Yuan and Dougherty, 2014). Both studies failed to detect common SNPs that reached genome wide significance, but the number of suggestive associations that did not overlap with their proband analyses indicated true maternal effects were most likely below their statistical ability to detect. In contrast to the unbiased GWAS approach, Kistner-Griffin et al. examined *SLC6A4* mediated maternal effects in ASD, focusing on the 5-HTTLPR (Kistner-Griffin et al., 2011). The inconsistency of 5-HTTLPR association studies in ASD led the authors to examine additional sources of risk that may underlie this heterogeneity. While the 5-HTTLPR short allele was associated with ASD in probands, an opposing maternal effect was found, with the long allele conferring risk. These findings highlight the utility of examining maternal effects in variants that have unclear relationships with ASD in traditional association studies.

In addition to human genetic studies, maternal effects on neurodevelopment are also being explored in animal models. While this field of research is still in its infancy,

there have been multiple reports of 5-HT-related mouse models exhibiting maternal effects on fetal development. Using *Tph1* KO animals, Côté et al. evaluated the impact of peripheral 5-HT production in dams on developing embryos (Cote et al., 2007). Interestingly, E12.5 offspring of *Tph1* KO dams, regardless of embryo genotype, were smaller and possessed gross brain abnormalities. Furthermore, these neuroanatomical changes were present despite *Tph2* expression in the developing midbrain at E10.5, indicating that maternal peripheral 5-HT function is critical for proper neurodevelopment.

While Cote et al. focused on developmental phenotypes resulting from maternal 5-HT dysfunction, a subsequent investigation of 5-HT_{1A} receptor (5-HT_{1A}R) KOs established that 5-HT mediated maternal effects could have a long lasting impact on offspring behavior (Gleason et al., 2010). Gleason et al. found that adult offspring of dams with partial or full 5-HT_{1A}R deletion exhibited increased anxiety-like behavior compared to the progeny of wildtype dams. To determine whether prenatal or postnatal maternal 5-HT_{1A}R function was required for the observed anxiety-like phenotype, the authors performed a series of intricate embryonic and early postnatal cross-fostering experiments. Surprisingly, results from these studies indicated that maternal 5-HT_{1A}R deficiency during pregnancy had a larger impact on offspring behavior in adulthood than the offspring's own 5-HT_{1A}R genotype.

Although the Côté and Gleason studies both demonstrated offspring phenotypes dependent on maternal genotype, it remains unclear 1) what aspects of maternal physiology during pregnancy are sensitive to changes in 5-HT homeostasis and 2) how these 5-HT mediated changes are then able to alter fetal development. In the Côté et al. study, it was hypothesized that the observed changes in embryos of *Tph1* KO dams

were due to altered maternal platelet 5-HT, which is dramatically reduced compared to wildtype. However, the transfer of maternal platelet 5-HT to the developing fetus has yet to be demonstrated experimentally and remains a controversial topic of debate (Bonnin et al., 2011). Interestingly, subsequent investigations of female *Tph1* KOs indicated that they exhibit gestational diabetes (Kim et al., 2010), a condition that is known to impact fetal development. Furthermore, while Gleason et al. established a link between hippocampal maturation and the anxiety-like behaviors of 5-HT_{1A}R KO offspring, the upstream maternal mechanisms of these phenotypes remain unknown. However, despite our current lack of understanding of these mechanisms, any change to maternal physiology that could impact neurodevelopment must ultimately act through the main interface between mother and fetus, the placenta.

While initially underappreciated as a vital organ that facilitates normal fetal development, the placenta is now being investigated for its role in the pathogenesis of psychiatric disorders such as ASD (Walker et al., 2013). The placenta is a specialized mammalian organ that primarily functions as the interface between the maternal and fetal blood supplies, allowing for the exchange of gases and other molecules. The organ is made up of both maternal and fetal components: the maternal decidua, vascularized tissue derived from endometrium, and fetal trophoblasts, a diverse group of specialized cells that differentiate from the trophectoderm layer of the blastocyst. In addition to the basic exchange of gas and nutrients, the placenta also serves as a protective barrier for the developing fetus from immunological challenges that occur during pregnancy. Furthermore, the placenta is the primary source of a number of hormones and growth factors during pregnancy. Unsurprisingly, stressors that significantly impact placental

function can cause fetal growth restriction and miscarriage (Rossant and Cross, 2001). However, the impact of more subtle changes in placental physiology on fetal development is only beginning to be explored.

As developmental perturbations of 5-HT signaling have long been implicated in ASD, placental 5-HT function is now being scrutinized for its role in the disorder. While the presence of 5-HT and 5-HT-related proteins in the placenta had been firmly established for decades (Yavarone et al., 1993), it was not until recently that we gained a basic understanding of placental 5-HT function and its interaction with fetal development. In a seminal study, Bonnin et al. demonstrated that the placenta has the ability to synthesize 5-HT from maternally derived sources of tryptophan (Bonnin et al., 2011). Moreover, this novel synthetic pathway provides the predominant source of 5-HT to the fetal forebrain before the arrival of serotonergic innervation from the midbrain raphe nuclei. The presumptive site of placental 5-HT synthesis occurs in syncytiotrophoblasts, a differentiated trophoblast cell type that is the cellular interface between the maternal and fetal blood supply. In addition to the enzymes required to synthesize 5-HT, syncytiotrophoblasts also express SERT (Balkovetz et al., 1989) and MAOA (Auda et al., 1998). It has been speculated that 5-HT uptake and degradation mechanisms are necessary to regulate fetal exposure to maternal sources of 5-HT, but further work is necessary to clarify how SERT and MAOA contribute to placental 5-HT homeostasis. Collectively, these findings highlight a novel developmental mechanism that impacts 5-HT signaling in the fetal brain. However, the long-term consequences of altered placental 5-HT synthesis remain unknown. Future studies will be required to

evaluate how potential ASD genetic and environmental risk factors may interact with this synthetic pathway.

Aims

Our understanding of how the 5-HT system intersects with the pathophysiology of ASD remains unclear. The clearest path forward to bridge this gap is to study functional variation in 5-HT-related genes associated with ASD in mouse models. With this idea in mind, Veenstra-VanderWeele and colleagues created the SERT Gly56Ala knock-in mouse line to evaluate how the most common rare SERT variant impacts murine brain development and behavior (Veenstra-Vanderweele et al., 2009). In Chapter 2, the initial biochemical and behavioral characterization of the SERT Ala56 mouse is described. In Chapter 3, we explore the developmental consequences of maternal and embryonic enhanced SERT function. In Chapter 4, we return to human studies to determine if common functional SERT variation, similar to the Ala56 variant, influences patterns of sensory behavior in ASD. The results of these studies and their implications for understanding the pathophysiology of ASD are discussed.

CHAPTER 2

INITIAL BIOCHEMICAL AND BEHAVIORAL CHARACTERIZATION OF THE SERT GLY56ALA KNOCK-IN MOUSE

As published in: Autism Gene Variant Causes Hyperserotonemia, Social Impairment and Repetitive Behavior*. Proc Natl Acad Sci U S A 109, 5469-74 (2012).*

Jeremy Veenstra-VanderWeele, Christopher L. Muller, Hideki Iwamoto, Jennifer E. Sauer, W. Anthony Owens, Charisma R. Shah, Jordan Cohen, Padmanabhan Mannangatti, Tammy Jessen, Brent J. Thompson, Ran Ye, Travis M. Kerr, Ana M. Carneiro, Jacqueline N. Crawley, Elaine Sanders-Bush, Douglas G. McMahon, Sammanda Ramamoorthy, Lynette C. Daws, James S. Sutcliffe, Randy D. Blakely

Introduction

ASD is a male-predominant disorder that is characterized by deficits in social interactions and communication, as well as repetitive behavior. Hyperserotonemia, or increased whole blood 5-HT, is a well replicated biomarker that is present in approximately 30% of subjects with ASD (Mulder et al., 2004; Schain and Freedman, 1961). Some data suggest an association of hyperserotonemia with stereotyped or self-injurious behavior, but results have been inconsistent (Kolevzon et al., 2010; Sacco et al., 2010). Despite the high heritability of whole blood 5-HT levels (Abney et al., 2001), a mechanistic connection between hyperserotonemia and specific components of the pathophysiology of ASD remains enigmatic. In blood, 5-HT is contained almost exclusively in platelets (Anderson et al., 1987) that lack 5-HT biosynthetic capacity but

accumulate the monoamine via the antidepressant-sensitive SERT. A genome-wide study of whole blood 5-HT as a quantitative trait found association with the SERT-encoding gene *SLC6A4*, as well as with *ITGB3*, which encodes the SERT-interacting protein integrin beta 3. In both cases, the strongest evidence for association was found in males (Carneiro et al., 2008; Weiss et al., 2005; Weiss et al., 2004). Linkage studies in ASD also implicate the 17q11.2 region containing *SLC6A4*, again with stronger evidence in males (Stone et al., 2004; Sutcliffe et al., 2005).

As common *SLC6A4* variants are only modestly associated with ASD (Devlin et al., 2005), we and our colleagues previously screened *SLC6A4* for rare variants in multiplex families that demonstrate strong linkage to 17q11.2. In this effort, we identified five rare SERT coding variants, each of which confers increased 5-HT transport in transfected cells as well as in lymphoblasts derived from SERT variant-expressing probands (Prasad et al., 2009; Prasad et al., 2005; Sutcliffe et al., 2005). We found the most common of these variants, Ala56 (allele frequency in subjects of European ancestry of 0.5–1%), to be overtransmitted to autism probands, and to be associated with both rigid-compulsive behavior and sensory aversion (Glatt et al., 2001; Sutcliffe et al., 2005). No such trait association is seen in families without linkage to this region (Sakurai et al., 2008). In transfected cells, SERT Ala56 also demonstrates increased basal phosphorylation and insensitivity to PKG- and p38 MAPK-linked signaling that normally produce increased transporter trafficking and catalytic activation, respectively (Prasad et al., 2005). These findings suggest that homeostatic control of 5-HT may be impaired in some children with ASD. Importantly, model system studies indicate that 5-HT and SERT are important determinants of normal brain development and that early

life perturbations in 5-HT signaling can have enduring effects on behavior (Ansorge et al., 2004; Bonnin et al., 2007; Jitsuki et al., 2011; Salichon et al., 2001).

To explore the dependence of juvenile and adult behavior on early life 5-HT manipulation and further understand the impact of the SERT Ala56 variant *in vivo*, we generated mice expressing SERT Ala56 from the native mouse *Slc6a4* locus (Veenstra-Vanderweele et al., 2009). Although SERT Ala56 mice exhibit normal growth and fertility, they display significantly increased CNS 5-HT clearance, enhanced 5-HT receptor sensitivity, and hyperserotonemia. Even more striking, SERT Ala56 animals display alterations in a number of ASD-relevant behaviors.

Methods

Mice

SERT Ala56 knock-in mice were constructed as previously described on a 129S6/SvEvTac genetic background (Veenstra-Vanderweele et al., 2009). Briefly, a targeting construct was created containing exons 2 to 5 of the mouse 129S6/SvEvTac *Slc6a4* gene with a floxed neomycin-resistance cassette inserted between exons 4 and 5 (SERT Ala56-Neo). This construct was electroporated into mouse 129S6/ SvEvTac embryonic stem cells, and correct targeting was identified by PCR screening and confirmed by Southern blot. Following blastocyst injection, resulting chimeric animals were bred with 129S6/SvEvTac female mice to generate germline transmission. To remove the floxed neomycin-resistance cassette, the knock-in mice were crossed with 129S4/Jae protamine-Cre mice, yielding the SERT Ala56 line used for experiments. All mice used in experiments were progeny of heterozygous pairings that were housed by

sex with three to five mixed-genotype littermate animals per cage. Mice used within each experiment were greater than eight weeks of age and were matched by birth date to generate cohorts of animals varying by no more than four weeks.

Synaptosome Preparation

WT and SERT Ala56 mice were rapidly decapitated, and the midbrain was immediately homogenized in 10 volumes (wt/vol) of cold 0.32 M sucrose using a Teflon-glass homogenizer under chilled water and centrifuged at 1,000 × *g* for 15 min at 4 °C. The resulting supernatant was centrifuged at 15,000 × *g* for 20 min and the pellet was washed by resuspending in 0.32 M sucrose and frozen for immunoblotting and binding assays or used immediately for phosphorylation assays. Protein assays used either the BCA method (Pierce) or DC protein assay (Bio-Rad).

Western Blotting

Mouse midbrain synaptosomes were solubilized with 250 mL RIPA buffer (50 mM Tris, pH 7.4, 150 mM NaCl, 1 mM EDTA, 1% Triton X-100, 1% sodium deoxycholate, 0.1% SDS) containing protease inhibitors (1:100; Sigma). Supernatants of detergent extracts (50 mg) were separated by 10% SDS/PAGE, electroblotted to PVDF membranes, and immunoblotted with affinity purified SERT antibody 48 (1:1,000) as described previously (Bauman et al., 2000). Immunoblotting for β-actin followed the same procedure with primary antibody anti–β-actin (1:50,000; Sigma). Optical densities of the bands were quantified with ImageJ software 1.4 (National Institutes of Health) after obtaining multiple gel exposures to ensure linearity of data capture.

[^{3}H]Citalopram Binding

Mouse midbrain synaptosomes were centrifuged at 15,000 × g for 20 min, and the pellet was lysed in binding buffer of 50 mM Tris(hydroxymethyl)aminomethane and 100 mM NaCl, pH 7.4. Each tube was prepared with 200 mg synaptosome protein in 500 µL binding buffer. 5 nM [^{3}H]citalopram was then added to each tube and incubated on ice for 20 min. Samples were harvested onto GF/B Whatman filters using a Brandel harvester. Filters were washed three times with ice-cold binding buffer and then immersed in scintillation liquid for 8 h before scintillation spectrometry (Beckman Coulter). Counts were corrected for nonspecific uptake by using parallel samples preincubated at 4 °C for 10 min with fluoxetine 500 µM.

SERT Phosphorylation

Synaptosomes were suspended in modified Krebs-bicarbonate buffer (25 mM Na2HCO3, 124 mM NaCl, 5 mM KCl, 5 mM MgSO4, 10 mM glucose, pH 7.3) that was saturated with 95% O2/5% CO_2 for 60 min at 22 °C. SERT basal phosphorylation was conducted by using 250 to 300 µg P2-synaptosomal protein with 5.0 mCi ^{32}P carrier-free orthophosphate per milligram protein with continuous shaking at 37 °C for 1 h. To study the effect of 8-Bromo-cGMP (8-Br-cGMP) or PD169316, synaptosomes were preincubated with 5.0 mCi ^{32}P carrier-free orthophosphate per mg protein for 30 min at 37 °C, followed by the addition of 100 µM 8-Br-cGMP, 20 µM PD169316, or vehicle with incubation for another 30 min at 37 ° C. Samples were then centrifuged at 15,000 × *g* for 20 min, and the pellet was resuspended in RIPA buffer supplemented with protease inhibitors (protease inhibitor mixture; Sigma) and phosphatase inhibitors (10 mM sodium

fluoride, 50 mM sodium pyrophosphate, 5 mM sodium orthovanadate, and 1 μM okadaic acid) by passing through a 25-gauge needle 10 times. The clear supernatant obtained after centrifuging the solubilized synaptosomes at 25,000 × *g* for 40 min at 4 °C was subjected to immunoprecipitation with SR-12 antibody as described previously (Ramamoorthy et al., 2007; Samuvel et al., 2005). The immunoadsorbents captured by protein A sepharose beads were washed with RIPA buffer before the addition of 60μL Laemmli sample buffer [62.5 mM Tris-HCl, pH 6.8, 20% (vol/vol) glycerol, 2% (wt/vol) SDS, and 5% (vol/vol) 2-mercaptoethanol] and incubated for 30 min at 22 °C. The eluates were subjected to SDS/PAGE (10% wt/vol) and the ^{32}P-radiolabeled SERT proteins were detected on autoradiograms. Quantification from digitized autoradiograms was evaluated on multiple exposures (4 and 7 d) of the film by using ImageJ software (National Institutes of Health).

High Performance Liquid Chromotography with Electrochemical Detection

Levels of 5-HT were quantified by previously described HPLC electrochemical detection methods (Bazalakova et al., 2007). Trunk blood and brain samples were harvested by rapid decapitation. Blood samples were collected into microcentrifuge tubes containing 25 μL of ACD anticoagulant solution A (BD). Trunk blood and brain samples were frozen on dry ice and maintained at −20 °C until analysis. Biogenic amines were determined by a specific HPLC assay using a Decade (oxidation, 0.7) electrochemical detector (Antec). Biogenic amines were eluted with a mobile phase consisting of 89.5% 100 mM TCA, 10 mM sodium acetate, .1 mM EDTA, and 10.5% (vol/vol) methanol (pH 3.8). Concentration was determined by comparison with

injections of known standards.

Immunohistochemistry

Mice were deeply anesthetized with sodium pentobarbital and intracardially perfused with 4% paraformaldehyde. Brains were postfixed overnight, transferred to 30% sucrose until sunk, and sectioned on a sliding freezing microtome to a thickness of 40µm. After blocking in 3% normal donkey serum and 0.1% Triton X-100 in PBS solution, pH 7.4, sections were incubated in anti-SERT (1:1,000; Abcam) and anti-tryptophan hydroxylase (1:1,000; Millipore) antibodies overnight at 4 °C. After washing with PBS solution, sections were incubated in DyLight 488-conjugated donkey anti-rabbit (1:200; Jackson ImmunoResearch) and DyLight 549-conjugated donkey anti-sheep (1:200; Jackson ImmunoResearch) secondary antibodies for 2 h at room temperature.

In Vivo Electrochemical Recordings

Clearance of 5-HT was measured by *in vivo* chronoamperometry as described previously (Daws et al., 1997). SERT Ala56 and littermate SERT Gly56 mice (20–30 g) were anesthetized by i.p. injection (2 mL/kg body weight) of chloralose (35 mg/kg) and urethane (350 mg/kg) and placed into a stereotaxic frame. High-speed chronoamperometric recordings were made using the FAST-12 system (Quanteon). Oxidation potentials consisted of 100 ms pulses of +0.55 V separated by a 90 ms interval at 0.0 V. An Ag/AgCl reference electrode was positioned in the extracellular fluid of the ipsilateral superficial cortex. Oxidation and reduction currents were digitally in-

tegrated during the last 80 ms of each 100 ms voltage pulse. Nafion-coated carbon fiber electrodes were pretested for selectivity ratio for 5-HT over 5-hydroxyindoleacetic acid greater than 500:1 and a linear response ($r^2 \geq 0.9$) to 5-HT. The detection limit for the measurement of 5-HT in these experiments averaged 35 ± 10 nM (n = 75).

In vivo electrochemical recording assemblies consisted of a Nafion-coated, single carbon fiber electrode attached to a glass micropipette such that their tips were separated by approximately 200 μm. The barrel was filled with 5-HT (200 μM) in artificial cerebrospinal fluid (aCSF), pH7.4. The electrode–micropipette recording assembly was lowered into the CA3 region of the dorsal hippocampus (anterior–posterior, −1.94; medial–lateral, +2.0; dorsal–ventral, −2.0) (9). Exogenous 5-HT was applied by pressure-ejection (5–25 psi for 0.25–3 s), in volumes ranging from 4 to 170 nL to produce signal amplitudes ranging from 0.1 to 4.2 μM in randomized order between mice. An electrolytic lesion was made for histological verification of electrode localization at the end of each experiment.

To evaluate the effect of 8-Br-cGMP on 5-HT clearance in WT and SERT Ala56 mice, 5-HT was first pressure-ejected in the CA3 region of hippocampus to achieve signals with amplitudes less than 1.0 μM (range, 0.44–0.90 μM; micropipette barrel concentration, 200 μM). Signal amplitudes did not differ between genotypes (WT, 0.61 ± 0.06 μM, n = 7; Ala56, 0.69 ± 0.06 μM, n = 6). When three reproducible 5-HT signals had been attained, 8-Br-cGMP was applied (micropipette barrel concentration, 12.5 μM; 25 nL ejected to deliver 0.5 pmol). Five minutes later, 5-HT was locally applied, and then again at 10 min and at 10 min intervals thereafter for 1 h. Two time course parameters were analyzed: T_{20} and T_{80}, defined as the time for 5-HT to be cleared by

20% and 80%, respectively, of the peak signal amplitude. T_{20} reflects 5-HT at a concentration at which SERT-mediated 5-HT clearance is near V_{max}, whereas T_{80} provides an index of 5-HT clearance at a concentration approximating the K_m for SERT-mediated 5-HT uptake. For both parameters, baseline 5-HT clearance time was fastest in SERT Ala56 mice; however, this reached significance only for the T_{80} parameter (T_{80}, WT 123 ± 13 s; Ala56 81 ± 5 s; t-test for independent samples, t(11) = 2.822, P=0.0166; T_{20}, WT 25 ± 4s; Ala56 16 ± 2s; t(11) = 1.806, P= 0.0984). Because of the difference in clearance time between genotypes, 8-Br-cGMP treatment data were analyzed as a percent of baseline (i.e. pre 8-Br-cGMP time course parameters).

Chronoamperometry Data Analyses

The oxidation current was converted to μM units of 5-HT concentration by using the calibration factor determined *in vitro*. V_{max} and apparent transporter affinity (K_T) values for 5-HT clearance were determined by fitting a one-site hyperbolic function to a plot of clearance rate (T_c) vs. signal amplitude, where T_c is defined as the slope of the decay curve from 20% to 60% of maximal signal amplitude (i.e. the most linear portion of the decay). Each point on the curves used for kinetic analyses of 5-HT clearance was derived from three to six mice. K_T values were corrected for a volume fraction (α) of 0.20 (Nicholson and Sykova, 1998).

Slice Preparation and Electrophysiological Recordings

Following rapid decapitation, brains were removed and blocked in cold sucrose-substituted aCSF. Coronal, midbrain slices (200 μm thickness) containing the dorsal

raphe nucleus were cut on a brain slicer (Campden Instruments) at ice-cold temperature and maintained in aCSF at room temperature for 1 h before recording. Neurons were visualized with an Axioskop microscope (Carl Zeiss) equipped for near-IR differential interference contrast imaging. Recording pipettes with resistance of 3 to 5 MΩ were filled with filtered, normal HEPES-buffered saline solution (Nunemaker et al., 2003). Cell-attached extracellular recordings were per- formed at 0 mV voltage-clamp condition at 35 °C. Raphe neurons were identified as likely serotonergic based on suppression of spontaneous spike frequency by 5-HT (4 μM). Spontaneous, basal firing rate was measured as the average of a 100 s record. The inhibition of the firing at various 5-HT concentrations was normalized by the basal firing frequency. Electrophysiological signals were processed and controlled by an Axopatch 1D amplifier and pClamp 10.0 software (Molecular Devices) in gap-free mode. The signals were low-pass filtered at 1 kHz, high-pass filtered at 1 Hz, and digitized at 5 kHz. All solutions contained 3 μM phenylephrine hydrochloride and 40 μM L-tryptophan to maintain the spontaneous firing rate in the absence of noradrenergic tone and tryptophan availability (Evans et al., 2008).

Behavioral Experiments

Four cohorts of adult male mice born consecutively to heterozygous SERT Ala56/Gly56 pairs were used for behavioral experiments. The first cohort of male SERT Ala56 (n = 22) and SERT Gly56 (WT littermate controls, n = 15) animals underwent the testing reported here in the following sequence: elevated plus-maze, open field activity, Crawley three- chamber sociability, acoustic startle and prepulse inhibition of acoustic

startle, Morris water maze, tube test for social dominance, forced swim test, and 8-OH-DPAT-induced hypothermia. The second cohort of male SERT Ala56 (n = 12) and SERT Gly56 (n = 10) animals underwent the testing reported here in the following sequence: Crawley sociability, acoustic startle and prepulse inhibition, tube test, and DOI-induced head twitch response. A third cohort of male SERT Ala56 (n = 13) and SERT Gly56 animals (n = 15) underwent the testing reported here in the following sequence: rotarod, a general examination of health and sensorimotor characteristics (14), and home cage monitoring (n = 10 of each genotype). A fourth cohort of male SERT Ala56 (n = 10) and SERT Gly56 (n = 10) underwent the marble burying test. A cohort of mixed-sex postnatal day 7 pups born consecutively to heterozygous SERT Ala56/Gly56 pairs was used for the ultrasonic vocalization experiment. A separate cohort of mixed-sex postnatal day 7 pups born consecutively to heterozygous SERT Ala56/ Gly56 pairs was used for the pup temperature measurements.

Elevated Plus-Maze

The elevated plus-maze was conducted as described previously under red light conditions in the first 4 h of the dark period to increase locomotion. The plus-maze consists of four arms, 10 × 10 × 30 cm, connected in a plus configuration and elevated approximately 50 cm. Two of the arms have walls 20 cm high, and two arms have no walls. Mice were placed in the center of the maze at the beginning of the 5 min session. The position of the mouse was tracked three times per second, and data were analyzed in real time on a Macintosh computer using Image EP (Miyakawa et al., 2001), a modification of ImageJ software (National Institutes of Health). Mice were placed in the

center of the maze at the beginning of the 5 min session. When the number of entries into the open and closed arms was noted to follow a bimodal distribution (Fig. S5B), animals with four or fewer entries (n = 6 Ala56, n = 5 Gly56) were excluded from the primary analysis.

Open Field Activity

Exploratory locomotor activity was evaluated by using activity monitors measuring 27.9 × 27.9 cm (MED Associates). Each apparatus contains 16 photocells in each horizontal direction, as well as 16 photocells elevated 4.0 cm to measure rearing. Exploratory locomotor activity was evaluated as described previously (Bazalakova et al., 2007) for 90 min under red light conditions in the first 4 h of the dark period.

Crawley Sociability Test

Social behavior was evaluated in a three- chamber polycarbonate apparatus with 4-inch sliding gates separating the 7 × 9 inch chambers (Moy et al., 2004). The subject mouse was initially allowed to explore all three chambers for 10 min to acclimate to the apparatus. A stimulus mouse (social stimulus) was then introduced inside an inverted wire pencil cup (Spectrum Diversified Designs) in one side chamber with a clean empty pencil cup (inanimate stimulus) introduced in the opposite side chamber. The stimulus mouse was an adult male WT mouse, previously habituated to the pencil cup in six 30 min sessions across three days. The subject mouse was then allowed to explore all three chambers for 10 min. A research assistant blinded to mouse genotype coded videos for time spent in each chamber. When the number of entries was noted to follow

a bimodal distribution (Fig. S5C), analysis of time spent in each stimulus chamber (social and inanimate) by repeated-measures two-way ANOVA with Bonferroni post-tests was performed excluding animals with four or fewer total entries during the sociability portion of the test (n = 14 Ala56, n = 12 Gly56).

Acoustic Startle and Prepulse Inhibition

Acoustic startle response and prepulse inhibition of acoustic startle were measured by using the Acoustic Startle Reflex Test Compartments (MED Associates). Mice were acclimated to background white noise of 65 dB for 5 min in a Plexiglas holding cylinder. Mice were then presented with seven trial types in six discrete, randomized blocks of trials for a total of 42 trials with an intertrial interval of 10 to 20 s. One trial measured baseline movement and one trial measured response to the 120-dB, 50-ms startle stimulus alone. The other five trials used an acoustic prepulse of 74, 78, 82, 86, or 90 dB preceding the acoustic startle stimulus by 100 ms. Startle amplitude was measured every millisecond over a 65 ms period beginning at the onset of the startle stimulus. The dependent variable was the maximum startle over the sampling period. Prepulse inhibition was calculated by dividing the difference between baseline startle and startle following prepulse by baseline startle.

Morris Water Maze

The water maze was a 122 cm circular pool in a room with multiple visual cues. Data were analyzed in real time on a Macintosh computer by using Image WM (O'Hara), a modification of the public-domain ImageJ software (National Institutes of

Health), which was used to track the mice for the length of time and swimming distance to a stationary submerged platform from four randomly ordered start locations. A subset of mice from cohort 1 (n = 10 per genotype) was used in the Morris water maze task, as described previously (Bazalakova et al., 2007). Four trials per day were given until each mouse within the cohort achieved an average time of less than 15 s to find the platform across four consecutive trials. On the final day of testing, a 1 min probe trial with no platform was used to measure the time spent in the quadrant of the pool that previously contained the platform. Reversal learning was tested the following week by switching the platform to the diagonally opposite position in the pool and repeating the aforementioned procedure.

Tube Test

Cohort 1 male mice used for the Morris water maze were paired with each other in the tube test for social dominance. Separately, animals from cohort 2 were paired with one another on the tube test. The apparatus is a 30 cm long, 3.5 cm diameter clear acrylic tube with small acrylic funnels added to each end to facilitate entry into the tube. On two separate days before testing, each mouse was exposed to the tube, with progress through the tube resulting in the mouse being returned to the home cage. Mice that did not initially enter the tube were encouraged to run forward with a gentle pull of the tail. Some mice (n = 8 of 22 Ala56/Ala56 and n = 7 of 20 Gly56/Gly56 animals) did not progress through the tube when attempting habituation, either taking more than 1 min to exit the tube, freezing in the tube, or backing out. These mice were not entered into pairings for the tube test. For the tube test bouts, one SERT Ala56 and one SERT

Gly56 mouse of the same sex and age cohort but from different home cages were placed at the opposite ends of the tube and released. A subject was declared a “winner” when its opponent backed out of the tube. Each mouse was tested against four to five individuals from other cages. Trials were repeated with each mouse beginning at either end to avoid position bias, for a total of 72 bouts in male cohort 1 and 68 bouts in male cohort 2. Wins and losses for each genotype were analyzed by McNemar exact test.

Forced Swim Test

Mice received an i.p. injection of fluoxetine 10 mg/kg or saline solution. After a 30-min delay for the drug to take effect, mice were gently lowered into a transparent Plexiglas cylinder (20 cm diameter) filled halfway with water (25 ± 1 °C) for a 6-min session, as described previously (Boyce-Rustay and Holmes, 2006). The presence/ absence of immobility (cessation of limb movements except minor involuntary movements of the hind limbs) was scored by stopwatch from 120 to 360 s, which corresponds to the time period that is sensitive to treatment with serotonin reuptake inhibitors (Lucki et al., 2001).

8-OH-DPAT–Induced Hypothermia

A subset of 12 mice per genotype were used. Once every 10 min for 80 min, each mouse had its core body temperature measured with a rectal probe (no. 50314; Stoelting) connected to a BAT-12 thermometer (Physitemp Instruments). Immediately before the third temperature measurement, mice were administered a 10 mL/kg s.c. injection of 0.1 mg/kg 8-OH-DPAT (Sigma-Aldrich) in PBS solution (recorded as 0 min).

Subsequently, the same procedure was used with an equivalent volume of PBS solution only. Finally, the procedure was repeated with the administration of a 10 mL/kg s.c. injection of 0.1 mg/kg WAY-100635 (Sigma-Aldrich) 30 min before injection of 8-OH-DPAT. Data were analyzed by piece-wise mixed- effects linear model by using SAS software (SAS Institute) for the 0 to 30 min time points to evaluate the hypothermia response. Hypoactivity response was not analyzed as a result of the low level of baseline activity.

DOI-Induced Head Twitch Response

A subset of 10 mice per genotype were used for this experiment. Injections (i.p.) of 1.0 mg/kg DOI (Sigma) in PBS solution were administered in a volume of 10 mL/kg. Each mouse was placed in a large glass beaker containing bedding 34 min after injection, and two research assistants who were blind to genotype independently counted head twitches over a 15-min period. More than one week later, the same mice were tested after pretreatment with 10 mL/kg of 0.25 mg/kg M-100907 (gift from Marion Merrell Dow) 17 min before injection with DOI. Finally, mice were tested for head twitch response to PBS solution alone.

Rotarod

Mice were run on an accelerating rotarod (Ugo Basile) on three consecutive days to assess motor learning. On each day, the mice underwent three trials on the rotarod with a 1-min break between trials. Each trial consisted of a maximum of 10 min, with rotation accelerating from four to 40 revolutions per minute.

Home Cage Monitoring

To evaluate possible repetitive behavior, individual mice of each genotype were video-recorded alone in their home cage for 24 h while maintaining their 12 h/12 h light/ dark schedule (Steele et al., 2007). Automated video analysis was conducted by using HomeCageScan (Clever Sys) to index time spent performing individual behaviors. The resulting data were condensed into 10 individual behaviors: awaken/sleep, chew/eat/drink, rear, groom, hang, remain low, sniff, stretch, twitch, and walk. To normalize distributions for analysis by two-way repeated-measures ANOVA, data were log10-transformed. Bouts of hanging behavior were defined as distinct periods of hanging separated by nonhanging behaviors. The number of bouts per animal was also log10-transformed before a t-test was performed.

Ultrasonic Vocalization

Progeny of heterozygous SERT Ala56/Gly56 pairs at postnatal day 7 were used to measure stress-induced communication. Pups were removed from their cage and placed in a Styrofoam chamber with bedding. Ultrasonic vocalizations were measured for 5 min using a Condenser ultrasound microphone (Avisoft-Bioacoustics, Berlin, Germany) and Avisoft SASLab Pro software (Avisoft-Bioacoustics, Berlin, Germany). Thresholds were set to detect only small frequency-modulated vocalizations within a 250-kHz range lasting at least 5 ms and occurring at least 20 ms apart.

Pup Temperature Measurement

Progeny of heterozygous SERT Ala56/Gly56 pairs at postnatal day 7 were used to measure body temperature. Pups were removed from their cage and placed in a Styrofoam chamber with bedding. After 5 min, rectal temperatures were measured by using a monochannel rodent thermometer (model BIO-TK885; eb Instruments) and rectal probe (model BIO-SEB BRET-3; eb Instruments).

Statistical Analysis

Two-tailed, unpaired Student t-test or two-way, repeated-measures ANOVA with Bonferroni post-tests were used to analyze the primary data, except where noted for linear or curve analyses. Specific statistical analyses for each data set are described in results or in the figure legends.

Results

As predicted from studies of SERT Ala56 transfected cells (Prasad et al., 2009; Prasad et al., 2005; Sutcliffe et al., 2005), midbrain SERT protein levels in Ala56 mice were found to be identical to those of WT, Gly56 littermate controls (Supplemental Fig. 1A), results that are paralleled by the results of antagonist binding (Supplemental Fig. 1B) and immunohistochemical studies (Supplemental Fig. 2). SERT proteins exhibit significant posttranslational regulation (Steiner et al., 2008), including Ser/Thr phosphorylation that involves PKG and p38 MAPK-linked pathways (Ramamoorthy et al., 2007; Samuvel et al., 2005). Consistent with our findings in transfected cells, we found phosphorylation of SERT Ala56 to be significantly elevated in midbrain

synaptosomes under basal conditions (P = 0.0002; Fig. 1A). Moreover, we found that activation of PKG with 8-Bromo-cGMP (8-Br-cGMP) fails to increase phosphorylation of SERT Ala56, whereas a robust increase in phosphorylation is observed for WT SERT (P = 0.0013; Fig. 1B). Basal SERT phosphorylation is dependent on p38 MAPK activity (Samuvel et al., 2005), and PKG activation leads to a p38 MAPK-dependent increase in SERT activity (Zhu et al., 2004). The gain of SERT activity following activation of p38 MAPK is paralleled by an increased affinity for 5-HT that can support an enhanced rate of transport at low 5-HT concentrations (Prasad et al., 2009; Prasad et al., 2005). When we incubated synaptosomes with the p38 MAPK inhibitor PD169316, we found significant reductions in basal phosphorylation of SERT Gly56 mice (P = 0.018; Fig. 1C). Importantly, the inhibitor also normalized the difference in phosphorylation between the WT and mutant transporters. These findings suggest that constitutive phosphorylation of SERT Ala56 precludes the flexibility exhibited by WT SERT to move between low and high activity states in parallel with changes in 5-HT release.

To complement our *ex vivo* phosphorylation studies and determine whether SERT Ala56 mice exhibit constitutively enhanced SERT activity in vivo, we monitored hippocampal 5-HT clearance by *in vivo* chronoamperometry (Daws et al., 1997). In these studies, we observed a significant increase in the rate of 5-HT clearance for Ala56 animals vs. WT littermates (P < 0.0001; Fig. 1D and Supplemental Fig. 3). Paralleling our findings in synaptosomes, we observed a significant increase in 5-HT clearance following infusion of 8-Br-cGMP in the WT animals but no significant response in SERT Ala56 animals (P = 0.022 and P = 0.009 for time to clear 20% and 80% of maximum 5-HT signal, respectively; Fig. 1E). Despite the significant increase in 5-HT clearance, no

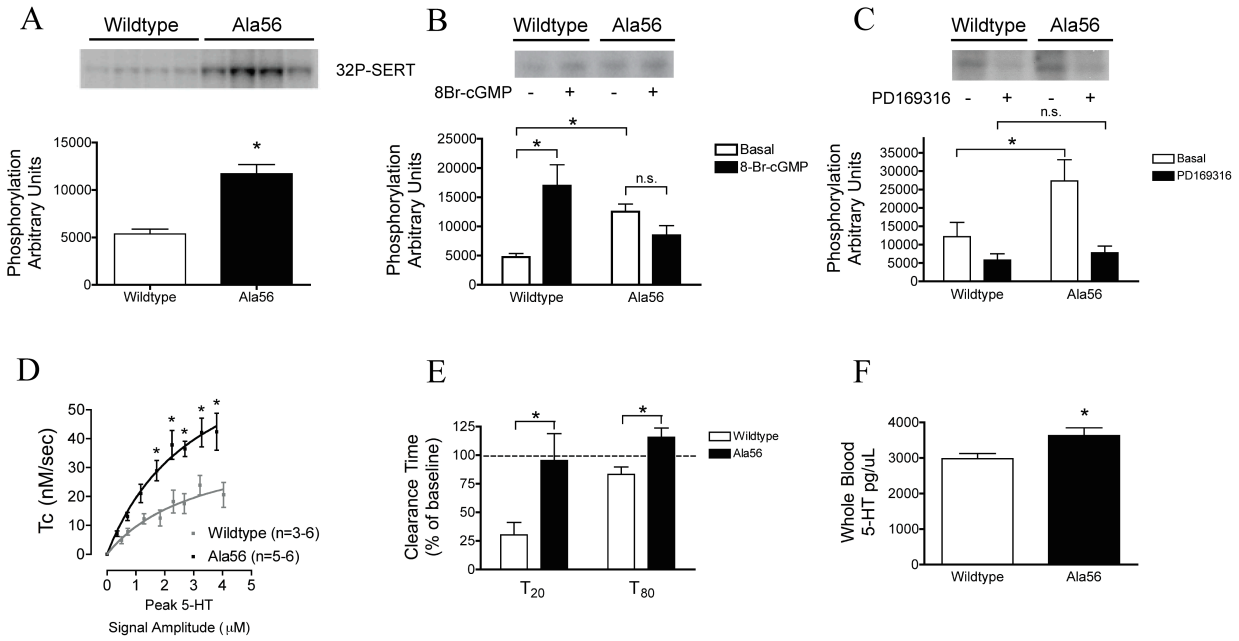

Figure 1. **Dysregulated SERT phosphorylation, increased 5-HT uptake, and hyperserotonemia in SERT Ala56 mice**. **(A)** Representative gel and cumulative graph of basal phosphorylation of SERT [Bartlett test statistic, 26.49, showing unequal variances ($P < 0.0001$); therefore, nonparametric Mann–Whitney test was used, U = 6.00, $P = 0.0002$, n = 12 per genotype]. **(B)** Representative gel and cumulative graph of 8-Br-cGMP–induced phosphorylation (two-way RM ANOVA interaction of cGMP treatment by genotype, F = 17.51, $P = 0.0013$; Bonferroni post-test in WT for cGMP treatment, t = 3.66, $P < 0.01$; Bonferroni post-test in Ala56 for cGMP, t = 2.26, $P > 0.05$; WT, n = 7; Ala56, n = 7). **(C)** Representative gel and cumulative graph of PD169316 inhibition of phosphorylation (two-way RM ANOVA interaction of PD169316 treatment by genotype, F = 8.815, P = 0.018; Bonferroni post-test of genotype difference in basal condition, t = 4.83, P < 0.01; Bonferroni post-test of genotype difference after PD169316 treatment, t = 0.63, $P > 0.05$; WT, n = 5; Ala56, n = 5). **(D)** 5-HT clearance rates in the CA3 region of the hippocampus as a function of increasing extracellular 5-HT concentrations. Clearance of 5-HT was significantly faster in Ala56 mice than that in WT controls (main effect genotype, $F_{1,73} = 64.69$, $P < 0.0001$; main effect 5-HT concentration, $F_{7,73} = 15.86$, $P < 0.0001$, two-way ANOVA with Bonferroni post hoc comparisons). Kinetic analysis reveals an approximate twofold increase in the apparent V_{max} for 5-HT clearance (t = 7.248, $P < 0.0001$; Ala56, 82 ± 20 nM/s vs. WT, 41 ± 15 nM/s) with no change in apparent transporter affinity (K_T) (corrected for volume fraction; Ala56, 64 ± 42 nM vs. WT, 64 ± 28 nM). **(E)** Time to clear 20% (T_{20}) and 80% (T_{80}) of the peak 5-HT signal amplitude 10 min after application of 0.5 pmol of 8-Br-cGMP, normalized to baseline 5-HT clearance. 8-Br-cGMP significantly shortened both T_{20} and T_{80} for 5-HT clearance in WT mice but was without effect in Ala56 mice (T_{20}, t = 2.65, P = 0.022; T_{80}: t = 3.195, $P = 0.009$; WT, n = 7; Ala56 n = 6). **(F)** HPLC measurement of 5-HT in whole blood. Unpaired t-test revealed a significant increase in whole blood 5-HT in the Ala56 animals compared with WT controls (t = 2.55, $P = 0.02$; WT, n = 11; Ala56, n = 9).

change was observed in midbrain or forebrain tissue 5-HT levels (Supplemental Fig. 4A&B). In contrast, in whole blood, in which 5-HT is sequestered by platelets that lack the capability to offset 5-HT accumulation with decreased 5-HT synthesis, SERT Ala56 mice exhibited significantly increased 5-HT levels relative to WT littermates (P = 0.02; Fig. 1F).

Genetic or pharmacological reductions in SERT activity produce diminished sensitivity of multiple 5-HT receptors (Fox et al., 2007). Therefore, we hypothesized that increased CNS 5-HT clearance could lead to decreased synaptic 5-HT availability and a compensatory increase in 5-HT receptor sensitivity. Consistent with this idea, enhanced 5-HT receptor sensitivity occurs in mice overexpressing SERT (Jennings et al., 2008). To explore this hypothesis in our mice, we first examined the sensitivity of animals to the 5-$HT_{2A/2C}$ receptor agonist 1-(2,5-dimethoxy-4-iodophenyl)-2-aminopropane (DOI), which produces a stereotyped head twitch response mediated by postsynaptic, cortical 5-HT_{2A} receptors (Willins and Meltzer, 1997). We observed a significantly elevated head twitch response in SERT Ala56 mice compared with WT littermate controls ($P < 0.01$; Fig. 2A). Next, we treated animals with the 5-$HT_{1A/7}$ agonist 8-hydroxy-2-(di-n-propylamino)-tetraline (8-OH-DPAT), which leads to hypothermia in mice, mediated by 5-HT_{1A} autoreceptors located on raphe 5-HT neurons (Rusyniak et al., 2007). As with DOI studies, SERT Ala56 mice displayed a significantly increased sensitivity to 8-OH-DPAT–induced hypothermia compared with WT controls ($P < 0.0001$; Fig. 2B).

To establish a physiological consequence of altered 5-HT receptor signaling in SERT Ala56 mice, we used loose-patch recordings of dorsal raphe 5-HT neurons in midbrain slices to examine basal firing rates and $5HT_{1A}$-mediated suppression of raphe

neuron excitability. Location of recordings was first established by using ePET-1:EYFP transgenic mice (Scott et al., 2005), centering on neurons of the medial division of the dorsal raphe. Under basal conditions, we observed a decrease in the firing rate of these neurons in SERT Ala56 brain slices (P = 0.0036; Fig. 2C), potentially arising from increased firing suppression by inhibitory 5-HT_{1A} autoreceptors (Wischmeyer and Karschin, 1996). Consistent with this hypothesis, dose–response studies of raphe neuron inhibition produced by bath-applied 5-HT revealed an enhanced inhibitory potency of bath-applied 5-HT (P < 0.0001; Fig. 2D).

Impaired social communication is often the first sign of ASD (Landa et al., 2007). To obtain a measure of early social communication, we measured ultrasonic vocalizations in pups that were separated from their dam at postnatal day 7. We observed a twofold decrease in vocalizations in SERT Ala56 pups in contrast to littermate controls (P = 0.015; Fig. 2G). As adults, SERT Ala56 and WT littermates exhibit a low baseline level of ambulatory activity in novel environments (Supplemental Fig. 6A–C), typical of 129S substrains (Moy et al., 2009; Moy et al., 2007). Thus, in analyses of adult animals that are dependent upon exploratory behavior, we included only data from mice with sufficient activity levels to allow a valid comparison between time spent in different arms or chambers (Supplemental Fig. 5B&C). In these studies, we observed no differences in anxiety-like behavior on the elevated plus-maze among mice with more than four arm entries (Supplemental Fig. 6D–F; pooled results from active and inactive animals are shown in Supplemental Fig. 6G). In cognitive or behavioral assays dependent on forced movement, including the Morris water maze test of spatial learning (Supplemental Fig. 7A–C), the rotarod test (Supplemental Fig. 6D),

and the forced swim test (Supplemental Fig. 6E), no significant differences were observed. However, when we tested SERT Ala56 mice for potential social interaction deficits in the three-chamber test of sociability (Moy et al., 2007; Yang et al., 2009), these animals, unlike their WT littermates, failed to demonstrate preference for another mouse vs. an inanimate object (Fig. 2E; pooled results from active and inactive animals are shown in Supplemental Fig. 6H).

To evaluate adult social interaction in a task that does not require high levels of ambulatory activity, we implemented the tube test of social dominance (Spencer et al., 2005). Mouse models of other disorders that display ASD traits, including Rett and Fragile X syndromes (Moretti et al., 2005; Spencer et al., 2005), show altered behavior on this task. After being trained to progress forward through an empty tube to be returned to their home cage, mice encounter an unfamiliar mouse that has entered from the opposite end of the tube. In these experiments, we found that SERT Ala56 animals more often withdrew from the tube upon encountering an age- and sex-matched WT littermate control ($P < 0.0001$; Fig. 2F).

In our studies that identified multiple, gain-of-function SERT variants in ASD subjects, we found the SERT Ala56 variant to be associated with rigid-compulsive behavior and sensory aversion in ASD (Sutcliffe et al., 2005). Several tests of sensorimotor function display deficits in subjects with ASD, including prepulse inhibition (Perry et al., 2007), a sensorimotor gating test that can be applied in mice. In a comparison with WT littermate controls, SERT Ala56 mice displayed a genotype by prepulse amplitude interaction effect on acoustic startle amplitude and prepulse inhibition of startle, reflecting an increased startle response at baseline that attenuated

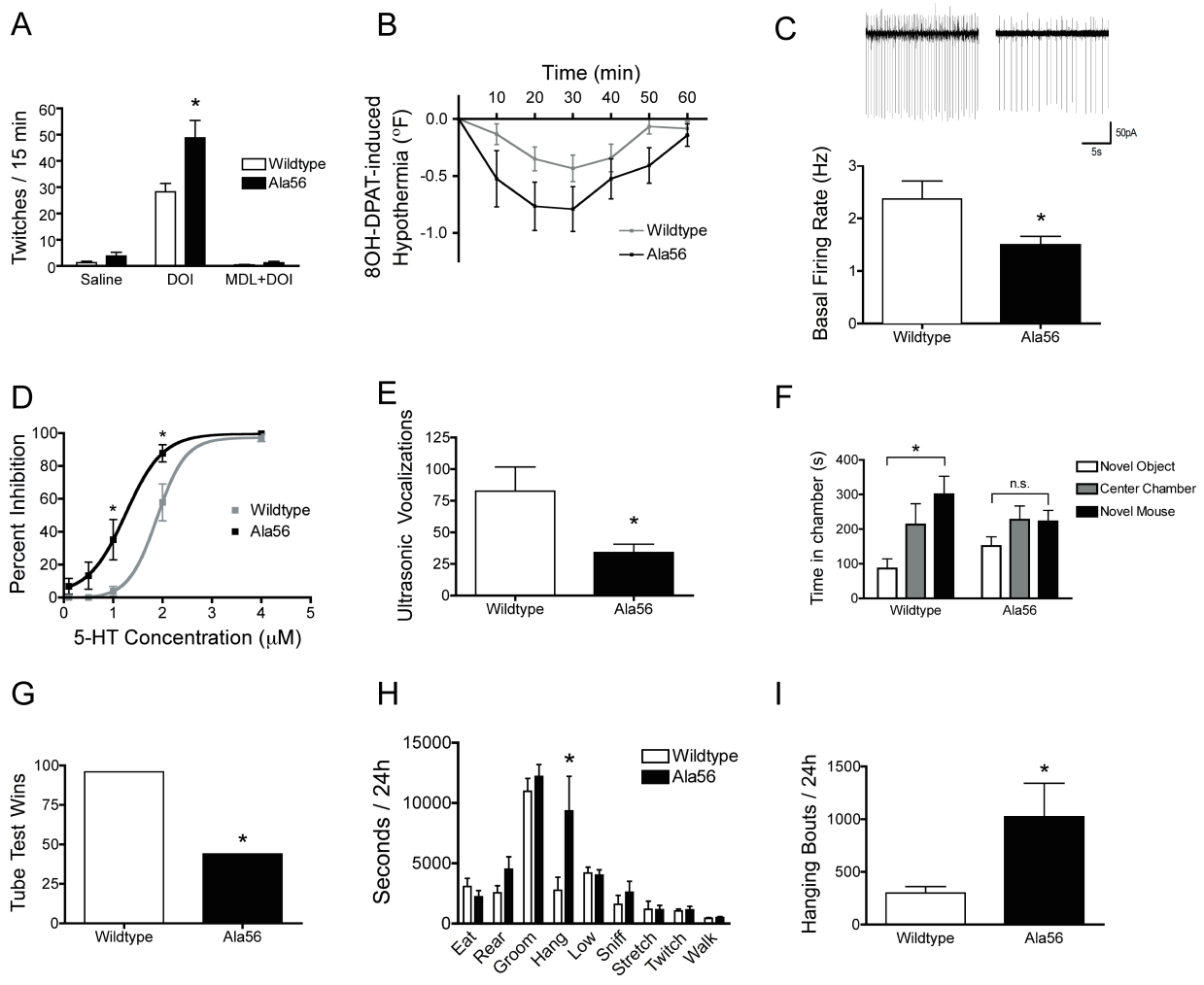

Figure 2. Increased receptor sensitivity and altered social, communication, and repetitive behavior in SERT Ala56 mice. (A) Head twitches recorded by two observers blind to genotype over 15 min following injection of saline solution, the 5-HT_2 agonist DOI, or the specific 5-HT_{2A} antagonist M-100907 followed by DOI. Two-way RM ANOVA revealed a significant genotype-drug interaction (F = 6.88, *P* = 0.0029, n = 10 per genotype), with a significant Bonferroni posttest result only for the difference between WT and SERT Ala56 animals in the DOI condition (*P* < 0.01). **(B)** Change in rectal temperature from baseline after administration of the 5-$HT_{1A/7}$ receptor agonist 8-OH-DPAT. Piecewise mixed linear model analysis revealed a significant genotype-drug–time interaction over the 30 min from baseline to maximal hypothermia response ($F_{1,177}$ *P* < 0.0001, n = 12 per genotype), reflecting a steeper slope in the SERT Ala56 animals compared with the WT controls. **(C)** Example traces with basal firing rates are shown for cell-attached extracellular recordings of dorsal raphe neurons in midbrain slices (n = 16 per genotype). Unpaired t test with Welch correction for unequal variances (F test to compare variances, $F_{15,15}$ = 4.345, *P* = 0.0036) revealed a significant decrease in firing rate in the Ala56 animals compared with the WT controls (t = 2.92, *P* = 0.032). **(D)** Percent inhibition of firing of dorsal raphe neurons as a function of varying, bath-applied 5-HT concentration. Curve fit analysis against log(5-HT concentration) with variable slope reveals a significant increase in sensitivity to inhibition of firing by 5-HT in the Ala56 animals compared with the WT controls ($F_{2,6}$ = 292.3, *P* < 0.0001). **(E)** Pup vocalizations upon separation from the dam for 5 min at postnatal day 7. Mann–Whitney test revealed a significant decrease in ultrasonic vocalizations in the SERT Ala56 animals in contrast with WT littermate controls (U = 85.5, *P* = 0.015; WT, n = 15; Ala56, n = 22). **(F)** Time in each chamber of the three-chamber Crawley sociability test is shown.

Animals with four or fewer total entries were excluded from the analysis as a result of inactivity. Two-way RM ANOVA revealed a main effect for chamber ($F = 23.25$, $P = 0.0006$) and a trend for an interaction between genotype and stimulus ($F = 3.92$, $P = 0.058$; WT, n = 11; Ala56, n = 17). Bonferroni posttest revealed a significant preference for the social chamber in the WT ($P < 0.01$) but not the SERT Ala56 animals ($P > 0.05$). **(G)** Wins for male animals on the tube test. McNemar exact test revealed a significant decrease in wins in the SERT Ala56 animals in contrast with WT littermate controls ($P < 0.0001$, n = 140 pairings). **(H)** Time spent performing individual behaviors over 24 h in the home cage. Two-way RM ANOVA of log10(time) revealed a significant genotype effect ($F = 5.84$, $P = 0.027$, n = 10 per genotype), with Bonferroni posttest showing a significant genotype difference only for time spent hanging ($P < 0.05$). **(I)** Number of bouts of hanging behavior in 24 h in the home cage. t-test of log10(bouts) revealed a significant increase in bouts of hanging in Ala56 SERT animals in comparison with WT littermate controls ($t = 2.567$, $P = 0.019$), with a significant correlation between log10(time) and log10(bouts) (Pearson $R = 0.749$, $P < 0.001$).

with increasing prepulse amplitudes (Supplemental Fig. 7A&B). To assess spontaneous repetitive behavior, we performed noninvasive, automated monitoring of animals in the home cage. Although many behaviors were found to be normal in these studies, we observed that SERT Ala56 mice spent a significantly greater time hanging from the wire cage lid relative to WT littermates ($P < 0.05$; Fig. 2H). Time hanging was significantly correlated with the number of bouts of hanging (Pearson R = 0.749, $P < 0.001$). Indeed, examination of recordings revealed that SERT Ala56 animals climbed up to hang briefly on the wire lid and then returned back to the floor of the cage, repeating this behavior an average of approximately 1,000 times over a 24 h recording period ($P = 0.019$; Fig. 2I). Other potential repetitive behaviors, including grooming, were not found in the home cage (Fig. 2H).

Discussion

These studies describe biochemical, physiological and behavioral traits that derive from the conversion of a single amino acid, Gly56, in SERT. Although conversion of Gly to Ala is a relatively minor change of structure, the SERT N terminus supports multiple SERT protein associations that may be impacted (Binda et al., 2006; Ciccone et al., 2008; Muller et al., 2006; Steiner et al., 2008). In this regard, SERT associates with proteins that influence the transporter's phosphorylation state, including the catalytic subunit of the Ser/Thr phosphatase PP2A (Bauman et al., 2000) and PKG1 (Steiner et al., 2009); although sites supporting these associations have not been defined. As the Ala56 variant does not create or alter a canonical phosphorylation site, we suspect that the alteration modifies the secondary structure of the N terminus to

permit enhanced access of one or more kinases (or restricted access of a protein phosphatase) to either the N terminus itself or a nearby cytoplasmic phosphorylation site. The SERT N terminus is directly connected to transmembrane domain 1, a domain that participates in 5-HT binding during the translocation process (Adkins et al., 2001; Yamashita et al., 2005). We hypothesize therefore that SERT Ala56-induced changes in N-terminal structure, protein associations, or phosphorylation, lock the transporter in a high-affinity conformation for 5-HT. Such an effect could lead to diminished availability of 5-HT for signaling and effectively eliminate the flexibility needed for SERT activity to track changes in 5-HT release. As proper control of 5-HT availability is vital to normal brain development (Gaspar et al., 2003), constitutively diminished 5-HT availability could lead to alterations in brain wiring and enduring changes in behavior.

The pattern of alterations in whole blood 5-HT levels, midbrain 5-HT neuron firing, and receptor sensitivities in the SERT Ala56 mouse reflects homeostatic changes in response to the primary change in SERT. Hyperserotonemia in the Ala56 mouse is consistent with the role of SERT in platelet 5-HT uptake and with prior studies showing that mice lacking SERT show essentially no whole blood 5-HT (Carneiro et al., 2008; Chen et al., 2001). Although no changes were found in brain tissue 5-HT levels in the SERT Ala56 mice, we suspect that tryptophan hydroxylase activity can be readily modified to reduce 5-HT biosynthetic capacity. Platelets lack this mechanism of homeostatic control, as they do not synthesize 5-HT but rather accumulate 5-HT released by duodenal enterochromaffin cells as they circulate through the gut (Chen et al., 2001). Moreover, tissue levels are a poor correlate of the synaptic availability of 5-HT, which likely depends more on smaller, readily releasable pools of neurotransmitter

and the inherent excitability of 5-HT neurons. Our findings of altered basal firing of raphe neurons *in vitro* and increased sensitivity of SERT Ala56 animals to challenge with $5HT_{1A}$ and $5HT_{2A}$ receptor agonists provides critical evidence that the changes seen in 5-HT clearance translate into behaviorally relevant changes in 5-HT signaling.

Substantial ethological differences exist between mice and humans, and scientists have, to date, generated only a few mouse models derived from gene variants identified in ASD (Etherton et al., 2009; Jamain et al., 2008; Kwon et al., 2006; Peca et al., 2011; Tabuchi et al., 2007). It is thus not possible to assert that a particular set of behavioral abnormalities directly models ASD in a mouse. We believe that, at this time, it is more reasonable to identify how genetic variation impacts mouse behavior, with the goal of identifying underlying changes in brain function that may be conserved in man and which can promote an understanding of the deficits arising in ASD. Given that SERT Ala56 represents a susceptibility variant, rather than a highly penetrant, monogenic cause of ASD (Sakurai et al., 2008; Sutcliffe et al., 2005), we do not expect animals expressing the variant to model all aspects of ASD. The impact of susceptibility variants is expected to vary depending on the presence of other genetic or environmental factors. Thus, the biochemical, physiological, and behavioral changes seen in an animal model of a susceptibility variant could offer many, or few, parallels to the human disorder. Further, individuals with ASD show considerable heterogeneity in clinical symptoms and genetic susceptibility, and an animal model of a susceptibility variant could therefore show some features that arise in only a subset of individuals (Silverman et al., 2010). Further research is needed to understand how other genetic or environmental factors modulate the phenotypes that we observed in the SERT Ala56

mice, as well as the interaction between this variant and other risk factors in individuals with ASD.

We find potential parallels of ASD-associated deficits in the SERT Ala56 mice. ASD is a disorder of pediatric onset. The decrease in ultrasonic vocalizations we observe in SERT Ala56 pups suggests an early emergence of the impact of 5-HT on the capacity or drive for communication. Social interaction deficits in ASD persist into adulthood. The tube test represents an ethologically valid mouse social interaction with a binary outcome that may be particularly sensitive to changes in social proficiency (Moretti et al., 2005). Interestingly, Duvall and colleagues identified a male-predominant, quantitative trait locus for social responsiveness in multiplex ASD families on chromosome 17q, including the *SLC6A4* gene region (Duvall et al., 2007). Consistent with this, we observed a lack of preference by adult SERT Ala56 mice for a social stimulus in the three-chamber test. Finally, SERT Ala56 has been associated with sensory aversion in ASD subjects (Sutcliffe et al., 2005). Although we observed only a modest enhancement in the startle response during prepulse inhibition tests, more sensitive studies are needed that examine the physiological properties of the sensory fields of mice and the ability of animals to integrate sensory information as these functions are known to be under the influence of 5-HT during development and in the adult (Bonnin et al., 2007; Jitsuki et al., 2011; Salichon et al., 2001).

Rigid-compulsive behavior is significantly elevated in SERT Ala56 carriers and in a combined group comprising SERT Ala56 carriers and other carriers of rare, hyperfunctional SERT coding variants (Sutcliffe et al., 2005). It is difficult to predict how a genetic determinant of rigid-compulsive behavior in humans will manifest in an animal

model. The repetitive bouts of hanging from the wire cage lid we observe in these mice may represent a novel parallel of the repetitive, nonfunctional routines that are common in ASD, although other interpretations are possible. Importantly, the repetitive hanging phenotype was identified in the context of many normal behaviors and in the animals' home cage, suggesting that we detected a spontaneous, rather than experimentally induced, repetitive behavior.

The biochemical, physiological, and behavioral results in the SERT Ala56 animals also have some important limitations. First, it is not clear how the specific change from Gly56 to Ala56 leads to increased p38-MAPK–sensitive basal phosphorylation, whether by way of altered SERT tertiary structure or disrupted protein–protein interactions in the N-terminal domain where Gly56 is expressed. Further work is needed to understand these mechanisms, including identifying the residues at which phosphorylation occurs and the kinases or phosphatases that act at these residues. Second, we studied only homozygous animals to maximize our ability to detect phenotypes. Future studies will be needed to understand whether similar biochemical, physiological, and behavioral phenotypes are found in animals with only one copy of the SERT Ala56 variant. Third, the low activity seen in some animals in the elevated plus-maze and three-chamber sociability test limit the interpretation of these data. This low activity level appears to be a result of the inbred strain background (Moy et al., 2009; Moy et al., 2007) and does not differ by genotype. When coupled with the ultrasonic vocalization and tube test results, however, the overall data are consistent with a change in social function. Further experiments conducted on other inbred strain backgrounds may clarify the lack of preference for social stimuli in the SERT Ala56

mice. Finally, in contrast with increased grooming behavior observed in some other mouse models of ASD-associated genetic variation (Etherton et al., 2009; Peca et al., 2011; Penagarikano et al., 2011), the increased climbing/hanging behavior we observed in the SERT Ala56 mice is a repetitive behavior that has not previously been described to our knowledge. The difference in the pattern of observed repetitive behavior in the SERT Ala56 mice, in contrast to other models of ASD susceptibility, could reflect the fact that expression of this susceptibility variant is limited to a single, neurochemically defined pathway. Further experiments will be necessary to connect this behavior to changes in underlying circuits.

As autism is a neurodevelopmental disorder, it will be important to now investigate the temporal profile and developmental requirements for constitutively elevated 5-HT transport in the changes we observe in the SERT Ala56 mice. Excess 5-HT clearance during early stages of development could influence neuronal migration, axonal projections, and synapse development in these mice, as indicated by other developmental manipulations that target 5-HT signaling (Gaspar et al., 2003). Our constitutively expressed variant also does not speak to the important sites of expression of SERT Ala56 in dictating phenotypes. SERT is not only expressed in the developing and mature brain but also in gut, platelet, adrenal gland, immune cells, pancreas, and lung. Moreover, Bonnin and coworkers have shown that the placenta, which expresses high levels of SERT (Prasad et al., 1996; Ramamoorthy et al., 1993), is a source of forebrain 5-HT during gestation and is important for normal axonal trajectories (Bonnin et al., 2011). Modulating 5-HT levels or transporter function to assess the reversibility of these phenotypes could yield insight into the developmental impact of increased and

dysregulated SERT function. Ultimately, studies that allow for temporal and spatial control of the SERT Ala56 variant are needed to answer these questions. Finally, ASD is a disorder with few therapies and none that consistently reverse major deficits. We believe that the SERT Ala56 model offers an opportunity to pursue genetic and pharmacological studies that can both probe ASD mechanisms and possibly identify novel therapeutic targets.

CHAPTER 3

MATERNAL SERT ALA56 GENOTYPE EFFECTS ON FETAL DEVELOPMENT

Christopher L. Muller, Tiffany D. Rogers, Carl G. Forsberg, Elizabeth Keller, Nick Goeden, George M. Anderson, Alexandre Bonnin, Randy D. Blakely, Jeremy Veenstra-VanderWeele

Introduction

Disruptions in the 5-HT system have been implicated in ASD for little over half a century (Schain and Freedman, 1961), but a clear understanding of how 5-HT contributes to the pathophysiology of ASD remains elusive. Besides its role as a modulatory neurotransmitter in adulthood, 5-HT is now appreciated as a signaling molecule during neurodevelopment. Several serotonergic proteins are transiently expressed in the developing forebrain before the arrival of 5-HT innervation originating from the midbrain raphe nuclei (Bonnin et al., 2006; Gaspar et al., 2003). This suggests that exogenous sources of 5-HT may play a functional role in developmental processes. Most notably, it has been recently shown that the placenta can synthesize and deliver 5-HT to the fetal forebrain from maternally derived tryptophan (Bonnin et al., 2011). While disruptions in this novel placental 5-HT synthetic pathway may impact fetal neurodevelopment, it has yet to be examined in animal models of ASD.

Due to its primary role as a regulator of 5-HT homeostasis, SERT has been heavily scrutinized for a potential role in ASD (Cook and Leventhal, 1996). Linkage studies have implicated the 17q region harboring the SERT gene (McCauley et al.,

2004; Yonan et al., 2003), *SLC6A4*, with stronger linkage found in families with only affected males. While there is only modest evidence to connect common *SLC6A4* variation to ASD, there have been a number of rare gain-of-function SERT variants discovered in families with evidence of linkage (Sutcliffe et al., 2005). However, the most common of the rare variants, Gly56Ala, is also found in unaffected carriers (Sakurai et al., 2008; Sutcliffe et al., 2005), suggesting there are other genetic or environmental factors that modulate ASD risk. Interestingly, there is evidence that variants associated with psychiatric disorders may also exert their effects through changes in the prenatal environment in maternal carriers of risk alleles(Gleason et al., 2010).

In the current study, we evaluated whether maternal SERT genotype in 129S6/S4 SERT Gly56Ala mice could impact fetal neurodevelopment. We find maternal effects on the developmental trajectory of the 5-HT system in the fetal brain that are indicative of altered placental function. Furthermore, we find parallel changes in the development of TCAs, a known 5-HT sensitive brain structure (Bonnin et al., 2007; Cases et al., 1996). While maternal SERT genotype does not appear to significantly affect placental 5-HT synthesis, RNAseq data suggests that altered maternal SERT function may have broader effects on placental development. Collectively, these findings suggest that some ASD risk alleles may exert transgenerational effects on neurodevelopment through impaired maternal-fetal interactions.

Methods

Mice

SERT G56A mice used for experiments were maintained on the 129S6/S4 inbred strain background. Timed breeding pairs were composed of wildtype, heterozygous, and homozygous Ala56 dams mated with sires of matching genotypes (i.e. WT x WT, etc.), with presence of vaginal plug considered E0.5. For all breeder schemes, 4-6 litters were harvested per developmental time point analyzed. For wildtype and homozygous Ala56 breeders, 2-4 samples per litter were randomly chosen for HPLC and TPH1 activity assay analyses, and a single representative sample for each litter for all other assays. For heterozygous breeders, multiple wildtype and Ala56 samples, if present, were collected per litter to increase statistical power for HPLC, and a single pair of littermates was chosen for all other assays. Initial HPLC data at E18.5 indicated no gender effects (data not shown), so samples were collapsed into single genotype groups regardless of sex for all subsequent analyses.

High-Performance Liquid Chromatography with Fluorometric Detection

Placental and embryonic brain samples were collected from PBS-perfused dams at E14.5 and E18.5. Embryonic brains were dissected to isolate forebrain and mid/hindbrain tissue. All tissues were weighed, flash frozen, and stored at -80°C until HPLC analysis with fluorometric detection of 5-HT, TRP, and 5-HIAA as previously described (Anderson et al., 1987). Briefly, an internal standard solution containing N-methylserotonin, ascorbic acid and sodium metabisulfite was added to the samples. After samples were vortex mixed, perchloric acid was added to the samples, which were

mixed and then kept on ice for 10 min prior to centrifugation at 6000 x *g* for 5 min. The supernatant was removed and analyzed by HPLC with fluorometric detection. Serotonin was determined with intra- and inter-assay coefficients of variation of less than 5 and 10%, respectively. At E14.5, forebrain 5-HIAA measurements were below our detection limit. Also, placental 5-HIAA could not be reliably measured due to an interfering spectra peak.

RNA Isolation

RNA from fresh frozen placental tissue was isolated using Qiagen RNeasy Mini Kit with DNase I treatment per manufacturer's instructions. RNA quality and yield were assessed by NanoDrop spectrophotometer (Thermo Scientific). For downstream RNAseq applications, sample integrity was also evaluated by Agilent Bioanalyzer (Agilent Technologies), with all samples possessing RINs > 9.0.

RNA-Seq

Isolated RNA from E14.5 placental tissue underwent cDNA library preparation (Illumina Tru Seq Sample Prep Kit) and whole transcriptome sequencing (30M reads/sample, single-end 50bp reads) on the Illumina HiSeq 2500 platform at the Vanderbilt Technologies for Advanced Genomics (VANTAGE) core facilities. Three biological replicates were sequenced per experimental group, with each replicate consisting of two unique samples pooled together.

RNA-Seq Analysis

Sequencing reads were mapped to the mouse genome mm10 using TopHat-2.0.10 (Kim et al., 2013) and quantified by samtools-0.1.19 (Li et al., 2009) and HTSeq-0.5.4p5 (Anders et al., 2014). To further assess sample quality, we examined intrasample correlation of normalized counts of the top 1000 expressed genes in the placenta. While intrasample correlation coefficients were generally high ($r > .90$), one sample from the KI(HET) experimental group consistently fell below this threshold and was omitted from further analysis. Count-based differential expression analysis was performed using edgeR_3.4.2 (McCarthy et al., 2012), which implements general differential analyses based on the negative binomial model. Differential expression analyses were performed for: 1) KI(KI) vs. WT(WT), 2) KI(HET) vs. WT(HET), and 3) the interaction between dam and embryo genotypes. Differentially expressed genes (DEGs) ($P < .05$) were input into web-based bioinformatics tool, WebGestalt, for pathway analyses (Zhang et al., 2005).

Quantitative PCR

For quantitative PCR (qPCR) experiments, cDNA was generated using High Capacity cDNA Reverse Transcription Kit (Life Technologies) per manufacturer's instructions. qPCR was performed using *Tph1* (Mm00493794_m1) and *GusB* (Mm00446953_m1) TaqMan gene expression assays run on a 7900HT system (Life Technologies). All samples were run in duplicate with a reverse transcriptase negative control. Differential gene expression was calculated using the ΔΔCT method with *GusB* as the endogenous control.

TPH1 Activity Assay

TPH1 activity was assayed in *in vitro* placenta preparations as previously described (Bonnin et al., 2011) with slight modifications. Frozen placental tissue was homogenized in 350 µl of extraction buffer containing .05 M Tris-HCL buffer pH 7.5, 1 mM EGTA, and 1 mM DTT. Homogenates were centrifuged at 21,000 x *g* for 15 minutes at 4 °C, and supernatant was collected for activity assay and protein quantification (DC Protein Assay, Biorad). For the activity assay, 20 µl of supernatant (~70 µg of protein) was added to 80ul of a reaction master mix, resulting in the final concentration of the following components: .05 M Tris-HCL buffer pH7.5, 1 mM EGTA, 100 µM L-tryptophan, .05 mg/ml catalase, 100 µM tetrahydrobiopterin, 1 mM ferrous ammonium sulfate. For negative controls, reaction master mix only contained Tris-HCL buffer, EGTA, and catalase. After incubation at 37 °C for 30 minutes, 100 µl of termination buffer, consisting of .2 M perchloric acid and 100 µM EDTA, was added to the reaction solution, which was then incubated on ice for 15 minutes. After centrifugation at 21,000 x *g* for 15 minutes at 4°C, supernatant was collected and flash frozen for subsequent HPLC with electrochemical detection of 5-hydroxytryptophan (5-HTP), the primary readout of TPH1 activity in this assay.

Netrin-G1a Immunohistochemistry & Quantification

Embryos were harvested from timed-pregnant dams at E18.5 and collected brains were fixed overnight in 4% paraformaldehyde. After cyroprotection in 30% sucrose, brains were embedded and sectioned (40 µm) on a cryostat. Prior to primary antibody application, peroxidase-quenched sections were blocked in PBS containing

3% donkey serum and .1% Triton X-100. Sections were then incubated overnight with Netrin-G1a antibody (1:100, R&D systems), washed, and incubated with peroxidase-conjugated donkey anti-goat secondary antibody (1:800, Jackson Immunoresearch). Per manufacturer's instructions, tyramide signal amplification was used for fluorescein labeling (1:100, Perkin Elmer), and sections were counterstained with DAPI mounting medium (Vector Labs). Fluorescent images were taken with a Zeiss Axio Imager M2.

Using ImageJ software, measurements of TCA and cortical thickness were collected from matched rostral and caudal brain sections by a research assistant blind to sample genotype. In each brain section, TCA/cortex thickness was measured at three separate locations along the TCA distal-proximal axis.

Results

To evaluate maternal SERT genotype effects on fetal neurodevelopment, experimental samples were collected from wildtype, heterozygous, and homozygous SERT Ala56 dams bred with sires of matching genotype. Thus, our experimental groups consisted of wildtype embryos from heterozygous dams [WT(HET)], Ala56 embryos from heterozygous dams [KI(HET)], wildtype embryos from wildtype dams [WT(WT)], and Ala56 embryos from Ala56 dams [KI(KI)]. While analysis of WT(HET) and KI(HET) littermates assessed embryo genotype effects, WT(WT) and KI(KI) group comparisons evaluated the impact of maternal genotype.

Using HPLC, we measured forebrain, hindbrain, and placenta tissue levels of 5-HT at embryonic day (E) 14.5, a developmental time point when the placenta predominantly supplies 5-HT to the fetal forebrain. While WT(HET) and KI(HET)

littermates exhibited no genotype differences in 5-HT content in any of the tissues studied, forebrain 5-HT levels were significantly decreased in KI(KI) compared to WT(WT) (P = .029; Fig. 3B). Paralleling these findings, KI(KI) placentas also exhibited significant decreases in 5-HT levels (P = .019; Fig. 3A). There were no changes in TRP, 5-HIAA, or 5-HT turnover in our collective E14.5 tissue group comparisons (Supplemental Fig. 8,9).

Tissue HPLC measurements were repeated at E18.5, when innervation from the midbrain raphe nuclei is the primary source of 5-HT in the fetal forebrain. In contrast to E14.5, KI(KI) forebrain 5-HT levels were now indistinguishable from WT(WT) (Fig. 3E). However, while forebrain 5-HT normalized, KI(KI) placental 5-HT levels remained significantly decreased compared to WT(WT) (P = .031; Fig. 3D). In littermates from heterozygous dams, there were again no significant genotype differences in forebrain, hindbrain, and placental 5-HT levels. While we did observe a significant decrease in KI(HET) hindbrain 5-HIAA levels compared to WT(HET) at E18.5 (Supplemental Fig. 9E) no other HPLC measures differed in our genotype group comparisons of interest.

To examine potential downstream effects of altered fetal forebrain 5-HT levels at E14.5, we performed NetrinG1a immunostaining of TCAs, which are sensitive to changes in 5-HT signaling during neurodevelopment. While TCAs appeared grossly normal in all experimental groups at E18.5 (Fig. 4A&D) the normalized thickness of TCA trajectories was significantly increased in rostral brain regions of KI(KI) embryos compared to WT(WT) (P = .001; Fig. 5B). However, this phenotype was attenuated in

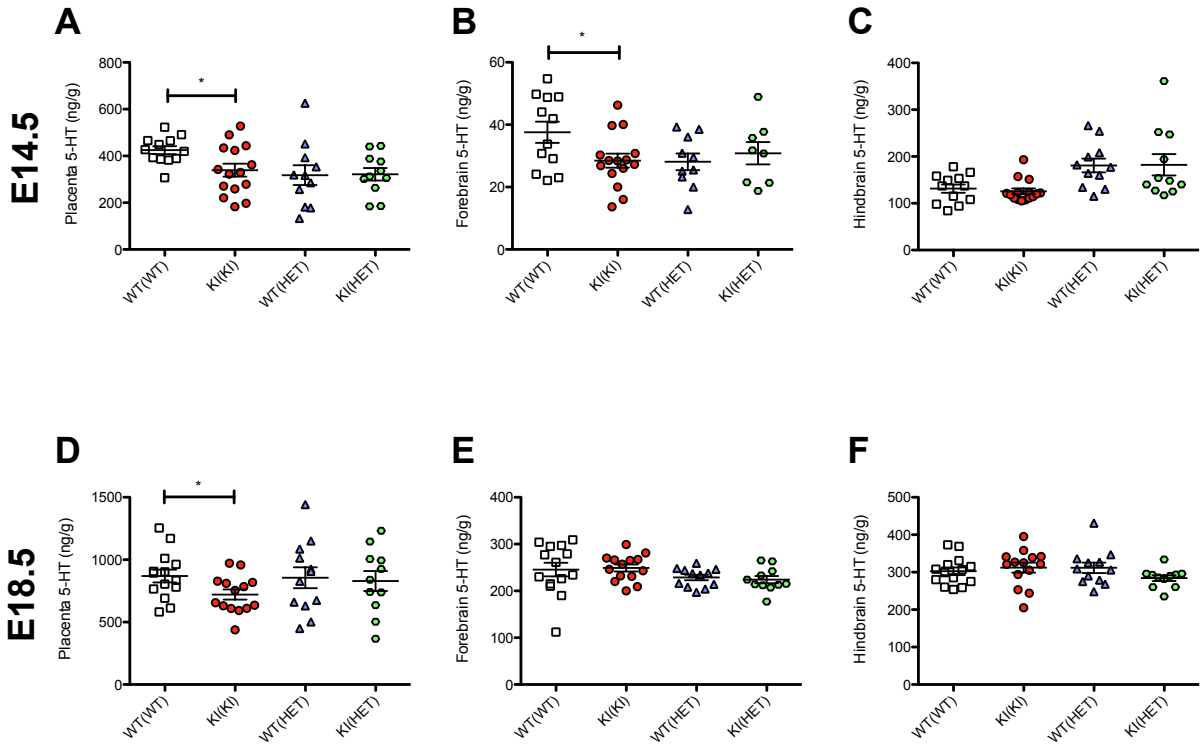

Figure 3. Examination of maternal and embryonic SERT Ala56 genotype effects on placenta and fetal brain 5-HT levels. At E14.5, 5-HT tissue levels were measured in **(A)** placenta, **(B)** forebrain, and **(C)** hindbrain collected from concepti of wildtype, heterozygous, and homozygous Ala56 dams. Unpaired t-tests revealed KI(KI) placental and forebrain 5-HT levels were decreased compared to WT(WT) (t = 2.493, *P* = .019; WT(WT) n = 12; KI(KI) n = 15; t = 2.316, *P* = .029; WT(WT) n = 12; KI(KI) n = 15, respectively). At E18.5, 5-HT tissue levels were once again measured in **(D)** placenta, **(E)** forebrain, and **(F)** hindbrain samples from our various breeder schemes. Unpaired t-test revealed KI(KI) placenta 5-HT levels were decreased compared to WT(WT) (t = 2.281, *P* = .031; WT(WT) n = 14; KI(KI) n = 14)

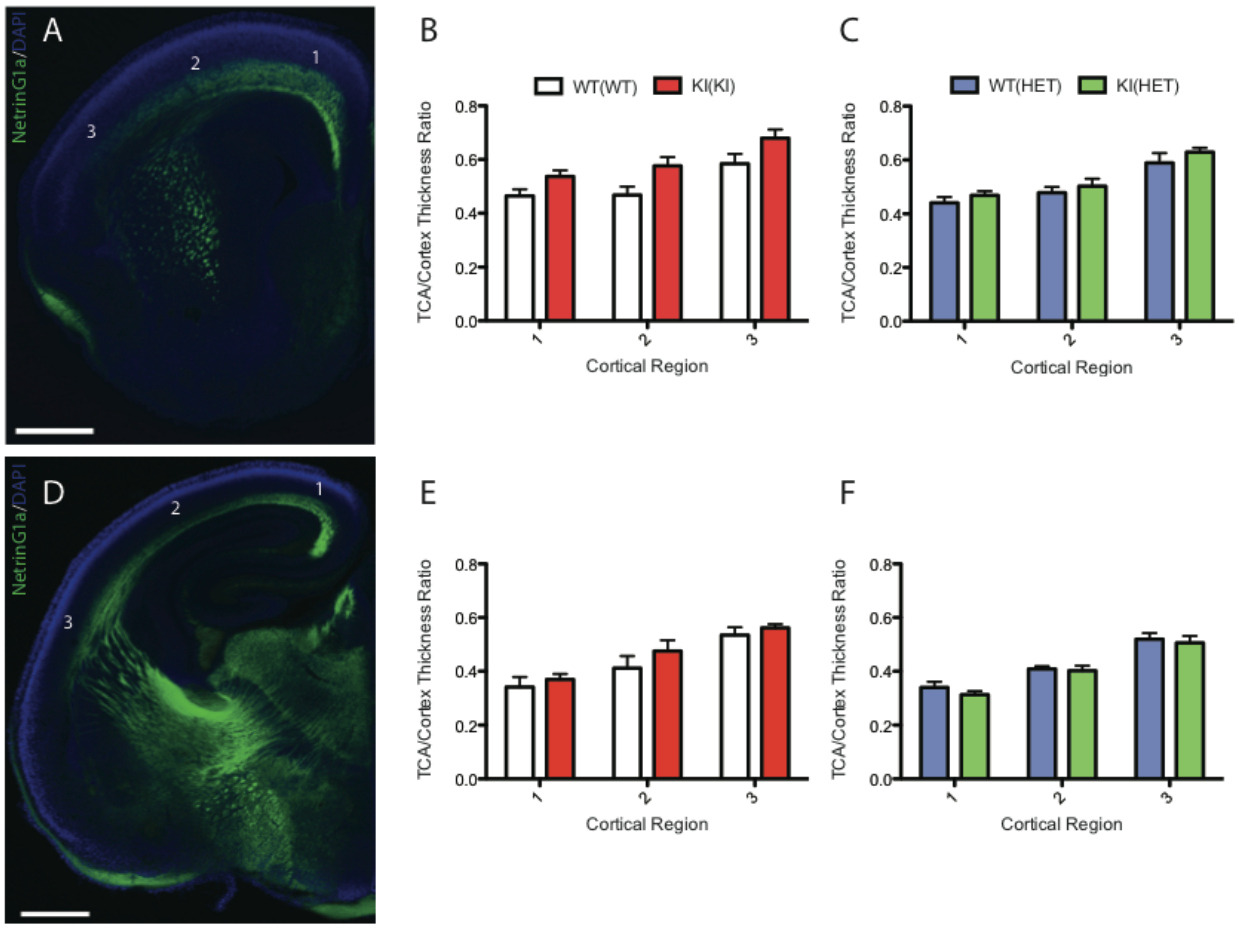

Figure 4. Examination of maternal and embryonic SERT Ala56 genotype effects on TCA trajectory thickness at E18.5. NetrinG1a immunostaining revealed no gross morphology changes in TCA development **(A)** and **(D)**. However, two-way ANOVA revealed that the TCA/Cortex thickness ratio in KI(KI) rostral brain sections **(B)** was significantly increased compared to WT(WT) (genotype main effect; $F_{1,24}$ = 13.64, *P* = .001). This phenotype was attenuated in KI(KI) caudal brain sections **(E)** (genotype main effect; $F_{1,24}$ = 2.19, *P* =.152). There were no significant genotype differences in TCA/Cortex thickness ratio between WT(HET) and KI(HET) littermates. White numbers in **(A)** and **(D)** indicate cortical regions measured along the TCA distal-proximal axis. Scale bar, 500 μm.

caudal brain regions (Fig. 4C). Similar to HPLC data, WT(HET) and KI(HET) littermates exhibited no genotype differences in normalized TCA trajectory thickness (Fig. 4E&F).

Decreased forebrain and placental 5-HT levels in E14.5 KI(KI) concepti may be the result of deficient placental synthesis of 5-HT. To evaluate this possibility, we examined tryptophan hydroxylase 1 (TPH1) activity using an *in vitro* placental preparation that utilizes HPLC measures of 5-hydroxytryptophan (5-HTP) as a readout of 5-HT neosynthesis. Interestingly, 5-HTP production was unchanged in KI(KI) E14.5 placentas compared to WT(WT) (Fig. 5A). Furthermore, no genotype differences were observed between WT(HET) and KI(HET). RT-PCR corroborated these findings, indicating no maternal or embryo genotype effects on placenta *Tph1* expression (Fig. 5B). Furthermore, altered KI(KI) placenta 5-HT levels were not due to changes in maternal TRP availability, as there were no changes in placenta TRP levels at E14.5 (Supplemental Fig 8A).

As an unbiased approach to examine changes in KI(KI) placenta physiology, we performed whole transcriptome RNA sequencing (RNAseq) on E14.5 placentas harvested from our various dam breeder schemes. We used two parallel approaches to analyze potential maternal effects on placental gene expression. First, we examined RNAseq data using a 2 x 2 ANOVA design, with dam genotype (homozygous KI or WT vs. heterozygous) and embryo genotype (KI vs. WT) as our variables of interest. Using this statistical design, a significant interaction effect highlights embryo genotype effects that are impacted by maternal genotype. While we discovered 411 differentially expressed genes (DEGs) with significant interaction effects ($P < .05$), high false

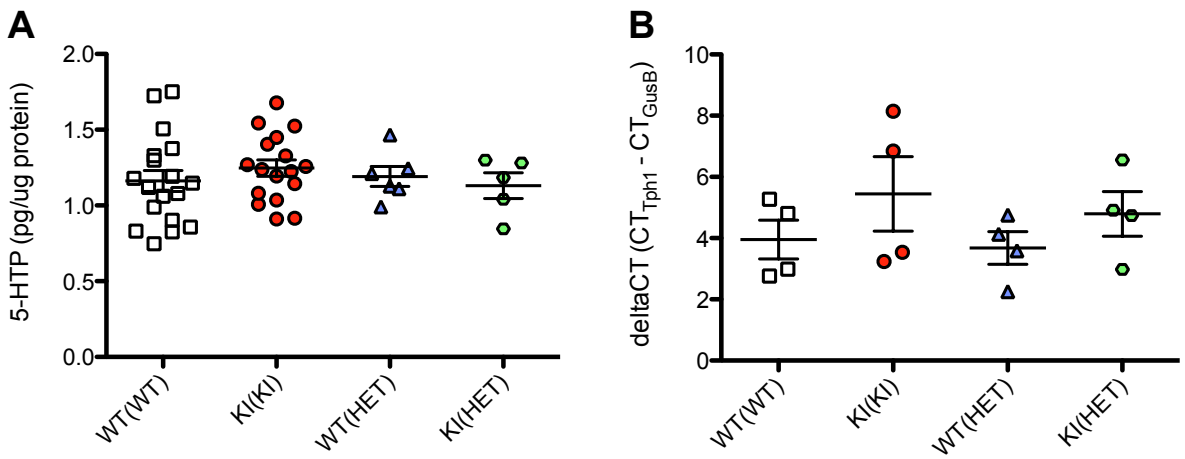

Figure 5. Examination of maternal and embryonic SERT Ala56 genotype effects on E14.5 placental TPH1 activity and *Tph1* expression. There were no significant maternal or embryo genotype effects found on TPH1 activity (i.e. 5-HTP neosynthesis) or *Tph1* expression as determined by unpaired t-tests of dam-embryo comparison groups of interest.

discovery rates (FDRs) for the dataset prevented us from identifying specific gene targets. To circumvent this limitation, we performed pathway analysis on the 411 DEGs to identify overarching molecular networks in the placenta that are impacted by maternal genotype. Both KEGG and WikiPathways analysis tools indicated a significant enrichment of genes in specific molecular pathways (Figure 6), with phagosome (KEGG adjP = .0002) and myometrial relaxation/contraction pathways (Wiki adjP = 3.07e-05) as top hits. Interestingly, both algorithms identified MAPK and cytokine signaling pathways as uniquely impacted in our interaction comparison (MAPK signaling: KEGG adjP=.0019, Wiki adjP=.0138; cytokine-cytokine receptor interaction: KEGG adJP = .0012; TGF beta signaling: Wiki adjP=.0207; chemokine signaling: Wiki adJ=.0326).

In a second approach to evaluate maternal effects on placental gene expression, we looked at the overlap between DEGs from the individual KI(KI) vs. WT(WT) and KI(HET) vs. WT(HET) group comparisons (Figure 7), identifying 264 DEGs that were uniquely altered in KI(KI) placentas. Similar to the 2 x 2 ANOVA statistical design, none of the 264 DEGs reached FDR thresholds to draw conclusions about individual genes. However, pathway analysis indicated a strongly significant enrichment of genes involved in complement and coagulation cascades (KEGG adjP = 5.38e-13, Wiki adjP = 8.34e-09). Moreover, genes documented in PPAR signaling pathways were also overrepresented (PPAR signaling: KEGG adjP = 0.0016, Wiki adjP = 0.0017).

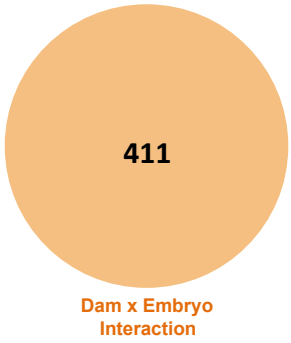

KEGG Pathway	Enrichment Statistics
Phagosome	C=176;O=13;E=2.49;R=5.21;rawP=1.52e-06;adjP=0.0002
Viral myocarditis	C=88;O=9;E=1.25;R=7.22;rawP=4.49e-06;adjP=0.0003
Cell adhesion molecules (CAMs)	C=149;O=11;E=2.11;R=5.21;rawP=9.72e-06;adjP=0.0004
Leishmaniasis	C=64;O=7;E=0.91;R=7.72;rawP=3.38e-05;adjP=0.0010
Cytokine-cytokine receptor interaction	C=245;O=13;E=3.47;R=3.74;rawP=5.30e-05;adjP=0.0012
MAPK signaling pathway	C=268;O=13;E=3.80;R=3.42;rawP=0.0001;adjP=0.0019
Rheumatoid arthritis	C=81;O=7;E=1.15;R=6.10;rawP=0.0002;adjP=0.0025
Type I diabetes mellitus	C=59;O=6;E=0.84;R=7.18;rawP=0.0002;adjP=0.0025
Hematopoietic cell lineage	C=82;O=7;E=1.16;R=6.02;rawP=0.0002;adjP=0.0025
Endocytosis	C=219;O=11;E=3.10;R=3.54;rawP=0.0003;adjP=0.0026

Wiki Pathway	Enrichment Statistics
Myometrial Relaxation and Contraction Pathways	C=158;O=13;E=2.24;R=5.81;rawP=4.45e-07;adjP=3.07e-05
Endochondral Ossification	C=67;O=8;E=0.95;R=8.43;rawP=4.77e-06;adjP=0.0002
MAPK signaling pathway	C=165;O=9;E=2.34;R=3.85;rawP=0.0006;adjP=0.0138
Prostaglandin Synthesis and Regulation	C=31;O=4;E=0.44;R=9.10;rawP=0.0009;adjP=0.0155
TGF Beta Signaling Pathway	C=59;O=5;E=0.84;R=5.98;rawP=0.0015;adjP=0.0207
G1 to S cell cycle control	C=65;O=5;E=0.92;R=5.43;rawP=0.0023;adjP=0.0265
Chemokine signaling pathway	C=184;O=8;E=2.61;R=3.07;rawP=0.0049;adjP=0.0326
cytochrome P450	C=44;O=4;E=0.62;R=6.41;rawP=0.0034;adjP=0.0326
Focal Adhesion	C=186;O=8;E=2.64;R=3.03;rawP=0.0052;adjP=0.0326
selenium	C=23;O=3;E=0.33;R=9.20;rawP=0.0041;adjP=0.0326

Figure 6. KEGG and Wiki Pathway analyses of 411 placental DEGs identified from dam x embryo genotype interaction analysis. Dam x embryo genotype interaction analysis identified 411 DEGs that exhibit maternal SERT Ala56 genotype effects. Top and bottom tables display top 10 statistically enriched pathways in KEGG and Wiki pathway analyses, respectively. Enrichment statistics description; number of reference genes in pathway category (C), number of DEGs in pathway category (O), expected number in category (E), ratio of enrichment (R), p-value from hypergeometric test (rawP), p-value adjusted for multiple comparisons (adjP).

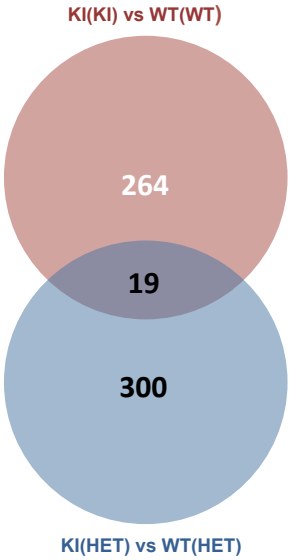

KEGG Pathway	Enrichment Statistics
Complement and coagulation cascades	C=76;O=14;E=0.69;R=20.27;rawP=7.69e-15;adjP=5.38e-13
Metabolic pathways	C=1175;O=29;E=10.68;R=2.72;rawP=1.19e-06;adjP=4.17e-05
Staphylococcus aureus infection	C=50;O=5;E=0.45;R=11.00;rawP=9.05e-05;adjP=0.0016
PPAR signaling pathway	C=80;O=6;E=0.73;R=8.25;rawP=9.11e-05;adjP=0.0016
Prion Diseases	C=35;O=4;E=0.32;R=12.58;rawP=0.0003;adjP=0.0042
Cell adhesion molecules (CAMs)	C=149;O=7;E=1.35;R=5.17;rawP=0.0004;adjP=0.0047
Glycerolipid metabolism	C=51;O=4;E=0.46;R=8.63;rawP=0.0012;adjP=0.0105
ECM-receptor interaction	C=86;O=5;E=0.78;R=6.40;rawP=0.0011;adjP=0.0105
Steroid hormone biosynthesis	C=55;O=4;E=0.50;R=8.00;rawP=0.0016;adjP=0.0112
Tight junction	C=136;O=6;E=1.24;R=4.85;rawP=0.0016;adjP=0.0112

Wiki Pathway	Enrichment Statistics
Complement and Coagulation Cascades	C=61;O=10;E=0.55;R=18.04;rawP=1.94e-10;adjP=8.34e-09
Blood Clotting Cascade	C=21;O=6;E=0.19;R=31.44;rawP=2.57e-08;adjP=5.53e-07
Statin Pathway	C=19;O=5;E=0.17;R=28.96;rawP=6.25e-07;adjP=8.96e-06
Matrix Metalloproteinases	C=29;O=4;E=0.26;R=15.18;rawP=0.0001;adjP=0.0011
PPAR signaling pathway	C=93;O=6;E=0.85;R=7.10;rawP=0.0002;adjP=0.0017
Myometrial Relaxation and Contraction Pathways	C=158;O=7;E=1.44;R=4.87;rawP=0.0006;adjP=0.0043
Triacylglyceride Synthesis	C=23;O=3;E=0.21;R=14.35;rawP=0.0011;adjP=0.0068
One Carbon Metabolism	C=39;O=3;E=0.35;R=8.46;rawP=0.0053;adjP=0.0285
Adipogenesis	C=133;O=5;E=1.21;R=4.14;rawP=0.0075;adjP=0.0358
Retinol metabolism	C=47;O=3;E=0.43;R=7.02;rawP=0.0090;adjP=0.0387

Figure 7. KEGG and Wiki pathway analyses of 264 placental DEGs unique to KI(KI) vs. WT(WT) comparison. Venn diagram of DEGs from KI(KI) vs. WT(WT) and KI(HET) vs. WT(HET) group comparisons identified 264 DEGs that were uniquely found in KI(KI) vs. WT(WT) comparison. Top and bottom tables display top 10 statistically enriched pathways in KEGG and Wiki pathway analyses, respectively.

Discussion

In the current study, we demonstrate that the ASD-associated SERT G56A variant can impact neurodevelopment independently of embryo genotype. Specifically, we find that embryos of Ala56 dams exhibit a unique pattern of neurodevelopmental perturbations, with parallel changes in forebrain 5-HT levels and TCA development. While maternal effects on fetal development have been explored in other mouse models of ASD, these studies have primarily focused on environmental stressors that negatively impact the maternal prenatal environment (Bronson and Bale, 2014; Malkova et al., 2012). However, recent work has indicated that genetic risk factors for psychiatric disorders may also influence neurodevelopment by altering maternal physiology during pregnancy (Toth, 2014). Interestingly, maternal genotype effects on fetal development have already been reported in 5-HT related mouse models, with offspring of *Htr1a* and *Tph1* knockouts displaying anatomical and behavioral abnormalities (Cote et al., 2007; Gleason et al., 2010). Our findings provide further evidence that disruptions in maternal 5-HT homeostasis are a risk factor for psychiatric disorders, such as ASD.

Due to the broad expression of SERT in the periphery and the brain (Qian et al., 1995), it is difficult to pinpoint what aspect of maternal physiology is affected by enhanced SERT function. However, the developmental trajectory of forebrain 5-HT in KI(KI) embryos suggests that altered maternal 5-HT homeostasis directly impacts placental function. At E14.5, during a developmental time period when the placenta provides the main source of forebrain 5-HT (Bonnin et al., 2011), 5-HT levels were specifically decreased in KI(KI) forebrain tissue compared to WT(WT). Furthermore, E14.5 KI(KI) placentas also possessed parallel decreases in 5-HT, suggesting deficient

placental 5-HT synthesis caused reduced KI(KI) forebrain 5-HT levels. Complementing these findings, KI(KI) forebrain 5-HT levels were normalized at E18.5, when endogenous sources of 5-HT originating from the midbrain raphe nuclei are predominant in the forebrain (Bonnin et al., 2011). While KI(KI) forebrain 5-HT was now indistinguishable from WT(WT) at E18.5, KI(KI) placenta continued to display decreases in 5-HT, indicating placental dysfunction may persist throughout pregnancy in Ala56 dams. Supporting this idea, we did observe a small, but significant increase in KI(KI) placenta weight compared to WT(WT) throughout embryonic development (Supplemental Fig. 10).

Maternal SERT genotype effects on TCA development were also noted in embryos from Ala56 dams. While not causally linked in our study, the maternal effect on TCA development may be reflective of placental-driven changes in forebrain 5-HT in KI(KI) embryos. During neurodevelopment, glutamatergic TCAs transiently express a number of serotonergic proteins, most notably SERT and $5\text{-HT}_{1B/1D}$ receptors. Consequently, alterations in extracellular 5-HT in the fetal forebrain impact multiple aspects of TCA development, including $5\text{-HT}_{1B/1D}$ modulation of netrin-1 mediated axon guidance cues (Bonnin et al., 2007). Decreased forebrain 5-HT levels, as found in KI(KI) embryos, may alter TCA $5\text{-HT}_{1B/1D}$ signaling, thereby affecting overall TCA trajectory. Furthermore, the rostral-caudal gradient of altered TCA trajectory thickness suggests that caudal TCAs are more resilient to changes in placental 5-HT delivered to the forebrain, presumably due to their proximity to endogenous 5-HT sources in the developing raphe nuclei.

The consistent decreases in KI(KI) placental 5-HT levels during development suggested maternally-induced deficits in placental 5-HT synthesis. The most parsimonious explanation for this phenotype is altered activity or expression of TPH1, the rate-limiting enzyme in the synthesis of 5-HT in peripheral tissues (Amireault et al., 2013). However, both TPH1 activity and mRNA expression were unaffected in KI(KI) placentas, which indicates altered maternal SERT function indirectly affects placental handling and storage of 5-HT. While this possibility was not addressed by the current study, future investigations are warranted in *ex vivo* placenta perfusion preparations that are ideally suited to examine placenta physiology in the context of different environmental and genetic manipulations (Goeden and Bonnin, 2013).

Although direct interrogation of the placental 5-HT system did not reveal a maternal effect on 5-HT synthesis, our unbiased RNAseq data indicate altered maternal SERT function causes broader placental dysfunction. In our collective approaches to identify maternal genotype mediated changes in placental gene expression, we were struck by two findings. First, the enrichment of DEGs related to MAPK signaling in our 2 x 2 interaction anaylsis is noteworthy in light of the fact that Ala56 SERT is insensitive to p38 MAPK regulation (Prasad et al., 2009; Sutcliffe et al., 2005). As placental syncytiotrophoblasts express SERT (Balkovetz et al., 1989), embryo genotype effects related to MAPK signaling were observed in littermates from heterozygous dams (Supplemental Fig. 11), corroborating previous data from midbrain synaptosomes in adult animals. However, enrichment of placental DEGs related to MAPK signaling are absent in the our KI(KI) vs. WT(WT) comparison. This indicates maternal Ala56

genotype effects on placental development act through divergent biological mechanisms than embryo genotype effects.

Lastly, pathway analyses identified several immune-related signaling pathways that are modulated by maternal Ala56 genotype. During pregnancy, the maternal immune system must be intricately balanced to prevent allogeneic rejection of the developing conceptus while still providing immunological protection (Mor and Cardenas, 2010). Maternal leukocytes, though located in close proximity to foreign fetal tissue (Aluvihare et al., 2004; Bulmer et al., 1988), are able to maintain immune tolerance through a number of mechanisms, including suppression of T-cell activity via tryptophan depletion (Munn et al., 1998). Moreover, various components of the innate and adaptive immune system express SERT and 5-HT receptors (Baganz and Blakely, 2013), allowing leukocytes to respond to 5-HT released from platelets. As 5-HT has been found to have numerous effects on leukocytes (Ahern, 2011; Baganz and Blakely, 2013), it is difficult to speculate about the exact nature of immune dysfunction observed in the KI(KI) placentas. However, SERT-mediated changes in maternal leukocyte function may disrupt immunosuppression mechanisms present at the placenta, thereby negatively impacting placental function and fetal development. This hypothesis is supported by concomitant maternal genotype mediated changes in PPAR signaling, which plays an essential role in placental development (Barak et al., 2008).

In conclusion, we have demonstrated a maternal SERT genotype effect on fetal development in offspring of SERT Ala56 dams. While the patterns of fetal abnormalities indicate disruption of the placental 5-HT synthetic pathway in SERT Ala56 dams, there is no apparent maternal effect on TPH1 function. Instead, we found evidence that

enhanced and dysregulated maternal SERT function causes broad immunological changes in the placenta, adding to a growing body of literature that suggests the immune system plays a role in the etiology of ASD (Braunschweig et al., 2013; Hsiao and Patterson, 2012). Collectively, our findings indicate ASD susceptibility factors, such as the Ala56 variant, may increase risk for the disorder by altering the maternal prenatal environment.

CHAPTER 4

GENETIC VARIATION IN SEROTONIN TRANSPORTER MODULATES TACTILE HYPERRESPONSIVENESS IN ASD

Christopher L. Muller, Kimberly B. Schauder, Jeremy Veenstra-VanderWeele, Carissa J. Cascio

Introduction

Although autism spectrum disorder (ASD) has been traditionally defined by social communication impairments and restricted, repetitive behavior, there is a growing appreciation that a significant proportion of individuals with ASD also exhibit sensory dysfunction (Crane et al., 2009; Leekam et al., 2007). Studies of sensory function in ASD have primarily focused on broad patterns of sensory behavior, which have been categorized as hyper- and hyporesponsiveness. While several reports indicate that hyporesponsiveness to sensory stimuli is highly prevalent in children with ASD and correlates strongly with clinical features (Foss-Feig et al., 2012), it remains unclear whether patterns of hyperresponsive sensory behaviors are a distinctive ASD characteristic (Baranek et al., 2006; Ben-Sasson et al., 2009; Rogers and Ozonoff, 2005; Tavassoli et al., 2014; Watson et al., 2011). To clarify these findings, recent investigations of sensory processing have also analyzed patterns of behavior across multiple sensory modalities (Kern et al., 2006; Little et al., 2011; O'Riordan and Passetti, 2006; Tomchek and Dunn, 2007; Wiggins et al., 2009). These studies report distinct differences in auditory, visual, and tactile processing in ASD, but the general patterns of sensory dysfunction are heterogeneous, with each modality exhibiting varying degrees

of impairment. While variation in sensory behavior documented in ASD may reflect differences in study methodology and demographics, heterogeneity in sensory processing could also indicate phenotypically and genetically distinct subpopulations of affected individuals.

One of the most replicated findings in ASD is elevated whole blood 5-HT levels, termed hyperserotonemia, in approximately 30% of children (Gabriele et al., 2014; Mulder et al., 2004). Due to its central role as a regulator of 5-HT homeostasis in the platelet as well as at the serotonergic synapse in the brain, SERT has been extensively studied as a candidate ASD risk gene. In particular, the impact of SERT function on human behavior has been scrutinized in the context of the *SLC6A4* promoter polymorphism, 5-HTTLPR, a variable tandem repeat polymorphism consisting of two primary alleles, the short allele and higher-expressing long allele (Heils et al., 1996; Lesch et al., 1996). More recent 5-HTTLPR studies have also taken into account the functional effects of a single nucleotide polymorphism (SNP), rs25531, which modulates long allele SERT expression (Hu et al., 2005). While consistent 5-HTTLPR/rs25531 associations with anxiety and affective behavior have been reported in the general population (Canli and Lesch, 2007), there have been inconsistent relationships found with the core behavioral features in ASD (Brune et al., 2006; Cook and Leventhal, 1996; Devlin et al., 2005; Mulder et al., 2004; Tordjman et al., 2001).

In addition to its role as a neurotransmitter, 5-HT is an important signaling molecule during neurodevelopment. Whereas SERT expression in the adult brain is limited to midbrain serotonergic neurons, the transporter is transiently expressed in a number of brain regions during neurodevelopment, including multiple areas involved in

sensory processing (Gaspar et al., 2003). Perinatal SERT function plays a key role in the topographical organization of cortical sensory maps, most notably rodent barrel field architecture in primary somatosensory cortex (Lebrand et al., 1996; Salichon et al., 2001). Changes in the somatotopic organization of primary somatosensory cortex have been described in individuals with ASD, but their relationship with altered 5-HT signaling is unknown (Coskun et al., 2009). In families with evidence for genetic linkage of autism to *SLC6A4*, the rare SERT Ala56 variant, which leads to increased and dysregulated SERT function, was associated with sensory aversion (Sutcliffe et al., 2005). While sensory aversion commonly comprises tactile hyperresponsiveness (Rogers et al., 2003; Tomchek and Dunn, 2007), specific sensory modalities were not evaluated in affected carriers of the Ala56 allele. Collectively, these findings suggest that enhanced SERT function could play a specific role in tactile hyperresponsiveness in ASD.

To test the hypothesis that higher-expressing SERT alleles are associated with tactile hypersensitivity, we evaluated sensory behavior in children with ASD and age-matched controls that were also genotyped for the 5-HTTLPR and rs25531 polymorphisms. Our findings provide further evidence of heterogeneous patterns of sensory disturbances in ASD, which exhibit previously noted relationships with age and repetitive behavior. In addition, we report that measures of tactile hyperresponsiveness are uniquely associated with high-expressing SERT genotypes in affected individuals

Methods

Participants

Participants were 47 (40 male) children with ASD and 38 (33 male) typically developing controls ages 4-10. Diagnosis of ASD was confirmed by research-reliable administration of the Autism Diagnostic Observation Schedule (ADOS) (Lord et al., 2000) and the Autism Diagnostic Interview-Revised (ADI-R) (Lord et al., 1994), as well as clinical diagnosis by a licensed clinical psychologist specializing in ASD. Children in the control group did not have any psychiatric, learning or behavioral diagnoses, did not have a first degree relative with ASD, and did not have elevated scores on an autism symptom screening measure, the Social Communication Questionnaire (SCQ) (Rutter et al., 2003). IQ was assessed for all participants with either the Kaufman Brief Intelligence Test, Second Edition (KBIT-2) (Kaufman and Kaufman, 2004) or the Weschler Abbreviated Scales of Intelligence (WASI) (Weschsler, 1999). When participants were unable to complete these measures due to poor language skills, the Mullen Scales of Early Learning (MSEL) (Mullen, 1995) was used to assess cognitive ability; however IQ was not able to be calculated because those individuals did not fall within the normed age range for this measure. Thus, IQ information was missing for four participants with ASD tested using the MSEL. Parents gave informed consent and participants gave informed assent, when able. Procedures were approved by Vanderbilt Institutional Review Board.

5-HTTLPR/rs25531 genotyping

5-HTTLPR and rs25531 SNP genotyping were performed as previously described with the following modifications (Dickel et al., 2007). Saliva samples were collected from each study participant using the Oragene DNA Collection Kit (DNA Genotek Inc., Kanata, Ontario, Canada). Forward primer, 5'-GGCGTTGCCGCTCTGAATGC-3', and reverse primer, 5'-AGGGACTGAGCTGGACAACCAC-3', were used for PCR amplification. The rs25531 SNP was genotyped by digesting 5-HTTLPR PCR product with HpaII, a restriction enzyme that cuts at the SNP site only if the G allele is present. To determine genotypes, 5-HTTLPR amplicons and HpaII digest products were analyzed by agarose gel electrophoresis. The resulting genotypes were combined to create composite 5-HTTLPR alleles (i.e. L_A, L_G, S_A, S_G). Individuals were categorized into two genotype comparison groups for statistical analysis: high SERT expressing genotypes (L_A/L_A) and low SERT expressing genotypes (L_A/L_G, L_A/S_A, L_G/S_A, and S_A/S_A).

Parent Questionnaires – Sensory Behaviors

Caregivers of study participants completed two sensory questionnaires about their child's current sensory behaviors, the Sensory Profile (Dunn, 1999) and Sensory Experience Questionnaire (SEQ) (Baranek et al., 2006). The Sensory Profile is a 125-item questionnaire measuring a child's sensory processing abilities across a variety of sensory modalities. The SEQ consists of 41 questions and was designed specifically to evaluate patterns of sensory processing in children with ASD. Both questionnaires ask caregivers to rate their child's behavior on a 5-point Likert scale.

To achieve the most comprehensive representation of each participant's sensory behavior, items from both questionnaires were used to calculate composite hypo- and hyper-responsiveness variables for tactile, visual, and auditory processing. Items used for the hyperresponsiveness variables were the low threshold items from the Sensory Profile and the hyperresponsive items from the SEQ. Composite hyporesponsiveness variables were created from the high threshold items from the Sensory Profile and the hyporesponsive items from the SEQ. Items from the Sensory Profile were reversed scored such that higher values represent greater sensory impairment, consistent with scoring on the SEQ. Within each composite variable, items that were identical in content or were not significantly correlated ($r < .2$, $P > .05$) with other included items were dropped. After excluding selected items, the composite variable score was averaged from the remaining items. Composite scores contained 4 to 14 items, with the auditory hyperresponsiveness score having the fewest and the tactile hyperrepsonsiveness score having the most items. Item-to-total composite score Spearman Rank correlation coefficient ranged from .38-.88.

Parent Questionnaire – Repetitive Behaviors

Parents in the ASD group completed the Repetitive Behavior Scale – Revised (RBS-R) (Lam and Aman, 2007), a questionnaire about their child's repetitive behaviors. The RBS-R contains 43 items that comprise six subscales corresponding to common repetitive behavior patterns in ASD. Parents rate each item on a scale from 0-3 based on how problematic each behavior is for their child. A total score, including all 43 items, was also calculated.

Statistics

Univariate ANOVAs were conducted to examine the effects of diagnostic groups on the composite sensory variables. A t-test was used to test the primary hypothesis, that the high-expressing genotype would be associated with somatosensory hyperresponsiveness within children with ASD. Exploratory two-way ANOVAs were conducted to examine possible interactions between diagnostic group and genotype. A correlation analysis with age and the six composite sensory variables was also performed to examine how age uniquely affects these sensory behaviors. Finally, relationships between the sensory variables and the total score from the RBS-R were explored using Pearson correlations. To further explore significant effects, additional correlations between the sensory variable and the six subscales of the RBS-R were conducted in order to determine the specific kind of repetitive behavior that was related to the sensory behavior. All statistical analysis was performed using SPSS Version 21.

Results

Participants with ASD did not differ from control participants on age ($t(83) = .188$, $P > .1$), gender ($\chi^2 = .05$, $P > .1$), or race ($\chi^2 = 4.69$, $P > .1$). Participants with ASD had significantly lower full scale IQ (FSIQ) scores than controls ($t(79) = 2.7$, $P < .01$). 5-HTTLPR ($\chi2 = .099$, $P = .95$) and rs25531 ($\chi2 = 0$, $P = 1$) were in Hardy-Weinberg equilibrium in our total sample population. Within each diagnostic group, individuals in the high expressing versus low expressing SERT groups did not differ in age, gender, race, or FSIQ.

All six univariate ANOVAs with each composite sensory variable as the dependent variable revealed a main effect of diagnostic group ($P < .001$), confirming more aberrant sensory behaviors across modalities and processing patterns in children with ASD. The primary analysis revealed a significant difference in tactile hyperresponsiveness by genotype within the ASD group ($t(45) = 2.07$, $P < .05$). These analyses were repeated including only the Caucasian participants. All ANOVA results remained highly significant ($P < .001$), and the effect of genotype for tactile hyperresponsive in the ASD group remained ($t(42) = 2.05$, $P < .05$), suggesting these effects are not due to race. This analysis was repeated including only the Caucasian participants ($t(42) = 2.05$, $P < .05$), which suggests the effect is not due to race. No other sensory domain showed a significant association with SERT genotype in the ASD group. Two-way ANOVA revealed a trend for an interaction between diagnostic and genotype group that was unique to tactile hyperresponsiveness ($F_{1,81} = 2.87$, $P = .094$). There were no main effects of genotype group on any of the composite sensory variables across both diagnostic groups. Visual inspection of group means suggests that children with ASD exhibit more tactile hyperresponsive behavior patterns; however, those with ASD and high expressing SERT show these behaviors to a greater degree (Fig. 8).

The six composite sensory variables were correlated with age and FSIQ separately in each group. There were no significant correlations in either group with any of the sensory variables and FSIQ. There were no significant relationships between age and any of the sensory variables in the TD control group. In the ASD group, age was

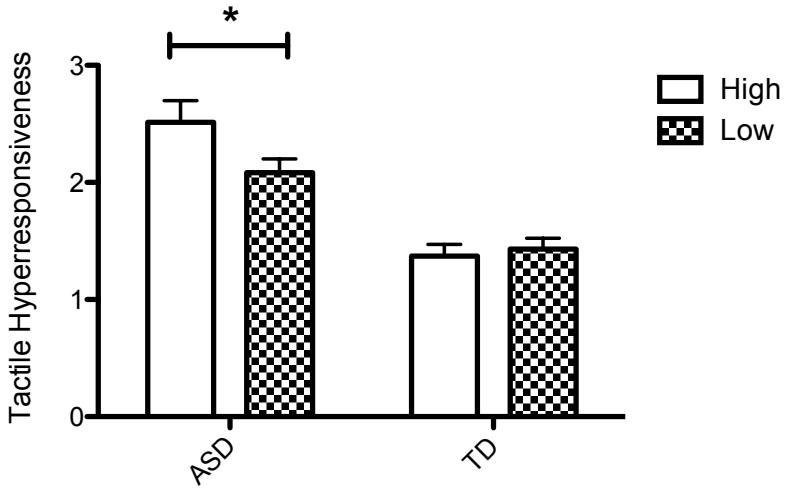

Figure 8. Tactile hyperresponsiveness in children with and without ASD, with high and low expressing SERT genotypes. In ASD group, children with high-expressing SERT genotypes display increased tactile hyperresponsiveness compared to children with low-expressing SERT genotypes ($t(45) = 2.07$, $P < .05$). SERT genotype effects on tactile hyperresponsiveness were absent in TD children.

		ASD	TD
		Age	
Auditory	Hyper-	-0.134	0.058
	Hypo-	**-0.298***	-0.305
Visual	Hyper-	-0.198	-0.075
	Hypo-	**-0.308***	-0.087
Tactile	Hyper-	-0.126	-0.211
	Hypo-	**-0.385****	-0.233
Overall	Hyper-	-0.179	-0.082
	Hypo-	**-0.409****	-0.232

Figure 9. Correlations between sensory variables and age. In ASD group, age was significant correlated with hyporesponsive patterns in all sensory modalities, in which older individuals showed fewer hyporesponsive sensory behaviors. * $P < .05$, ** $P < .01$

A

		RBS-R Overall Score
Auditory	Hyper-	**0.392***
	Hypo-	0.078
Visual	Hyper-	0.236
	Hypo-	0.295
Tactile	Hyper-	**0.582*****
	Hypo-	0.266
Overall	Hyper-	**0.512****
	Hypo-	0.261

B

RBS-R Subscale	Auditory Hyper-	Tactile Hyper-
Stereotyped	0.14	0.40*
Self-Injurious	0.18	0.29
Compulsive	0.27	0.40*
Ritualistic	0.21	0.33
Sameness	0.44**	0.65***
Restricted	0.51**	0.52**

Figure 10. Correlations between sensory variables and RBS-R overall/subscale scores. Overall repetitive behavior score as measured by RBS-R was significantly positively correlated with hyperresponsive patterns in auditory and tactile modalities **(A)**. Auditory and tactile hyperresponsive behaviors were positively related to all subscales of the RBS-R, with the sameness and restricted behaviors scales showing the strongest relationships. *$P < .05$, **$P < .01$, ***$P <. 001$.

negatively correlated with sensory hyporesponsiveness variables, with older individuals displaying fewer sensory behaviors (Fig. 9).

Visual inspection of the data revealed one extreme outlier (greater than 3 SD above the mean) on the RBS-R. After excluding this outlier, the six composite sensory variables were correlated with the overall score from the RBS-R in the ASD group only. Repetitive behaviors were positively related to all sensory scores. This relationship was significant for tactile (r = .58, P < .001) and auditory (r = .51, P < .01) hyperresponsiveness, with the tactile domain showing the strongest correlation to repetitive behaviors (Fig. 10A). Additional correlations between tactile and auditory hyperresponsiveness and the subscales of the RBS-R revealed strongest relationships with the sameness and restricted behaviors subscales (Fig. 10B). Analyses including the single outlier revealed similar results; however, correlations with the repetitive behavior score and both visual hyper- and hypo- responsiveness also became significant.

Discussion

To our knowledge, this is the first study to examine the influence of SERT genetic variation on specific patterns of sensory behavior. While all measures of auditory, visual, and tactile processing impairment were significantly increased in children with ASD compared to TD participants, only patterns of tactile hyperresponsive behavior in ASD exhibited a relationship with SERT genotype. Specifically, we found that tactile hyperresponsiveness scores were significantly increased in affected individuals with high SERT expressing genotypes, matching our primary hypothesis.

The relationships of age and repetitive behaviors with sensory processing patterns in our population were supported by previous literature. Although ASD is associated with sensory dysfunction throughout life (Crane et al., 2009), the degree of sensory impairment appears to decrease with age (Ben-Sasson et al., 2009; Kern et al., 2006). Our data matches this trend; however, only hyporesponsive, and not hyperresponsive, behaviors decrease within the 4-10 year age range in our study, suggesting these behaviors are more malleable early in life.

Whereas age was more related to hyporesponsive behavior patterns, repetitive behaviors were related to hyperresponsive patterns, consistent with a prior study in a similar age demographic (Boyd et al., 2010). Furthermore, we found that repetitive behaviors, specifically sameness and restricted behavior subscales, were most strongly associated with tactile hyperresponsiveness in ASD. However, in contrast to tactile hyperresponsiveness, RBS-R scores were not associated with SERT genotype. While a link between common SERT polymorphisms and repetitive behavior in ASD has remained elusive, the rare gain-of-function SERT Ala56 variant is associated with ADI-R measures of rigid-compulsive behavior in addition to sensory aversion (Sutcliffe et al., 2005). Interestingly, due to the relationship between sensory hyperresponsiveness and repetitive behavior, it has been proposed that these behaviors may share common neurobiological mechanisms (Baranek et al., 1997; Boyd et al., 2010; Chen et al., 2009). Consequently, it is possible that enhanced SERT function may impact shared brain circuits that underlie tactile hyperresponsiveness and repetitive behavior in ASD.

While our work is the first to implicate SERT genetic variation in tactile function in ASD, there are some notable limitations in our study design. First, our sample size gave

us limited statistical power to detect genotype/phenotype relationships. In addition, children with ASD in our study were generally high-functioning, which prohibits us from generalizing our findings to more impaired individuals. Altered patterns of sensory behavior are reported to be more prevalent in low-functioning cases of ASD (Patten et al., 2013; Watson et al., 2011), potentially further limiting our power. Furthermore, the SERT promoter polymorphisms are, at best, an indirect assessment of SERT expression and function, hindering our ability to directly test the effects of SERT on sensory functioning. Beyond genotype analyses, it would be of great interest to examine the relationship between sensory behavior and whole blood 5-HT levels in ASD, which are partially influenced by SERT genetic variation (Anderson et al., 2002; Coutinho et al., 2004; Cross et al., 2008). Finally, whereas common variation in a single gene is unlikely to significantly impact subjective measures of human behavior, gene variants of modest effect size may have stronger relationships with endophenotypes: heritable, biological measures associated with a disease state. Using this approach, some ASD neuroimaging studies have had success relating changes in brain structure and activity to SERT function (Wassink et al., 2007; Wiggins et al., 2012). To date, there have been few empirical studies of tactile processing in ASD (Blakemore et al., 2006; Cascio et al., 2008; Cascio et al., 2012; Coskun et al., 2009; Marco et al., 2012; O'Riordan and Passetti, 2006; Tommerdahl et al., 2007), with a limited understanding of the biological mechanisms underlying sensory dysfunction.

In conclusion, the current study highlights a unique association in ASD between high-expressing SERT genotypes and tactile hyperresponsiveness, as measured by parent report. Supplementary analyses with age and repetitive behaviors, factors known

to influence sensory behaviors, replicated previous findings in the literature and specified that age is more related to hyporesponsive patterns and repetitive behaviors are more related to hyperresponsive patterns, particularly in the tactile domain. These findings provide an initial foundation to explore the biological mechanisms underlying abnormal sensory behavior in ASD. Previous attempts to relate 5-HT system dysfunction to specific ASD behavioral impairments, such as repetitive behaviors, have produced inconsistent results, but evaluating a potential relationship between 5-HT and sensory processing may be able to connect variation in this key system and its neurodevelopmental sequelae. While our present findings point to a relationship between SERT and tactile processing deficits, future studies will be needed to connect more direct measures of SERT expression and function with aberrant sensory behavior and somatosensory neural circuitry.

CHAPTER 5

FINAL DISCUSSION

While we have known about disruptions in whole blood 5-HT levels in ASD for little over half a century, we are still struggling to identify how hyperserotonemia relates to central serotonergic function and the pathophysiology of ASD. Due to the substantial overlap of serotonergic proteins that exist in the periphery and the brain, a fundamental assumption has been made that disturbances in 5-HT homeostasis in the periphery will elucidate 5-HT dysfunction in the brain. Although there have been many studies that individually examine either the central or peripheral 5-HT system in ASD, there is shockingly only one human imaging study that has attempted to simultaneously evaluate platelet 5-HT measures and cortical 5-HT function. In 2009, Goldberg and colleagues found evidence of global decreases in cortical 5-HT_{2A} binding in a small sample of parents with at least two children with ASD, with a significant negative correlative between PET binding measures and blood 5-HT levels (Goldberg et al., 2009). While there are logistical and ethical concerns with PET imaging that effectively limit studies of this nature, investigators that examine more commonplace MRI and fMRI measures in ASD would be hard-pressed to justify not examining blood 5-HT levels in their imaging cohorts. A simple blood draw would greatly contribute to our understanding of how hyperserotonemia is related to brain development and function.

Analyses of the genetic determinants of blood 5-HT levels in founder populations have clearly indicated a significant role for SERT. However, functional platelet studies demonstrate that while genetic variation in SERT impacts 5-HT transport, it has

surprisingly little effect on overall 5-HT blood levels (Anderson et al., 2002). These findings address another key assumption that many researchers have made about the nature of hyperserotonemia in ASD. While increased platelet 5-HT levels could result from enhanced SERT function, increased 5-HT production in enterochrommafin cells or reduced degradation of 5-HT are equally plausible explanations. It is more likely that enhanced SERT function only causes hyperserotonemia in a subset of individuals with ASD. In Chapter 2, we present data that indicate that the rare gain-of-function Ala56 variant causes elevated whole blood 5-HT in mice bred on the 129S6/S4 background. Interestingly, our laboratory has found that hyperserotonemia is attenuated in C57Bl/6 Ala56 mice (Kerr et al., 2013), indicating genetic modifiers of SERT function and/or peripheral 5-HT production/degradation. Furthermore, it is important to note that despite reported changes in lymphoblast 5-HT uptake, human carriers of the Ala56 allele were never specifically evaluated for hyperserotonemia or central 5-HT dysfunction. While a single case study has found evidence of decreased cerebral spinal fluid (CSF) 5-HIAA levels in an affected heterozygous Ala56 carrier (Adamsen et al., 2011), future studies that thoroughly examine peripheral and central 5-HT function in individuals that possess rare SERT variants would be of great interest.

In Chapter 2, we present *in vivo* evidence that the SERT Ala56 variant causes global changes in 5-HT homeostasis and alters rodent behavior relevant to the diagnostic core features of ASD. In contrast to the vast majority of published mouse models of ASD, the SERT Ala56 mouse exhibits strong construct validity, as it accurately recapitulates a known genetic risk factor for the disorder. While mouse knockout models may be more informative about gene function, knock-in models

provide a stronger platform to test specific hypotheses about ASD pathophysiology and novel therapeutics. Since SERT influences numerous aspects of behavior and physiology, it was difficult to predict the *in vivo* impact of enhanced and dysregulated SERT. However, due to the collective association of the rare, hyperfunctional SERT variants with rigid-compulsive behavior, we hypothesized that Ala56 mice would exhibit some manifestation of repetitive behavior. While we did report a repetitive climbing behavior in the home cage, our most robust behavioral phenotype in Ala56 mice by far was decreased wins in the tube test for dominance. This phenotype even persisted in C57Bl/6 Ala56 mice, which exhibit an overall attenuated phenotype compared to our 129S6/S4 mouse line. As our strongest behavioral phenotype, the tube test for social dominance necessitates future mechanistic dissection. While the neural circuitry underlying mouse behavior in commonly used assays is generally unknown, there is previous literature highlighting the key neural substrates that mediate performance in the tube test for dominance. Wang and colleagues demonstrated that rodent social hierarchy, as measured by tube test, is sensitive to changes in excitatory neurotransmission in medial prefrontal cortex (mPFC) (Wang et al., 2011). The authors noted that socially dominant mice possess enhanced AMPA-mediated currents in layer V of mPFC, which could be modulated to affect behavioral performance in the tube test. Interestingly, in addition to being linked to changes in social standing in non-human primates (Myers et al., 1973), analogous regions of mPFC have also been implicated in social impairments in ASD (Happe et al., 1996). Collectively, these findings suggest SERT Ala56 mice possess mPFC dysfunction that is relevant to impairment found in ASD.

A major hurdle faced by neuroscientists trying to evaluate how changes in SERT function affect behavior and physiology is determining the critical sites of SERT expression that underlie a given phenotype. In addition to its seemingly ubiquitous presence in the brain and periphery, SERT also displays a unique temporal pattern of expression, with the transporter transiently found in non-serotonergic neurons during perinatal development. Fortunately, an impressive collection of molecular and genetic tools has been developed in the mouse to manipulate gene expression in a cell type and temporally restricted manner. Thus, the creation of conditional and inducible SERT Ala56 mouse models will be instrumental in mechanistically exploring the various phenotypes we have documented in the constitutive knock-in line. Furthermore, a critical conceptual question that exists in ASD research is whether the features associated with the disorder can be prevented or reversed by interventions that occur after initial development. While we have collected some data that suggests pharmacological blockade of SERT in adulthood ameliorates social deficits in Ala56 mice (data not shown), inducible and conditional expression of the Ala56 variant will give us the ability to evaluate whether enhanced SERT function during neurodevelopment has specific, irreversible long-term consequences.

In addition to traditional genotype effects, we have also presented evidence that suggests the SERT Ala56 variant may cause more profound changes in neurodevelopment by altering the prenatal environment in maternal carriers. However, a number of major questions remain from this work. While offspring of Ala56 dams exhibit parallel decreases in E14.5 placenta and forebrain 5-HT levels as well as neuroanatomical changes in TCAs at E18.5, it is unclear whether these phenotypes are

causally linked and lead to meaningful changes in postnatal behavior. To begin to address these questions, it will be necessary to isolate the upstream SERT mediated changes in maternal physiology that impact placental/fetal development. Interestingly, there are several aspects of maternal physiology that are dynamically regulated during pregnancy that interact with the 5-HT system. As discussed in Chapter 3, the maternal immune system must be intricately balanced during pregnancy to prevent allogeneic rejection of developing concepti while still conferring protection of the fetus. Since virtually all leukocytes express SERT and/or 5-HT receptors, it is certainly plausible that Ala56 SERT mediated changes in 5-HT homeostasis may have cascading effects on immune system function at the maternal-fetal interface. Remarkably, whereas our genome wide approach to interrogate maternal effects on placental function did not find alterations in central hubs of the 5-HT system (i.e. TPH1, 5-HT receptors, etc), RNAseq analyses highlighted extensive immunological dysfunction in E14.5 placentas from SERT Ala56 dams. These findings converge with emerging evidence that maternal immunological dysfunction during pregnancy may be a risk factor for ASD (Braunschweig et al., 2013; Schwartzer et al., 2013). Thus, future work examining components of the innate and adaptive immune system in Ala56 dams during pregnancy is warranted.

As described in the introduction, the developmental role of 5-HT was firmly established by observations that excessive extracellular 5-HT alters the formation of rodent barrel cortex. While these studies have provided circumstantial evidence connecting 5-HT dysfunction to neurodevelopmental disorders, there has not been an emphasis in the literature connecting 5-HT mediated changes in TCA development to

relevant sensory-related features in ASD. Moreover, one of the findings that struck us most about the SERT Ala56 variant was its unique association with sensory aversion in ASD. Consequently, my initial work with SERT G56A mice involved a thorough examination of barrel cortex development in hopes of identifying the neural substrates responsible for altered sensory processing in affected Ala56 carriers. Similar to other mouse models with reductions in extracellular 5-HT (van Kleef et al., 2012), we discovered that early postnatal and adult SERT Ala56 mice possess no overt changes in barrel field architecture (Supplemental Fig. 12). Interestingly, despite the lack of gross morphological changes in Ala56 mice, we do observe basal increases in cFos+ cells in layer IV of barrel cortex (Appendix 2), suggesting subtle alterations in somatosensory processing. To complement these indirect measures of neural activity, electrophysiological studies of TCA neurotransmission are needed to mechanistically dissect the potential excitatory-inhibitory imbalance present in barrel cortex of Ala56 mice.

Although mice are an excellent model system to explore the molecular mechanisms underlying sensory processing, behavioral manifestations of sensory dysfunction in mouse models of ASD are difficult to evaluate. As a parallel approach to our mouse studies, we evaluated whether common genetic variation in SERT was associated with patterns of sensory behavior in children with ASD. Remarkably, we found a unique relationship between high-expressing SERT genotypes and tactile hyperresponsiveness in ASD, mirroring the association of the hyperfunctional SERT Ala56 variant with sensory aversion. To evaluate potential neural substrates underlying this relationship, we have also performed diffusion tensor imaging (DTI) of

thalamocortical connectivity to primary somatosensory cortex (S1), analogous to the 5-HT sensitive structures studied in rodents. Initial evidence indicates that the volume of the thalamus-S1 tract is increased in children with ASD, with a significant positive correlation between tract volume and measures of tactile hyperresponsiveness (C. Cascio, unpublished observations). While further work is necessary to directly connect changes in SERT function to altered thalamic connectivity and sensory behavior, these findings suggest that altered TCA development observed in SERT Ala56 mice may be relevant to pathophysiology underlying sensory dysfunction in ASD.

In summary, we have determined that 129S6/S4 mice expressing the rare, gain-of-function SERT Ala56 variant possess hyperserotonemia, global changes in central 5-HT system function, and behavioral abnormalities relevant to ASD. Moreover, we demonstrate the Ala56 variant may also impact neurodevelopment by disrupting the maternal prenatal environment, providing further evidence that non-genetic forms of inheritance may underlie the 'missing heritability' in ASD. Finally, we established a connection between SERT genetic variation and patterns of sensory behavior in children with ASD, supporting the original genetic association of the Ala56 variant with sensory aversion. Collectively, these studies have provided the foundation for future mechanistic work in the SERT Ala56 mouse model that will shed light on the elusive pathophysiology of ASD.

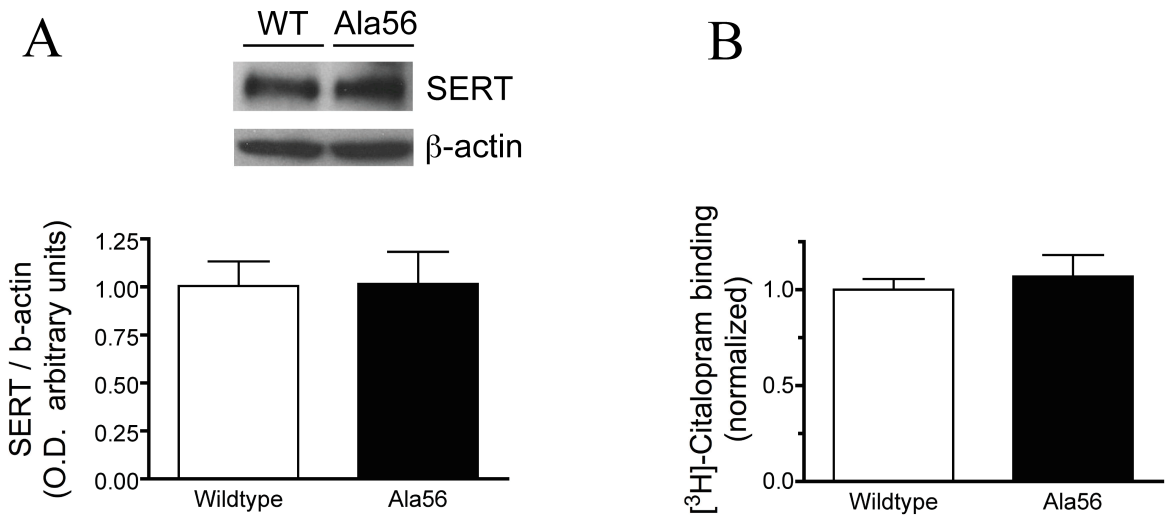

Supplemental Figure 1. **No change in midbrain SERT protein expression or citalopram binding in SERT Ala56 knock-in mice. (A)** Immunoblot of midbrain synaptosomes for β-actin and SERT (n = 3 per genotype). **(B)** [^{3}H]Citalopram binding of midbrain synaptosomes normalized to the mean WT value (n = 6 per genotype, two replicates per sample).

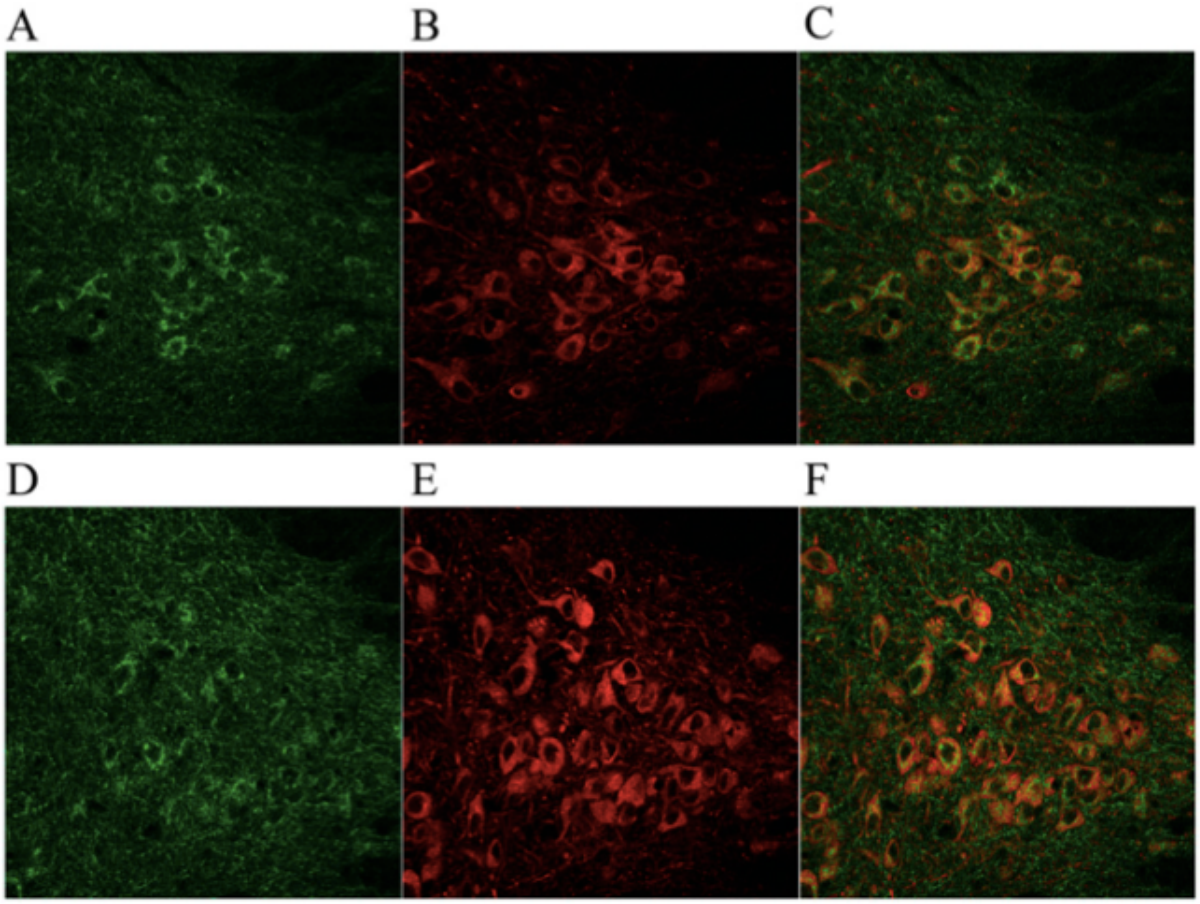

Supplemental Figure 2. No change in midbrain SERT distribution in SERT Ala56 knock-in mice. (A–C) Representative midbrain confocal images of a WT littermate (SERT Gly56) animal stained for SERT **(A)** and tryptophan hydroxylase **(B)**. **(C)** Superimposed image shows both antibodies. **(D–F)** Representative midbrain confocal images of an SERT Ala56 animal stained for SERT **(D)** and tryptophan hydroxylase **(E)**. **(F)** Superimposed image shows both antibodies.

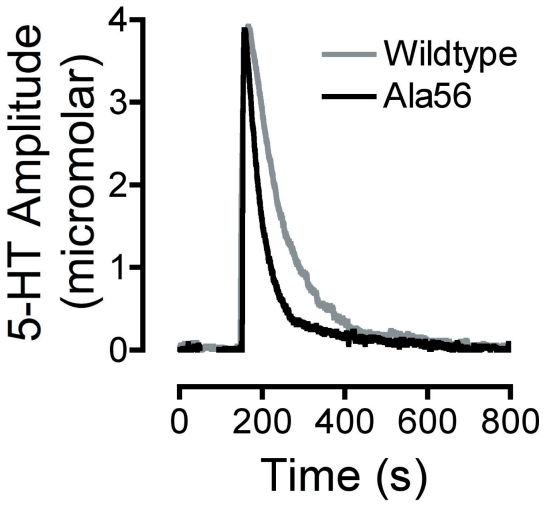

Supplemental Figure 3. Elevated 5-HT clearance in hippocampus of SERT Ala56 knock-in mice. Representative oxidation currents for serotonin pressure ejected into the CA3 region of the hippocampus of Ala56 and littermate WT mice. The oxidation currents are converted into micromolar units as described in Chapter 2 Methods.

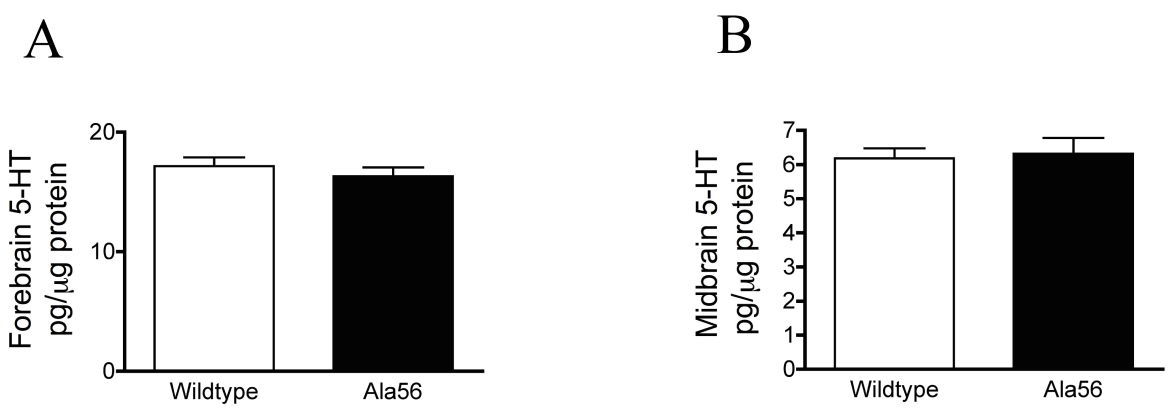

Supplemental Figure 4. No change in midbrain or forebrain 5-HT levels in adult SERT Ala56 knock-in mice. (A) HPLC measurement of 5-HT levels in the forebrain (unpaired t test, t = 0.79, *P* = 0.45; WT, n = 7; Ala56, n = 6). **(B)** HPLC measurement of 5-HT levels in the midbrain (unpaired t test, t = 0.25, *P* = 0.80; WT, n = 7; Ala56, n = 6).

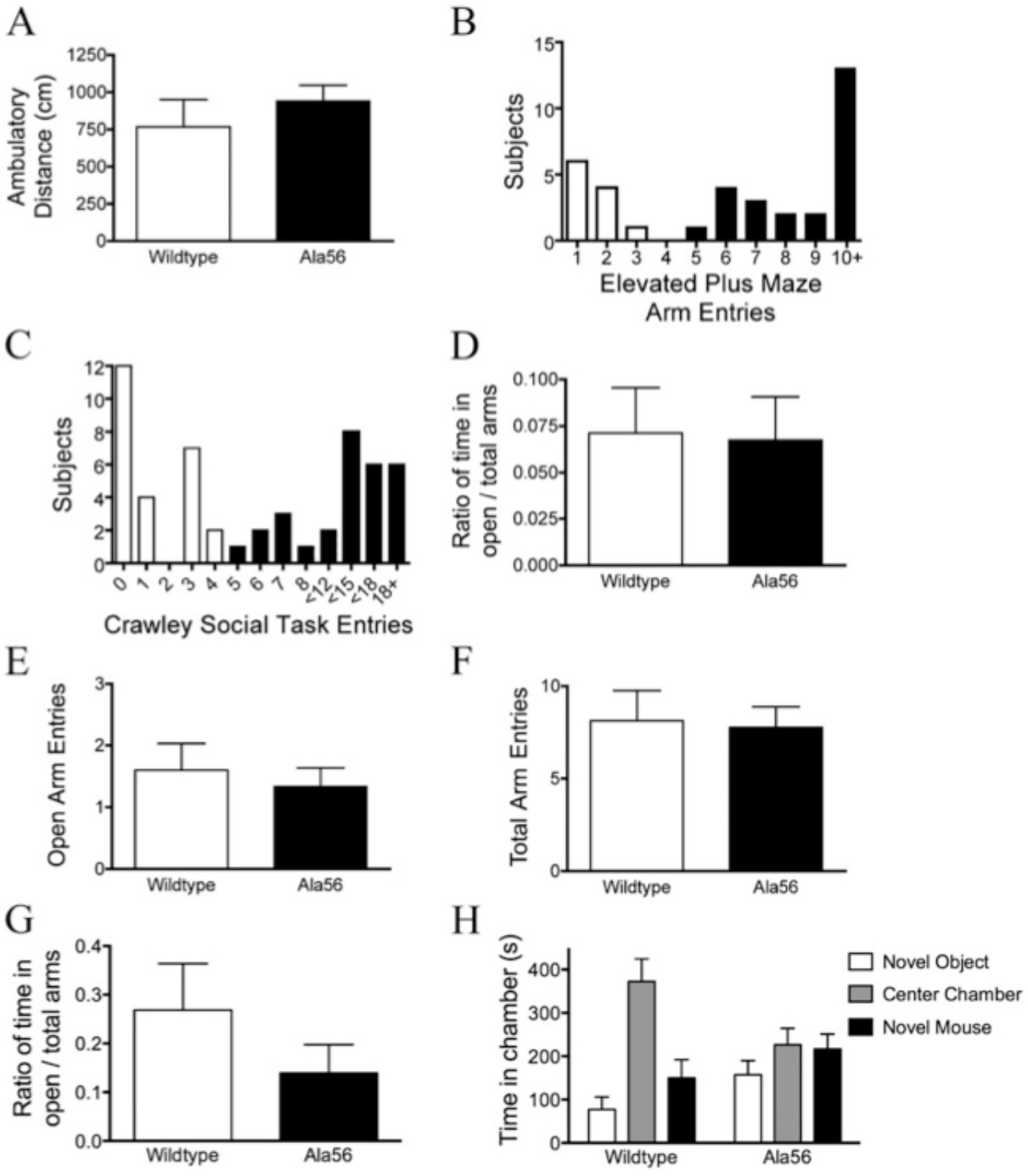

Supplemental Figure 5. No change in activity, anxiety-like behavior, or spatial learning in SERT Ala56 knock-in mice. (A) Distance traveled in the open field. WT and SERT Ala56 animals did not differ in their baseline activity (t = 0.86, P = 0.40; WT, n = 15; Ala56, n = 22). **(B)** A histogram of the number of arm entries on the elevated plus-maze is shown. A significant minority of mice, shown in white, had minimal entries, remaining largely stationary during the test. These mice significantly increased the variability of the test, as some of them remained in a single open or closed arm for the

duration of the test. The number of entries for each mouse followed an apparently bimodal distribution, and therefore, only mice with more than four entries were included in the primary analysis shown in D. **(C)** A histogram of the number of chamber entries on the Crawley sociability test is shown. A substantial minority of mice, shown in white, had four or fewer entries, typically entering only one or none of the stimulus chambers, and remaining largely stationary during the test. The number of entries for each mouse on this test also followed an apparently bimodal distribution, with a cluster of mice with four or fewer entries and an extended range of mice with more than four entries that were included in the primary analysis shown in Fig. 2E. **(D)** The ratio of time in the open arm divided by total time in either open or closed arms is shown. Mice with four or fewer total entries were excluded from the analysis because of inactivity (A and B). WT and SERT Ala56 animals did not differ in their anxiety-like behavior on the elevated plus-maze ($t = 0.11$, $P = 0.92$; WT, $n = 10$; Ala56, $n = 15$). **(E)** The total number of entries to the open arms of the elevated plus-maze is shown. No difference was seen between genotypes ($t = 0.52$, $P = 0.61$). **(F)** The total number of entries to the open or closed arms is shown. No difference was seen between genotypes ($t = 0.19$, $P = 0.85$). **(G)** The ratio of time in the open arm divided by total time in either open or closed arms is shown for active and inactive mice ($t = 1.22$, $P = 0.18$; WT, $n = 15$; Ala56, $n = 21$). **(H)** Time in each chamber of the three-chamber Crawley sociability test is shown for both active and inactive mice. Two-way RM ANOVA revealed a trend for a main effect for chamber ($F = 2.90$, $P = 0.095$), a significant effect of genotype for total time spent in a side chamber ($F = 5.49$, $P = 0.023$), and no interaction between genotype and stimulus ($F = 0.03$, $P = 0.86$; WT, $n = 22$; Ala56, $n = 31$). Bonferroni post-test revealed no significant preference for the social chamber in the WT ($P > 0.05$) or SERT Ala56 animals ($P > 0.05$) when active and inactive mice are analyzed together.

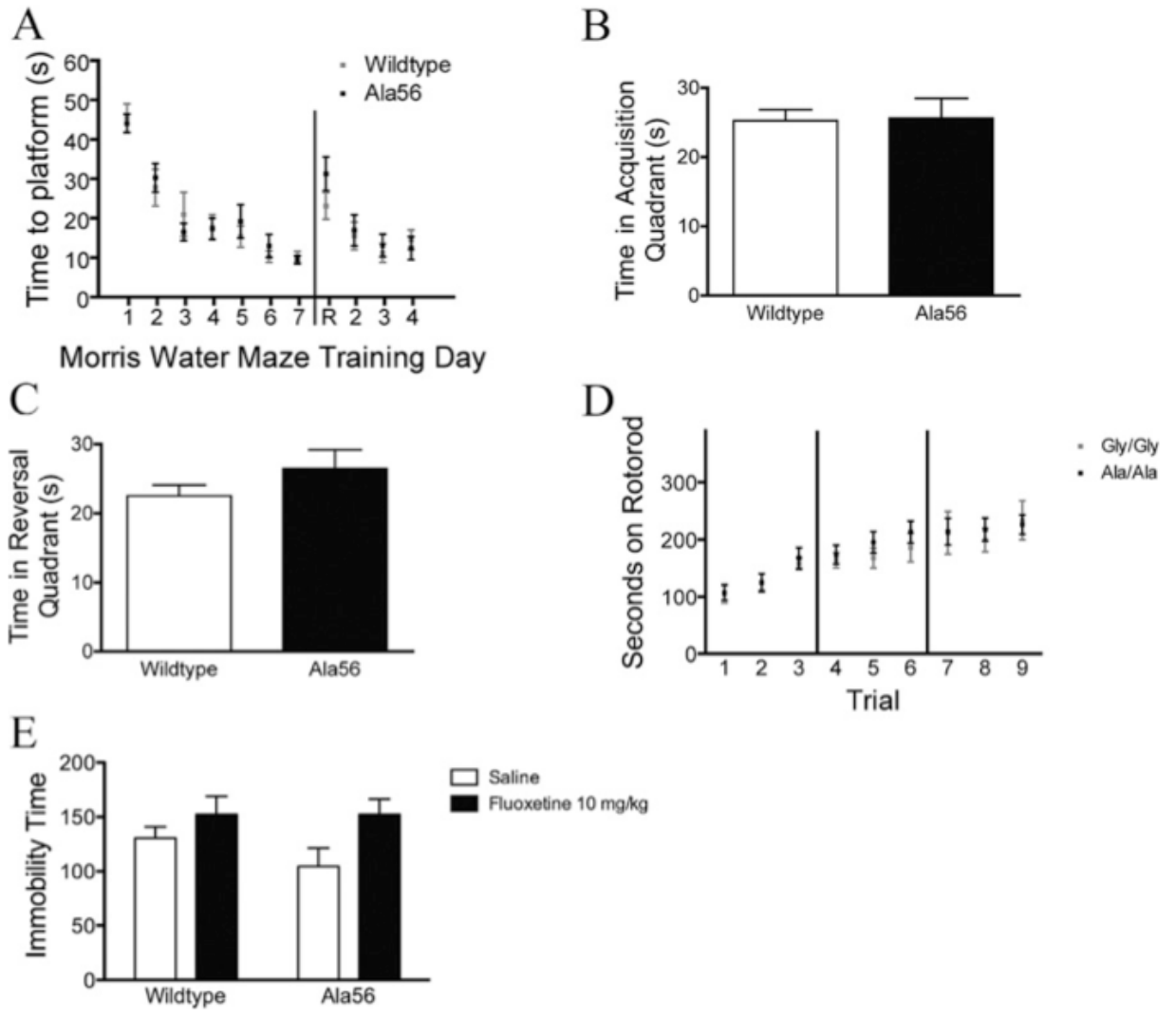

Supplemental Figure 6. No change in spatial memory on the Morris water maze, motor memory on the accelerating rotarod, or immobility in the forced swim test in SERT Ala56 knock-in mice. (A) Acquisition of the platform location in the Morris water maze is shown to the left of the vertical line and to platform reversal is shown to the right. Both genotypes successfully acquired the initial platform location and reversal location (two-way RM ANOVA, main effect of day, $F = 20.55$, $P < 0.0001$; main effect of genotype, $F = 0.68$, $P = 0.41$; genotype–day interaction, $F = 0.57$, $P = 0.80$; n = 10 per genotype). **(B)** The time spent in the platform quadrant during the 1 min probe trial following acquisition of the initial platform location on the Morris water maze is shown. No difference was seen between genotypes ($t = 0.12$, $P = 0.90$; WT, n = 10; Ala56, n = 10). **(C)** The time spent in the reversal platform quadrant during the 1-min probe trial following acquisition of the reversal platform location on the Morris water maze is

shown. No difference was seen between genotypes (t = 1.25, P = 0.23). **(D)** Latency to fall off the rotarod apparatus is shown for each genotype. No significant difference was seen between the genotypes (two-way RM ANOVA, main effect of trial, F = 21.57, P < 0.0001; main effect of genotype, F = 1.32, P = 0.26; genotype–trial interaction, F = 0.45, P = 0.89; WT, n = 15; Ala56, n = 13). **(E)** Immobility in the last 4 min of the 6-min forced swim test is shown for each genotype for both the saline solution and fluoxetine 10 mg/kg treated animals. No significant difference was seen between the genotypes at baseline (t = 1.32, P = 0.21). A significant increase in immobility was seen with fluoxetine, but no significant interaction was seen between drug and genotype (two-way ANOVA, main effect of drug, F = 5.34, P = 0.029; main effect of genotype, F = 0.74, P = 0.40; drug–genotype interaction, F = 0.76, P = 0.39; Bonferroni post-test revealed a significant effect of fluoxetine in Ala56 mice (P < 0.05) but not in WT controls (P > 0.05); WT saline solution, n = 8; WT fluoxetine, n = 8; Ala56 saline solution, n = 9; Ala56 fluoxetine, n = 9).

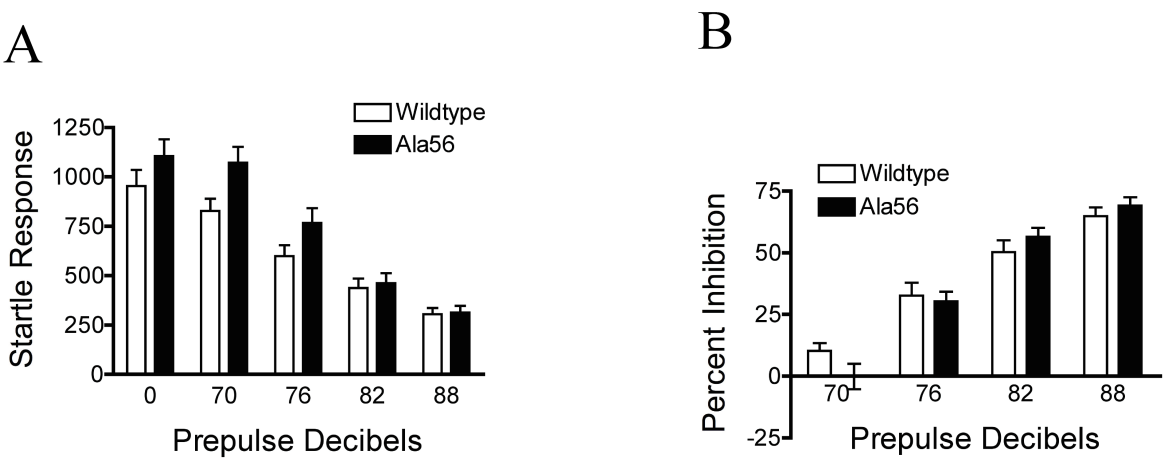

Supplemental Figure 7. Alteration in prepulse inhibition in SERT Ala56 knock-in mice. (A) Acoustic startle response to the 120-dB startle cue across a range of prepulse amplitudes is shown, including the baseline acoustic startle with no prepulse (0 dB). Mice that showed negative prepulse inhibition at three or more prepulse amplitudes were excluded (WT, n = 1; Ala56, n = 2). Two RM ANOVA revealed a significant interaction between genotype and prepulse amplitude ($F = 3.47$, $P = 0.009$). **(B)** Prepulse inhibition across a range of prepulse amplitudes is shown. A two-way RM ANOVA revealed a significant interaction between genotype and prepulse amplitude ($F = 2.91$, $P = 0.036$; WT, n = 26; Ala56, n = 30).

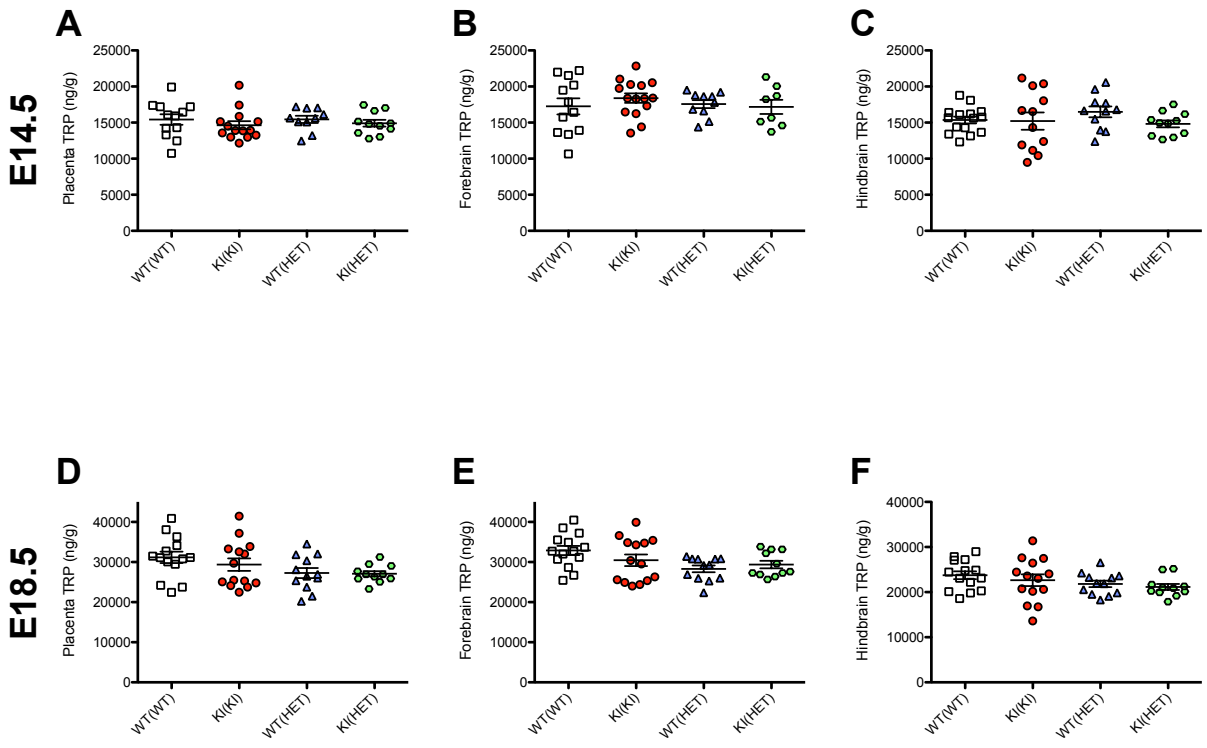

Supplemental Figure 8. Examination of maternal and embryonic SERT Ala56 genotype effects on placenta and fetal brain TRP levels. At E14.5, TRP tissue levels were measured in **(A)** placenta, **(B)** forebrain, and **(C)** hindbrain collected from concepti of wildtype, heterozygous, and homozygous Ala56 dams. At E18.5, TRP tissue levels were once again measured in **(D)** placenta, **(E)** forebrain, and **(F)** hindbrain samples from our various breeder schemes. Unpaired t-tests indicated no significant genotype effects in any of the tissue sources at both of our embryonic time points.

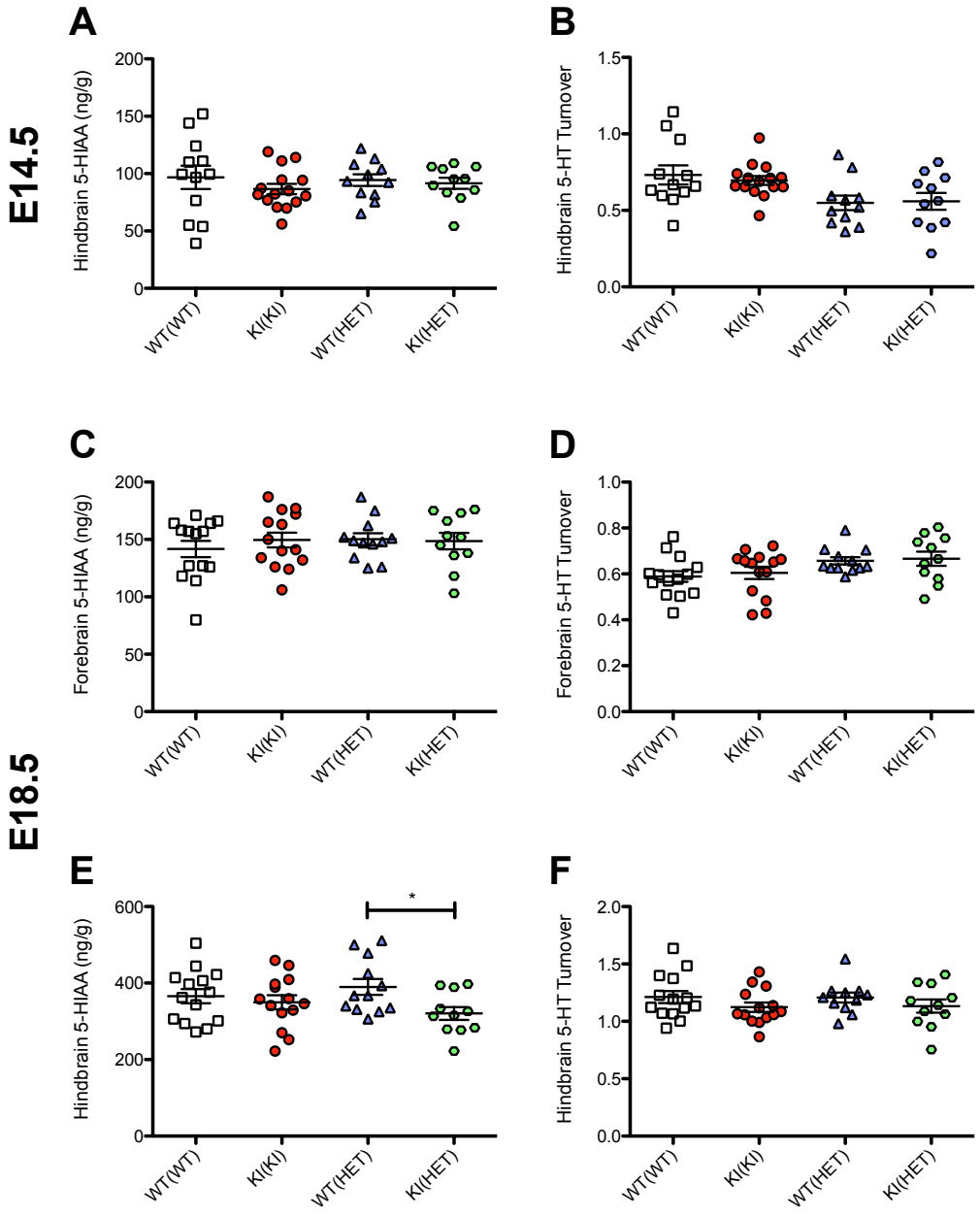

Supplemental Figure 9. Examination of maternal and embryonic SERT Ala56 genotype effects on fetal forebrain and hindbrain 5-HIAA and 5-HT turnover. At E14.5, **(A)** 5-HIAA and **(B)** 5-HT turnover (i.e. 5-HIAA/5-HT) were determined for hindbrain collected from embryos of wildtype, heterozygous, and homozygous Ala56 dams. Unpaired t-tests revealed no significant genotype differences. At E18.5, forebrain **(C)** 5-HIAA and **(D)** 5-HT turnover as well as hindbrain **(E)** 5-HIAA and **(F)** 5-HT turnover were determined tissue levels were also evaluated. Unpaired t-test revealed KI(HET) hindbrain 5-HIAA levels were decreased compared to WT(HET) ($t = 2.557$, $P = .018$; WT(HET) n = 12; KI(HET) n = 11).

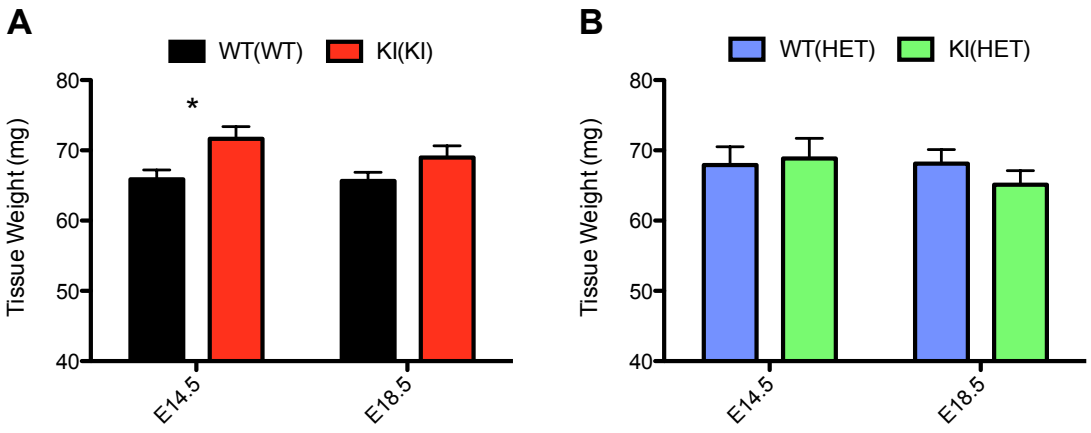

Supplemental Figure 10. Examination of maternal and embryonic SERT Ala56 genotype effects on placenta tissue weight. (A) Two-way ANOVA indicated a main genotype effect on placental tissue weight ($F_{1,107}$ = 8.32, *P* = .0047), with KI(KI) placentas weighing more than WT(WT) samples. This effect was more pronounced at E14.5, as bonferroni post-hoc test was significant at this time point (*P* < .05). **(B)** In contrast, no genotype differences in placental weight were noted in littermates from heterozygous breeders.

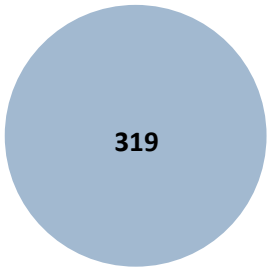

KI(HET) vs WT(HET)

KEGG Pathway	Enrichment Statistics
Ribosome	C=99;O=11;E=1.09;R=10.07;rawP=1.33e-08;adjP=1.13e-06
MAPK signaling pathway	C=268;O=14;E=2.96;R=4.73;rawP=1.95e-06;adjP=8.29e-05
Phagosome	C=176;O=10;E=1.94;R=5.15;rawP=2.81e-05;adjP=0.0006
Antigen processing and presentation	C=78;O=7;E=0.86;R=8.13;rawP=2.52e-05;adjP=0.0006
Focal adhesion	C=199;O=10;E=2.20;R=4.55;rawP=7.92e-05;adjP=0.0013
Endocytosis	C=219;O=10;E=2.42;R=4.14;rawP=0.0002;adjP=0.0024
Chemokine signaling pathway	C=183;O=9;E=2.02;R=4.46;rawP=0.0002;adjP=0.0024
Viral myocarditis	C=88;O=6;E=0.97;R=6.18;rawP=0.0004;adjP=0.0043
Leukocyte transendothelial migration	C=119;O=6;E=1.31;R=4.57;rawP=0.0021;adjP=0.0198
Allograft rejection	C=52;O=4;E=0.57;R=6.97;rawP=0.0026;adjP=0.0201

Wiki Pathway	Enrichment Statistics
Cytoplasmic Ribosomal Proteins	C=78;O=11;E=0.86;R=12.78;rawP=1.00e-09;adjP=5.70e-08
Adipogenesis	C=133;O=9;E=1.47;R=6.13;rawP=1.78e-05;adjP=0.0005
MAPK signaling pathway	C=165;O=9;E=1.82;R=4.94;rawP=9.65e-05;adjP=0.0018
Chemokine signaling pathway	C=184;O=9;E=2.03;R=4.43;rawP=0.0002;adjP=0.0029
Splicing factor NOVA regulated synpatic proteins	C=58;O=5;E=0.64;R=7.81;rawP=0.0005;adjP=0.0057
Wnt Signaling Pathway	C=61;O=5;E=0.67;R=7.43;rawP=0.0006;adjP=0.0057
Hypertrophy Model	C=20;O=3;E=0.22;R=13.59;rawP=0.0013;adjP=0.0106
Myometrial Relaxation and Contraction Pathways	C=158;O=7;E=1.74;R=4.01;rawP=0.0019;adjP=0.0135
IL-2 Signaling Pathway	C=92;O=5;E=1.02;R=4.92;rawP=0.0036;adjP=0.0228
Focal Adhesion	C=186;O=7;E=2.05;R=3.41;rawP=0.0048;adjP=0.0249

Supplemental Figure 11. KEGG and Wiki Pathway analyses of 319 placental DEGs identified from KI(HET) vs. WT(HET) group comparison. Comparison of KI and WT littermate placental samples identified 319 DEGs that exhibit embryo SERT Ala56 genotype effects. Top and bottom tables display top 10 statistically enriched pathways in KEGG and Wiki pathway analyses, respectively.

APPENDIX 1

EVALUATION OF WHOLE BLOOD SEROTONIN AND TRYPTOPHAN LEVELS DURING PREGNANCY IN SERT ALA56 DAMS

Although the uptake of 5-HT from placental syncytiotrophoblasts has been documented *in vitro*, it remains unclear whether changes in maternal whole blood 5-HT negatively impact placental physiology. To begin to answer this question, we conducted a longitudinal study of whole blood 5-HT and TRP levels during pregnancy in SERT Ala56 dams and WT controls. While no statistically significant genotype differences were found in our study, we discovered that whole blood 5-HT and TRP levels exhibit a dynamic trajectory during pregnancy. Whole blood 5-HT steadily declines until E14.5, at which point 5-HT levels increase and eventually exceed pre-pregnancy levels at E18.5 and persist post partum. In contrast, whole blood TRP is relatively stable until a sudden decrease at E18.5 that normalizes to pre-pregnancy levels after birth. Further studies are needed to understand the source of peripheral 5-HT system changes during pregnancy and their contribution to maintaining 5-HT homeostasis in the placenta.

Methods

Blood Collection

Beginning three days prior to the experimental protocol, virgin female mice were handled daily to minimize stress reactivity during blood draw procedures. Using submandibular bleeds, blood was drawn from unanesthetized females at various time points during their pregnancy. Blood draws occurred a week prior to pregnancy, 7.5

days post conception, 14.5 days post conception, 18.5 days post conception, and a week post partum. After the E18.5 time point, sires were removed from breeding cages to prevent impregnation of dams after birth of offspring. Blood was collected into K_2EDTA coated tubes (BD Biosciences) and stored at -80 °C until HPLC analysis with fluorometric detection as previously described.

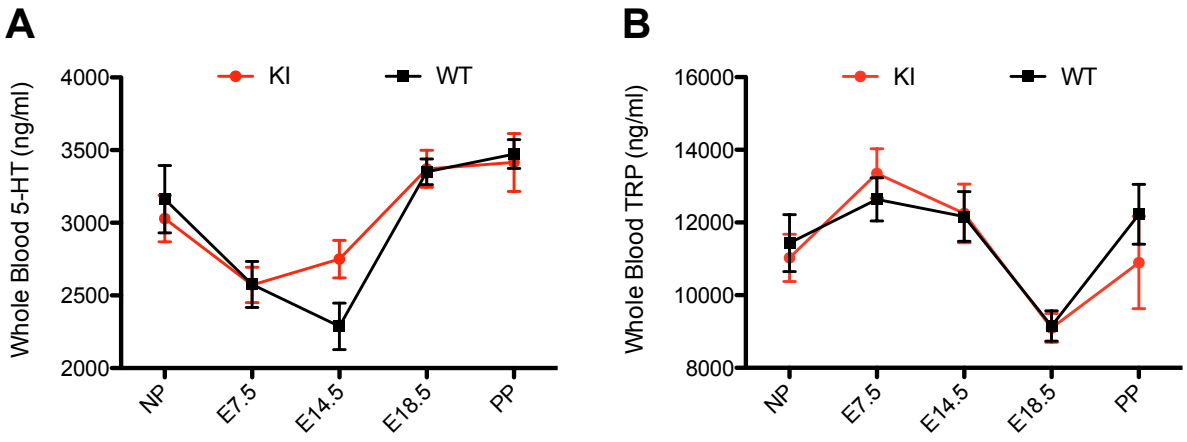

Appendix Figure 1. No changes in the trajectory of whole blood 5-HT and TRP levels during pregnancy in SERT Ala56 dams. (A) Two-way RM ANOVA indicated a significant main effect of pregnancy time point ($F_{4,48}$ = 15.96, P < .0001; WT n = 7; KI n = 7) on whole blood 5-HT, but no genotype main effect. Bonferroni post hoc test was not significant at E14.5. **(B)** Two-way RM ANOVA also found a significant main effect of pregnancy time point ($F_{4,48}$ = 8.46, P < .0001; WT n = 7; KI n = 7) on whole blood TRP. NP – Not Pregnant, PP – Post Partum.

APPENDIX 2

INITIAL EXAMINATION OF SENSORY FUNCTION IN SERT ALA56 MICE

Due to the original association with sensory aversion in affected SERT Ala56 carriers, our lab has had an interest in characterizing sensory function in SERT Ala56 mice. Our initial attempts to evaluate sensory-related behavior utilized von Frey monofilament sensitivity and the hot plate test, two common assays to assess somatosensation and nociception respectively in mice. Using a cohort of adult male littermates, we found that SERT Ala56 mice possess normal sensitivity to von Frey monofilaments and noxious thermal stimuli, indicating intact basic sensory processing.

For a more fine-grained measure of sensory function, we also examined patterns of neuronal activation in barrel cortex upon whisker stimulation. Specifically, we quantified the induction of cFos expression in barrel cortex of freely behaving SERT Ala56 mice that were allowed to explore a novel environment. Interestingly, while we saw no genotype differences in barrel cortex activation upon whisker stimulation, SERT Ala56 mice exhibited increased cFos expression across multiple cortical layers in barrel field architecture at baseline, with the largest differences observed in cortical layer IV, the main thalamic input layer. As a baseline measure of somatosensory neuronal activity in our experimental paradigm, whiskers on the left side of the snout were trimmed to the skin to prevent peripheral stimulation of barrel cortex. Future studies are required to study the nature of this excitatory imbalance in barrel cortex and whether this imbalance is found globally in the brain or is specific to sensory systems.

Methods

von Frey

Tactile sensitivity was assessed using plastic von Frey monofilaments applied to plantar surface of the subject's right hind paw. Briefly, each subject was placed into a plexiglass chamber with a wire mesh flooring for experimental access to the mouse footpad. Subjects were allowed to habituate to the testing chamber for 5 minutes before the assessment of tactile sensitivity. Von Frey monofilaments (Stoetling Co.) of ascending diameter were applied to the subject's hind paw until reaching the target force (i.e. bending of the filament). The lowest force required to elicit a paw withdrawal response was considered a subject's tactile sensitivity threshold.

Hot Plate Test

Thermal sensitivity was assessed using the hot plate test as previously described. Briefly, experimental mice were allowed to acclimate to the testing room for 30 min prior to testing. For each test trial, a mouse was placed onto a hot plate heated to 55 °C with plexiglass cylindrical barrier surrounding the test area. The latency to demonstrate a nociceptive response (i.e. hind paw lick, hind paw flick, jumping) was recorded by an observer blind to genotype, and the mouse was immediately removed from the hot plate. If mice did not show a clear response after 30 sec, the trial was terminated and the subject was excluded from the dataset.

Novelty-Induced Whisker Stimulation Behavioral Paradigm

The day before the behavioral whisker stimulation paradigm, adult WT and SERT Ala56 littermate male mice were put under light isoflurane sedation to trim whiskers on their left snout. After whisker trimming, mice were individually housed to prevent additional whisker barbering from cagemates. On the day of procedure, mice were habituated to testing room for 30 min prior to behavioral assay. Following the habituation period, mice were transferred to novel cage with various inanimate objects placed in the cage bedding to facilitate exploratory behavior and whisker stimulation. Under low light conditions, mice were allowed to explore the novel cage environment for 2 hr and their activity was recording by video. There were no genotype differences in activity during this task (data not shown). At the conclusion of the 2 hr exploration period, mice were administered sodium pentobarbital, perfused with 4% paraformaldehyde in .1 M phosphate buffer (PB) pH 7.4, and their brains were harvested for downstream immunohistochemistry (IHC) applications. To help differentiate whisker stimulated vs. unstimulated brain hemispheres, a small part of the left ventral brain was removed to indicate the stimulated side.

cFos Immunohistochemistry and Quantification

Perfused brains were postfixed overnight in 4% paraformaldehype, transferred to 30% sucrose in .1 M PB until sunk, and sectioned on a microtome to a thickness of 40 µm. Barrel field containing sections were peroxidase quenched in .3% H_2O_2 in methanol for 30 min, blocked in PBS with 5% normal donkey serum and 0.3% Triton X-100 for 2 hr at room temperature, and incubated in anti-cFos primary antibody (1:5000; Santa

Cruz) for 72 hr at 4 °C. After washing in PBS with .3% Triton X-100, sections were incubated in biotinylated donkey anti-rabbit (1:500; Jackson ImmunoResearch) secondary antibody for 2 hr at room temperature. Washed sections were incubated with ABC reagent and DAB substrate (Vector Labs) per manufacturer's instruction for visualization of stained cells. cFos immunostaining was quantified using Image J by a research assistant blind to sample genotype. Areas corresponding to cortical layers were traced, and cFos expression was quantified as % of area stained. Quantification of outer most cortical layer (layer I) was excluded due to defects caused by tissue processing.

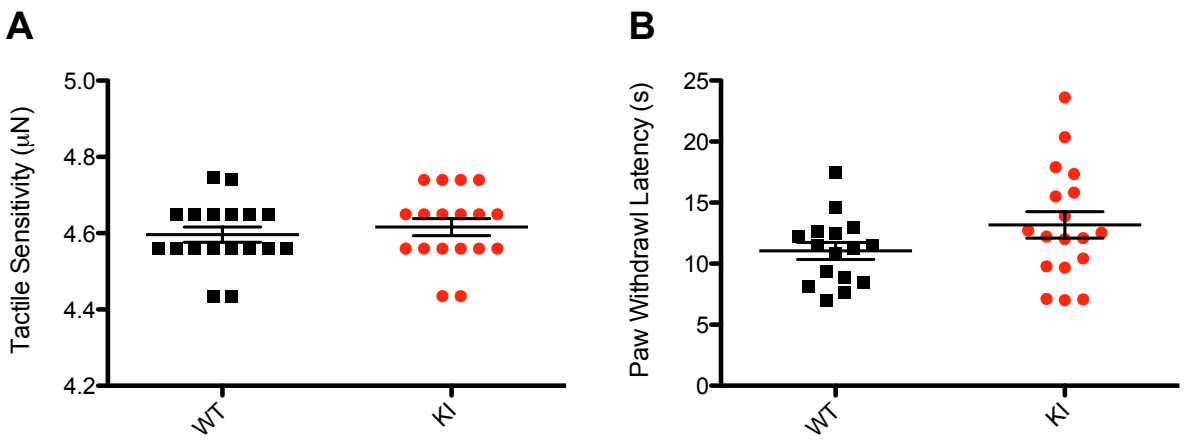

Appendix Figure 2. No changes in basic measures of somatosensation and nociception in SERT Ala56 mice. (A) Unpaired t-test indicated no significant genotype difference in von Frey tactile sensitivity (t = .66, *P* = .52; WT n = 18; KI n = 18) **(B)** Similarly, unpaired t-test indicated no significant genotype difference in paw withdrawl latency (t = 1.65, *P* = .11; WT n = 16; KI n = 18). μN – Micronewton.

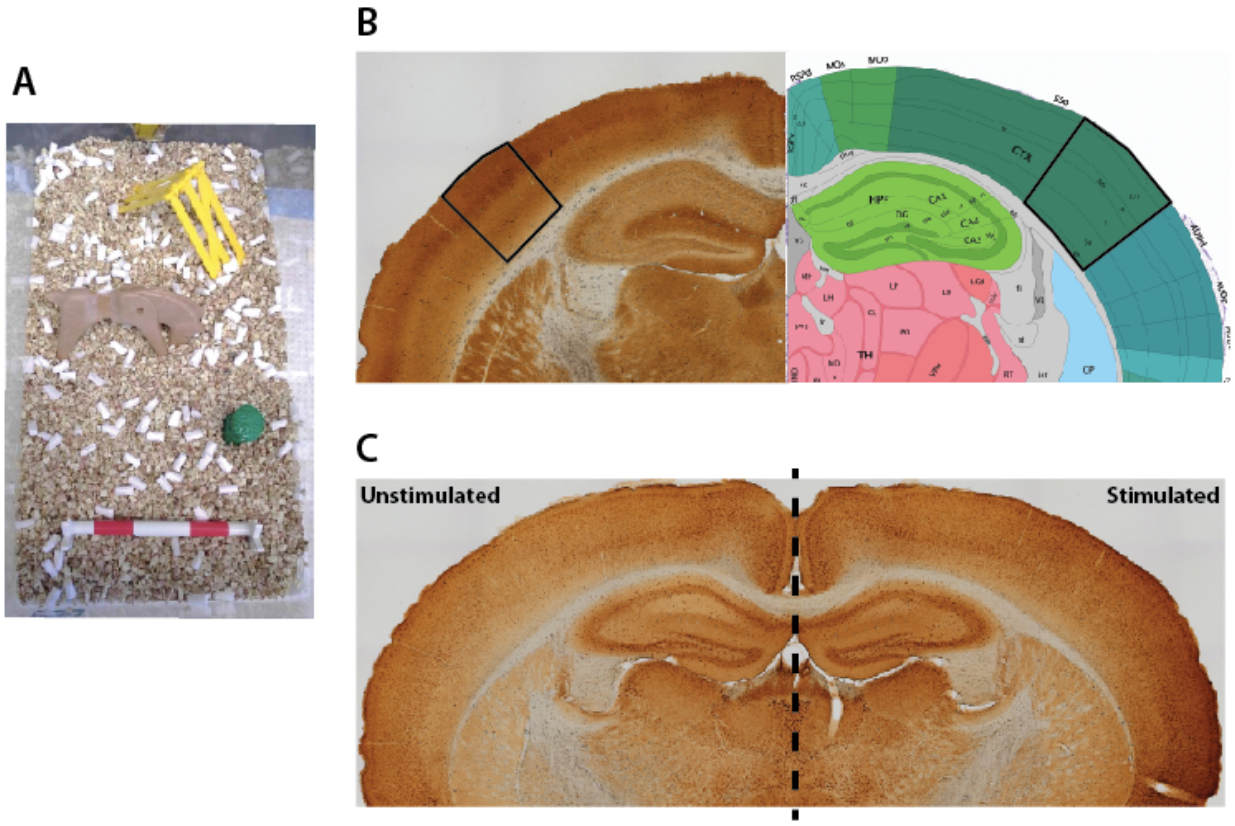

Appendix Figure 3. Whisker stimulation paradigm to examine sensory processing in barrel cortex. (A) Mice were allowed to explore a novel cage environment that was enriched with various inanimate objects. **(B)** Cytochrome oxidase (CO) histochemistry of coronal brain sections confirmed barrel field regions of interest as outlined by the Allen Brain Atlas. **(C)** Representative image of barrel cortex cFos expression in mice that underwent whisker stimulation behavioral paradigm. The 'stimulated' brain hemisphere received stimulation from intact whiskers on the rodent snout. In contrast, the 'unstimulated' brain hemisphere received minimal stimulation from trimmed whiskers.

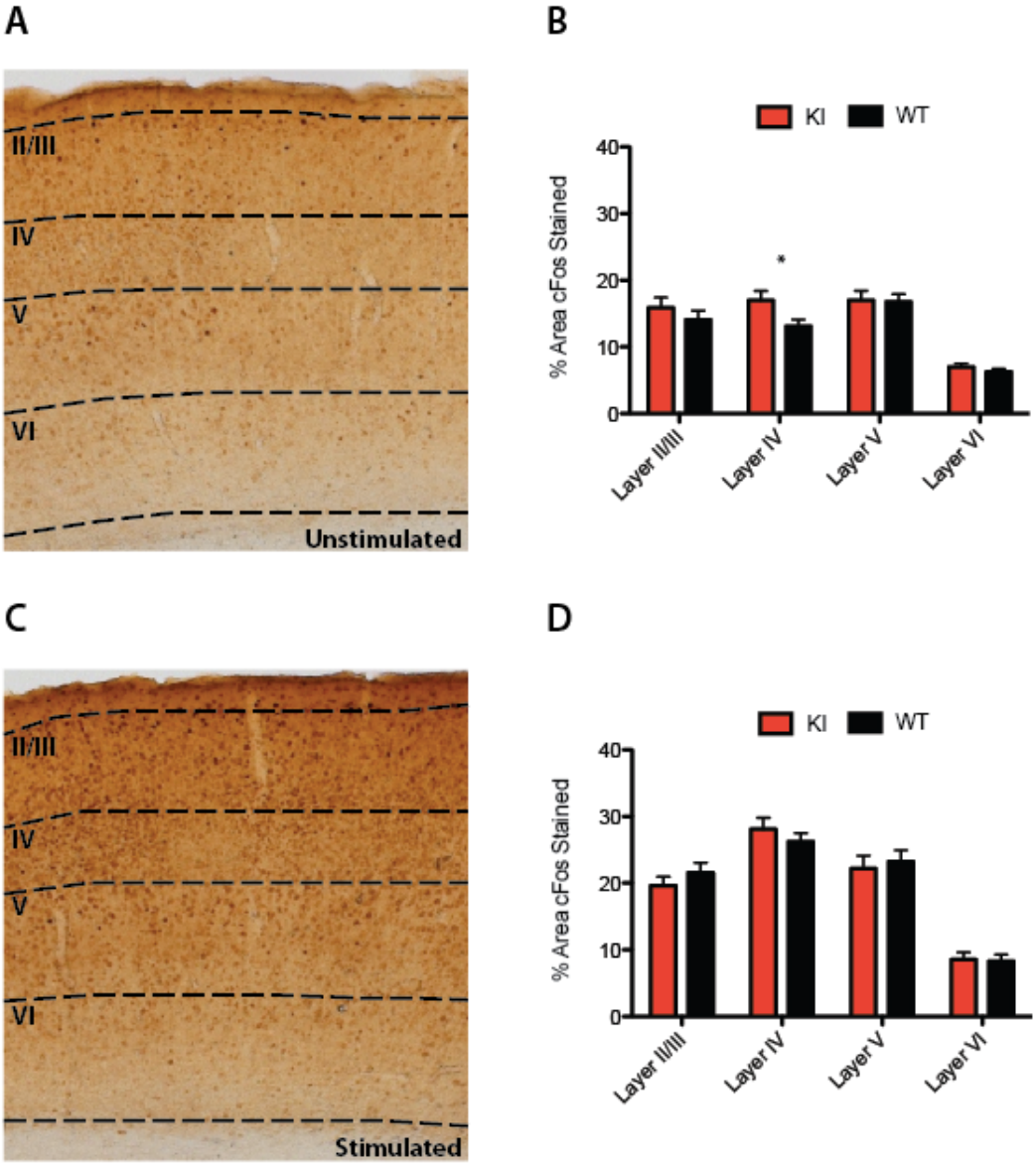

Appendix Figure 4. cFos expression in 'unstimulated' layer IV of barrel cortex is increased in SERT Ala56 mice. (A) Representative image of 'unstimulated' barrel cortex used for quantification (WT n = 9; KI n = 9). CO histochemistry (Appendix Figure 3B) helped define cortical layer landmarks. **(B)** Two-way RM ANOVA indicated main effects of both cortical layer ($F_{3,32}$ = 19.53, P < .0001) and genotype ($F_{1,32}$ = 8.42, P = .0067) on cFos expression in 'unstimulated' barrel cortex, with Ala56 mice displaying increased cFos expression. Bonferroni post hoc test was significant at cortical layer IV (P < .01). **(C)** Representative image of 'stimulated' barrel cortex used for quantification. **(D)** Two-way RM ANOVA again indicated a significant main effect of cortical layer on cFos expression ($F_{3,32}$ = 38.16, P < .0001), but there were no significant genotype differences in whisker 'stimulated' barrel cortex.

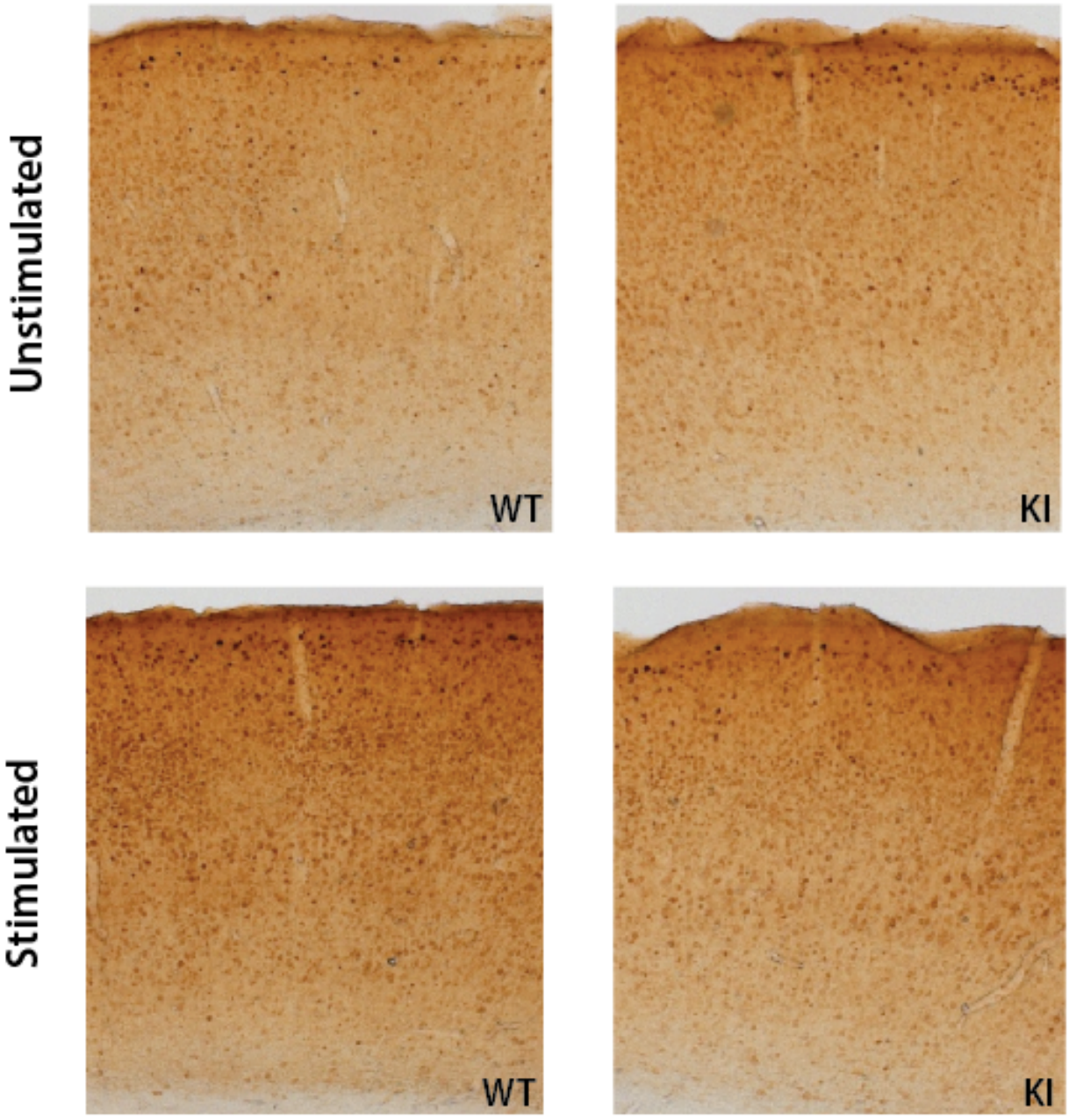

Appendix Figure 5. Representative comparison images demonstrating basal increases in barrel cortex cFos expression in SERT Ala56 mice.

APPENDIX 3

CHARACTERIZATION OF BARREL CORTEX INTERNEURONS IN SERT ALA56 MICE

Although the pathophysiology of ASD remains poorly understood, several investigators have hypothesized that subtle imbalances between excitatory and inhibitory neurotransmission may underlie the deficits observed in the disorder. Consequently, several mouse models of ASD have been scrutinized for abnormalities in the development and function of GABAergic interneurons, the primary neuronal regulators of inhibitory signaling in the brain. As an initial attempt to examine inhibitory function in SERT Ala56 mice, we conducted a series of immunostaining experiments to characterize the distribution of interneurons in barrel cortex. Besides providing an easily identifiable anatomical region for quantification, we focused on interneuron distribution in barrel cortex due to basal increases in barrel field cFos expression that were found in SERT Ala56 mice (Appendix Figure 4B). In our first immunostaining experiment, we discovered that SERT Ala56 mice have statistically significant decreases in the number of interneurons expressing GAD67, one of the enzyme isoforms that decarboxylates glutamate to produce GABA. To follow up on these findings, we then examined the distribution of interneurons expressing two different calcium-binding proteins commonly used to subclassify interneurons into functionally distinct groups, parvalbumin and somatostatin. However, in contrast to our GAD67 data, there were no significant genotype differences in the number of parvalbumin or somatostatin expressing cells in barrel cortex. In addition to electrophysiological studies confirming deficits in inhibitory

neurotransmission in SERT Ala56 mice, future work will be required to identify the specific interneuron subpopulations that are sensitive to enhanced SERT function.

Methods

GAD67 Immunohistochemistry

Perfused brains were processed as previously described in appendices. Barrel field containing sections were peroxidase quenched in .3% H_2O_2 in methanol for 30 min, blocked in PBS with 5% normal donkey serum and 0.001% Triton X-100 for 2 hr at room temperature, and incubated in anti-GAD67 (1:2000, Millipore) primary antibody for 72 hr at 4 °C. After washing in PBS with .001% Triton X-100, sections were incubated in biotinylated donkey anti-mouse (1:1000, Jackson ImmunoResearch) secondary antibody for 1.5 hr at room temperature. Washed sections were incubated with ABC reagent and DAB substrate (Vector Labs) per manufacturer's instructions for visualization of stained cells.

Parvalbumin and Somatostatin Immunohistochemistry

Perfused brains were processed as previously described in appendices. Barrel field containing sections were peroxidase quenched in .3% H_2O_2 in methanol for 30 min, blocked in PBS with 5% normal donkey serum and 0.1% Triton X-100 for 2 hr at room temperature, and incubated in either anti-parvalbumin (1:500, Sigma) or anti-somatostatin (1:400, Millipore) primary antibody for 72 hr at 4 °C. After washing in PBS with .1% Triton X-100, sections were incubated for 1.5 hr at room temperature in biotinylated donkey anti-mouse or donkey anti-rat secondary antibody (1:1000, Jackson ImmunoResearch) for parvalbumin and somatostatin IHC, respectively. Washed

sections were incubated with ABC reagent and DAB substrate (Vector Labs) per manufacturer's instructions for visualization of stained cells.

Quantification

Interneuron immunostaining was quantified using Image J by a research assistant blind to sample genotype. Areas corresponding to cortical layers were traced, and GAD67, parvalbumin, and somatostatin positive cells were counted. Quantification of outer most cortical layer (layer I) was excluded due to defects caused by tissue processing.

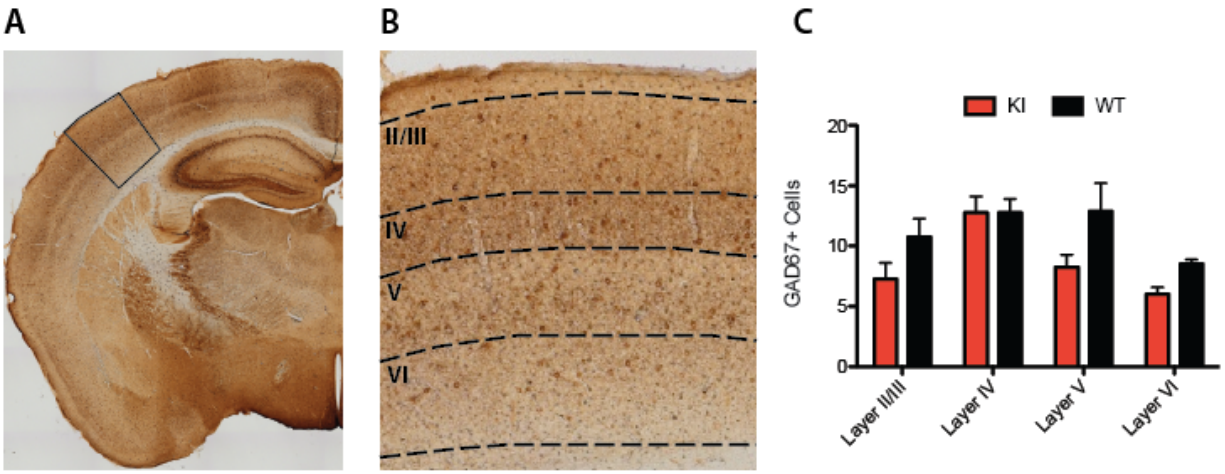

Appendix Figure 6. The number of GAD67 expressing interneurons in barrel cortex is decreased in SERT Ala56 mice. (A) Matching coronal sections containing barrel cortex were chosen to examine the distribution of GAD67+ interneurons (WT n = 8; KI n = 8). The black outline designates cortical region isolated for measurements. **(B)** Representative image used to quantify number of GAD67 + cells in each cortical layer. **(C)** Two-way RM ANOVA indicated main effects of cortical layer ($F_{3,28}$ = 5.32 , *P* = .005) and genotype ($F_{1,28}$ = 9.24 , *P* = .005), with Ala56 mice possessing fewer GAD67+ interneurons than littermates controls.

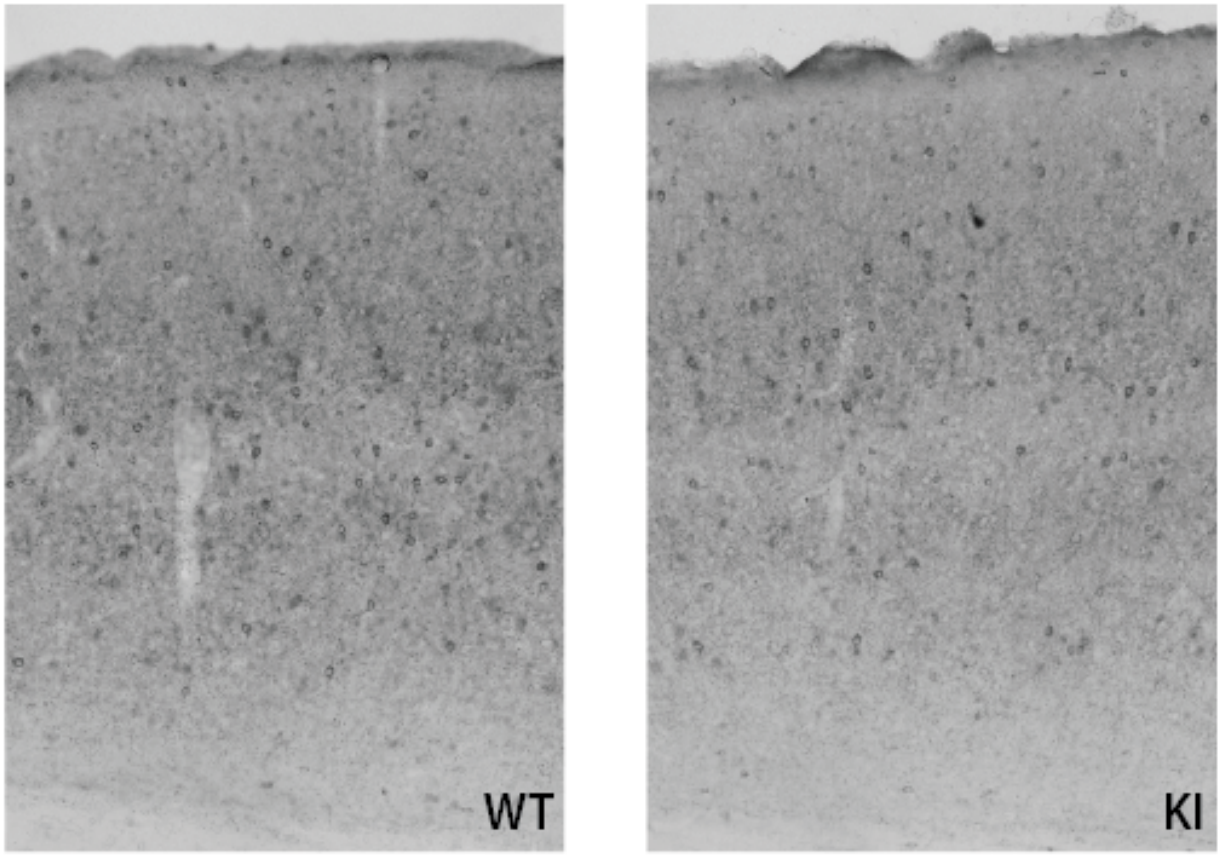

Appendix Figure 7. Representative comparison images demonstrating decreased number of GAD67+ interneurons in barrel cortex of SERT Ala56 mice.

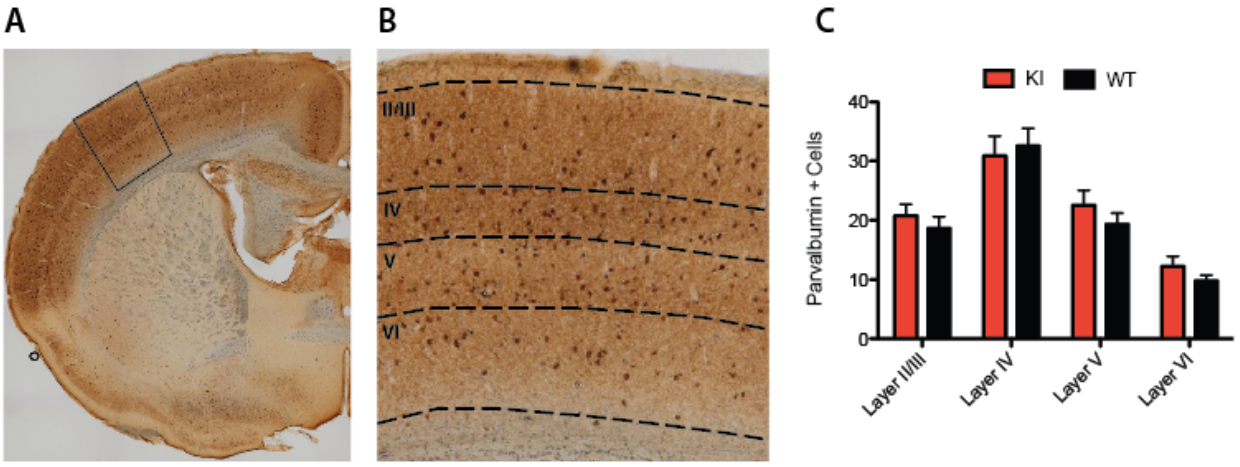

Appendix Figure 8. No changes in parvalbumin expressing interneurons in barrel cortex of SERT Ala56 mice. (A) Matching coronal sections containing barrel cortex were chosen to examine the distribution of parvalbumin+ interneurons (WT n = 9; KI n = 9). The black outline designates cortical region isolated for measurements. **(B)** Representative image used to quantify number of parvalbumin+ cells in each cortical layer. **(C)** Two-way RM ANOVA indicated a main effect of cortical layer ($F_{3,64}$ = 27.77 , *P* < .0001), but no genotype differences in the number of parvalbumin+ interneurons.

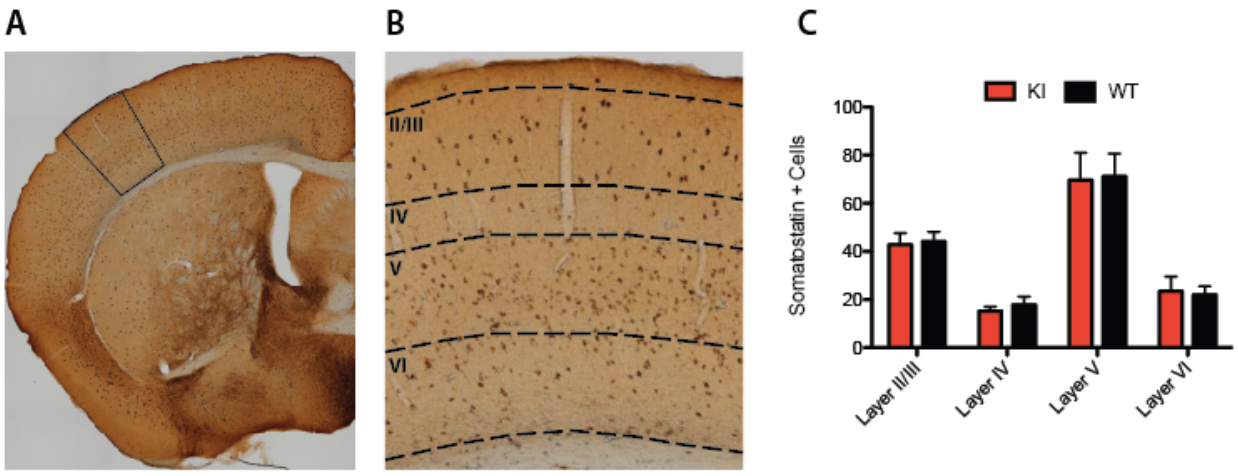

Appendix Figure 9. No changes in somatostatin expressing interneurons in barrel cortex of SERT Ala56 mice. (A) Matching coronal sections containing barrel cortex were chosen to examine the distribution of somatostatin+ interneurons (WT n = 8; KI n = 8). The black outline designates cortical region isolated for measurements. **(B)** Representative image used to quantify number of somatostatin+ cells in each cortical layer. **(C)** Two-way RM ANOVA indicated a main effect of cortical layer ($F_{3,28}$ = 16.47 , *P* < .0001), but no genotype differences in the number of somatostatin+ interneurons.

APPENDIX 4

ANATOMICAL CHARACTERIZATION OF BARREL CORTEX IN SERT ALA56 MICE

Alterations in 5-HT signaling during rodent neurodevelopment disrupt the formation of primary sensory structures, most notably whisker barrel field architecture in primary somatosensory cortex. While perturbations that increase extracellular 5-HT levels cause dramatic anatomical changes in barrel cortex, decreased extracellular 5-HT results in only subtle changes in morphology, with some studies reporting small, but significant decreases in barrel area in tangential brain sections. Since the SERT Ala56 variant causes increased, dysregulated 5-HT transport, we hypothesized that SERT Ala56 mice may possess subtle anatomical changes that would mirror findings in extracellular 5-HT depletion models. Moreover, these potential changes in SERT Ala56 barrel cortex may be relevant to the pathophysiology underlying sensory aversion observed in Ala56 carriers with ASD. Our examination of adult male littermates revealed no genotype differences in the size or spatial configuration of barrel cortex. Further characterization of SERT Ala56 barrel cortex during the first postnatal week of life revealed no changes in the maturation of barrel field architecture. Additionally, there were no significant differences in the orientation of barrel cortex relative to other primary sensory cortical areas in SERT Ala56 mice. Although these studies indicate that the Ala56 variant does significantly impact the basic anatomy of barrel cortex, further work is needed to evaluate the functional activation of the whisker-to-barrel pathway in SERT Ala56 mice.

Methods

Tissue Preparation for Tangential Brain Sections

P7 and P56 littermates from heterozygous SERT Ala56 breeding pairs were perfused and cortices were dissected from each brain hemisphere. Cortices were flattened between two slides and placed in 30% sucrose in .1 M PB overnight for cyroprotection. Flattened cortices were then sectioned on a sliding freezing microtome to a thickness of 40 μm. The order of the sections relative to the pial surface was maintained during all histochemical and immunohistochemical procedures.

Cytochrome Oxidase Histochemistry

In P56 male animals, barrel field architecture was visualized with cytochrome oxidase (CO) histochemistry as previously described. Briefly, PB washed sections were incubated at 37 °C for 2 hr in 1 mL of a CO reaction solution containing: 100 mL .1 M PB, 4 g sucrose, 75 mg cytochrome C, and 50 mg DAB. After 2 hr incubation, washed sections were mounted onto subbed slides.

Serotonin Immunohistochemsitry

In P7 male animals, barrel cortex and surrounding primary sensory structures were visualized with 5-HT immunohistochemistry. Sections were blocked in PBS with 3% normal donkey serum and .1% Triton X-100 for 1.5 hr at room temperature, and incubated in anti-serotonin (1:500, Sigma) primary antibody overnight at 4 °C. After washing in PBS with .1% Triton X-100, sections were incubated for 2 hr at room temperature in Alexa Fluor 488 donkey anti-rabbit secondary antibody (1:500, Jackson

ImmunoResearch). Sections were counterstained with DAPI mounting medium (Vector Labs).

P56 Barrel Cortex Size and Shape Morphometric Analysis

Tangential section images were overlaid in Adobe Photoshop CS6 to reconstruct the posteromedial barrel subfield (PMBSF) corresponding to the major facial whiskers on the rodent snout. The reconstructed PMBSF was traced for subsequent size and shape morphometric analyses. 'Area' and 'centroid' measurements were obtained in Image J for each traced barrel. In addition, the total barrel field area encapsulating the PMBSF was measured to calculate septa area (i.e. 'total barrel field area' – 'sum of individual barrels area' = septa area). Using the *R* shapes statistical package, barrel centroid coordinates were utilized to perform generalized Procrustes analysis.

P7 Primary Sensory Area Shape Morphometric Analysis

Tangential section images were overlaid in Adobe Photoshop CS6 to reconstruct primary somatosensory (S1), visual (V1), and auditory cortex (A1). The reconstructed primary sensory cortices were traced for shape morphometric analysis. 'Centroid' measurements were obtained in Image J for each traced sensory area (i.e. S1-barrel cortex, S1-body, V1, and A1). Using the *R* shapes statistical package, sensory area centroid coordinates were utilized to perform generalized Procrustes analysis.

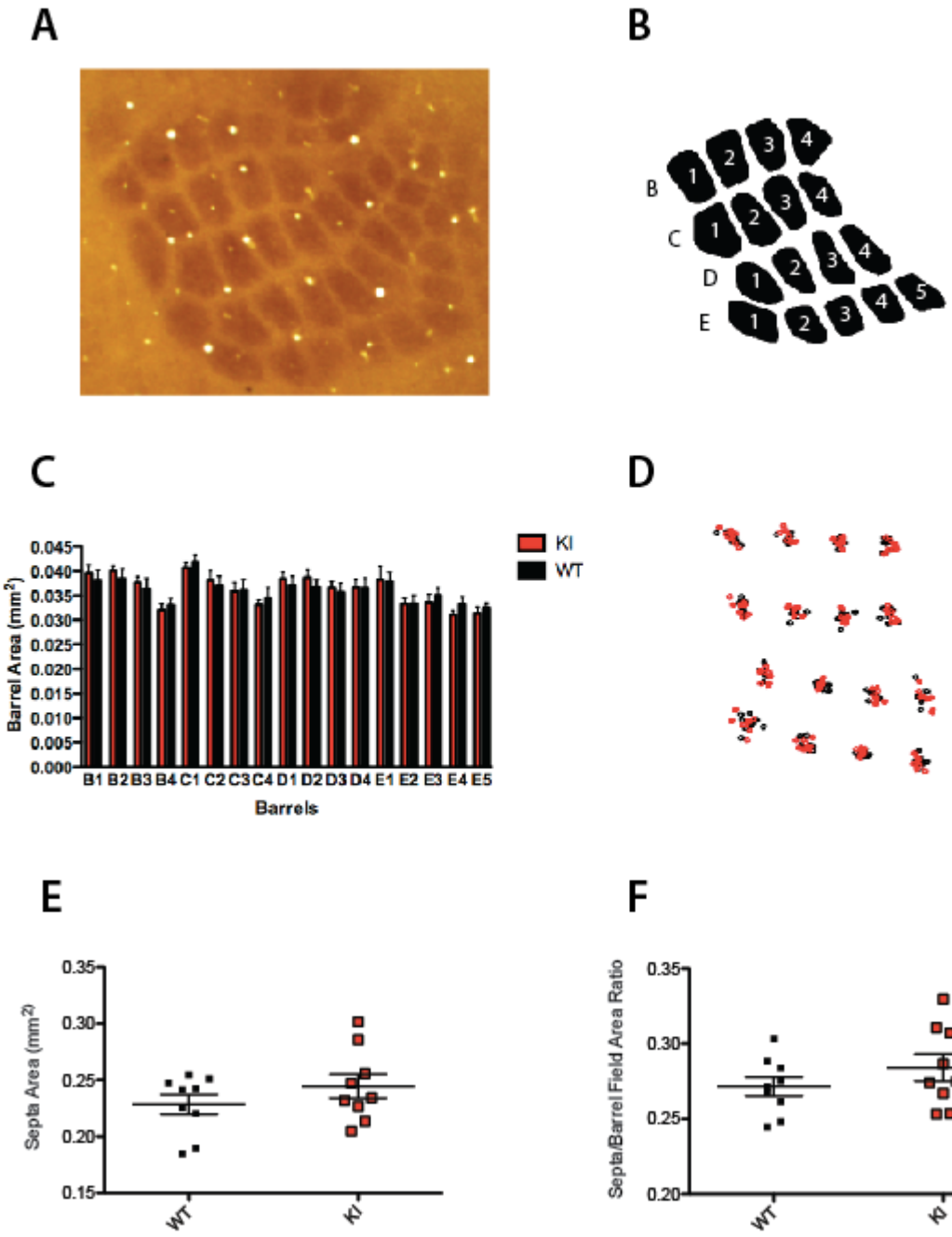

Appendix Figure 10. No anatomical changes in adult SERT Ala56 barrel cortex. **(A)** Representative image of SERT Ala56 barrel cortex in the tangential plane as visualized with CO histochemistry (WT n = 9; KI n = 9). **(B)** Major barrels of the PMBSF in rows B-E were traced for size and shape morphometric analysis. **(C)** There were no significant genotype differences found in individual or overall barrel area. **(D)** Procrustes superimposition of 17 barrel centroid landmarks from wildtype (black) and SERT Ala56 mice (red). Goodall's F test indicated no differences in the spatial orientation of barrel field architecture in SERT Ala56 mice. **(E)** Septa area and the **(F)** septa/barrel field area ratio was also unchanged in SERT Ala56 mice.

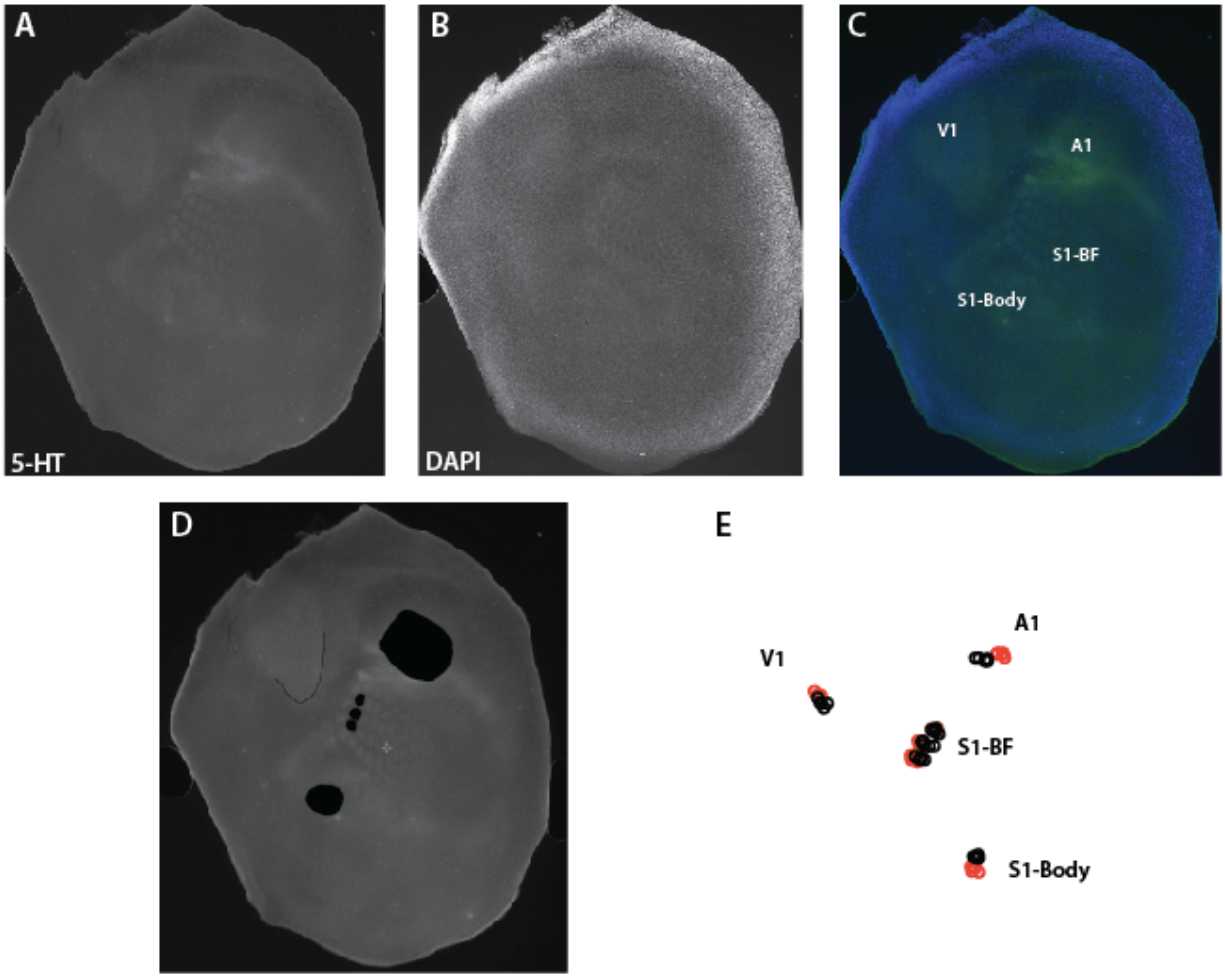

Appendix Figure 11. No changes in the cortical topography of primary sensory areas in P7 SERT Ala56 mice. A combination of **(A)** 5-HT immunohistochemistry and **(B)** DAPI counterstaining was used to **(C)** visualize primary sensory areas in tangential brain sections. **(D)** Landmarks in S1, V1, and A1 were traced for shape morphometric analysis. **(E)** Procrustes superimposition of 6 cortical centroid landmarks from wildtype (black) and SERT Ala56 mice (red). Goodall's F test indicated no differences in the spatial orientation of primary sensory areas in SERT Ala56 mice. A1 – Primary Auditory Cortex, S1 – Primary Somatosensory Cortex, V1 – Primary Visual Cortex, BF – Barrel Field

APPENDIX 5

GENETIC BACKGROUND MODULATES PHENOTYPES OF SEROTONIN TRANSPORTER ALA56 KNOCK-IN MICE

Portions published in: Genetic Background Modulates Phenotypes of Serotonin Transporter Ala56 Knock-in Mice*. Mol Autism 4, 35 (2013)*

Travis M. Kerr, Christopher L. Muller, Mahfuzur Miah, Christopher S. Jetter, Rita Pfeiffer, Charisma Shah, Nicole Baganz, George M. Anderson, Jacqueline N. Crawley, James S. Sutcliffe, Randy D. Blakely, Jeremy Veenstra-VanderWeele

As 5-HT is a modulator of multiple CNS pathways subserving complex behaviors, we hypothesized that SERT coding variation could be influenced by genetic variation in other genes, which might account for the variable phenotype observed in humans with the SERT Ala56 allele. To explore this hypothesis, we moved the SERT Ala56 allele to a C57BL/6 (B6) background for two purposes: 1) to examine autism-relevant behavior in a more active and social strain than 129, and 2) to study strain dependence of SERT function, the 5-HT system, and resulting behavior. Previous work identified a functional and behavioral impact of variation at two amino acids that differ between 129 and B6 inbred strains. We therefore also backcrossed the 129 SERT onto the B6 background to allow a comparison with the mutant SERT on this background. Our findings reveal a striking influence of genetic background on the impact of the SERT Ala56 variant, suggesting that further dissection of strain differences could illuminate other genes modulating risk of ASD.

Methods

Backcross

Male SERT Ala56 mice (Glu39/Ala56/Arg152) on a mixed 129S6/SvEvTac and 129S4/ImJ background were crossed with C57BL/6 females, with male progeny from each generation crossed again to C57BL/6 females for at least 8 generations. The Jackson Lab Genome Scanning Service was used to verify congenic status with C57BL/6. In parallel, wildtype 129S6/S4 mice from the same colony (SERT Glu39/Gly56/Arg152) were backcrossed at least 10 generations to C57BL/6 and verified congenic with C57BL/6 to serve as valid control animals. SERT Gly56Ala and SERT Arg152/Lys genotyping was performed as described previously. Sanger sequencing was used to verify that the SERT Ala56 was maintained after the full backcross.

Behavioral Testing

Co-housed littermate progeny of heterozygous pairs (SERT Gly56/Ala56) were used for all behavioral testing. A cohort of 20 matched male Ala56/Ala56 and Gly56/Gly56 littermates, as well as 16 co-housed matched male Ala56/Gly56 littermates, was used in behavioral experiments in the following order to minimize order effects on testing: Elevated Zero Maze, Light-Dark Test, Open Field Activity, Three-Chamber Sociability Test, Tube Test, Y Maze Spontaneous Alternation, von Frey filament test. A subset of this cohort was used for Home Cage Monitoring (12 Ala56/Ala56 and 12 Gly56/Gly56). A cohort of 20 matched female Ala56/Ala56, Ala56/Gly56, and Gly56/Gly56 littermates was used in behavioral experiments in the following order: Elevated Zero Maze, Light-Dark Test, Open Field Activity.

Elevated Zero Maze

Assessment of anxiety-like behaviors were evaluated using an elevated zero maze, as described previously for 5 min under standard fluorescent light (Frederick et al., 2012).

Light-Dark Exploration

Anxiety-like responses were evaluated using activity monitors (Med Associates, Inc.) divided in half to create a light compartment and a dark compartment, as described previously, with the subject mouse placed in the light compartment at the beginning of the test and activity recorded for 5 minutes (Bazalakova et al., 2007).

Open Field Activity

Exploratory locomotor activity was evaluated in activity monitors (Med Associates, Inc.), as described previously (Veenstra-VanderWeele et al., 2012).

Three-Chamber Sociability Test

Social behavior was evaluated in a three-chamber polycarbonate apparatus with 4-inch sliding gates separating the 7 × 9-inch chambers. The subject mouse was initially allowed to explore all three chambers for 10 min to acclimate to the apparatus. A stimulus mouse (social stimulus) was then introduced inside an inverted wire pencil cup (Spectrum Diversified Designs) in one side chamber with a clean empty pencil cup (inanimate stimulus) introduced in the opposite side chamber. The stimulus mouse was an adult male 129S4/ImJ mouse, previously habituated to the pencil cup in six 30-

minute sessions across 3 days. The subject mouse was then allowed to explore all three chambers for 10 minutes. A new stimulus mouse was then introduced inside a pencil cup in the previous inanimate stimulus chamber. The subject mouse was finally allowed to explore all three chambers for 10 minutes. A research assistant blinded to mouse genotype coded videos for time spent in each chamber and within 1 cM of each pencil cup.

Tube Test

The tube test was conducted in male mice as described previously. The apparatus is a 30-cm-long, 3.5-cm-diameter clear acrylic tube with small acrylic funnels added to each end to facilitate entry into the tube. On two separate days before testing, each mouse was exposed to the tube, with progress through the tube resulting in the mouse being returned to the home cage. Mice that did not initially enter the tube were encouraged to run forward with a gentle pull of the tail. For each bout, a mouse was paired with a stranger mouse from a different cage. The “winner” mouse was declared when the other mouse backed out of the tube. Trials were repeated from either end to avoid a side bias. Each mouse was tested against four to five individuals from other cages.

Home Cage Monitoring

To evaluate possible repetitive behavior, 12 Ala56/Ala56 and 12 Gly56/Gly56 mice were video-recorded alone in their home cage for 24 hours while maintaining their light/dark schedule. Automated video analysis was conducted by using HomeCageScan

(CleverSys, Inc.) to index time spent performing individual behaviors. The resulting data were condensed into 10 individual behaviors: awaken/sleep, chew/eat/drink, rear, groom, hang, remain low, sniff, stretch, twitch, and walk. To normalize distributions for analysis, data were log_{10}-transformed. Bouts of hanging behavior were defined as distinct periods of hanging separated by non-hanging behaviors. The number of bouts per animal was also log_{10}-transformed for analysis.

Y-Maze

To evaluate for perseverative exploratory behavior, mice were tested for spontaneous alternation in the Y-maze, with maze arms of 6 x 35.5 cm, as previously described. The subject mouse was placed facing the center in one of the three arms of the maze and then allowed to explore for 6 minutes. Each trial was video recorded and then scored for spontaneous alternation, which was defined as entry into a different arm than on the previous two entries.

von Frey

Tactile sensitivity was assessed using plastic von Frey monofilaments applied to plantar surface of the subject's right hind paw. Briefly, each subject was placed into a plexiglass chamber with a wire mesh flooring for experimental access to the mouse footpad. Subjects were allowed to habituate to the testing chamber for 5 minutes before the assessment of tactile sensitivity. Von Frey monofilaments (Stoetling) of ascending diameter were applied to the subject's hind paw until reaching the target force (i.e.

bending of the filament). The lowest force required to elicit a paw withdrawal response was considered a subject's tactile sensitivity threshold.

Resident Intruder

A subset of 18 male mice of each homozygous genotype was used, with two littermate cages removed due to previous fighting injuries. The test mouse, the resident, was isolated in its home cage for seven days. A novel mouse, the intruder, was then introduced to the resident's home cage for 5 minutes. The intruder was an adult male 129S4/ImJ mouse. Interactions were recorded and a researcher blind to genotype scored videos for time of the initial aggressive behavior of the resident.

Ultrasonic Vocalization

Progeny of heterozygous SERT Ala56/Gly56 pairs at postnatal day 7 were used to measure ultrasonic vocalizations, as described previously. Pups were removed from their cage and placed in a Styrofoam chamber with bedding. Ultrasonic vocalizations were measured for 5 min using a Condenser ultrasound microphone (Avisoft-Bioacoustics) and Avisoft SASLab Pro software (Avisoft-Bioacoustics). Thresholds were set to detect only small frequency-modulated vocalizations within a 250-kHz range lasting at least 5 ms and occurring at least 20 ms apart.

DOI-Induced Head Twitch Response

A separate cohort of 12 littermate pairs was used to evaluate head twitch response to DOI as described previously. Briefly, each mouse was administered an

intraperitoneal injection of 1.0 mg/kg DOI (Sigma-Aldrich) and then allowed to acclimate to a standard housing cage with clean bedding for 34 minutes. Two research assistants who were blind to genotype then independently counted head twitches over 15 minutes.

8-OH-DPAT-Induced Hypothermia

A separate cohort of 10 littermate pairs was used to evaluate hypothermia response to 8-OH-DPAT. Briefly, core temperature was measured every 10 minutes for 80 minutes with a rectal probe (no. 50314; Stoelting) connected to a BAT-12 thermometer (Physitemp Instruments). Immediately after the third temperature measurement, mice were administered a subcutaneous injection of 0.1 mg/kg 8-OH-DPAT (Sigma-Aldrich).

Whole Blood and Midbrain Harvest

Twelve SERT Ala56 mice and matched littermate controls at postnatal day 7 were rapidly decapitated and trunk blood was collected in 1.5 ml microcentrifuge tubes containing 37 USP units of lithium heparin and mixed by inversion. Samples were immediately placed on dry ice and then stored at -80° C until analysis.

High-performance Liquid Chromatography (HPLC)

HPLC was conducted as described previously. Briefly, an internal standard solution (ISS) containing N-methylserotonin, ascorbic acid and sodium metabisulfite was added to the samples. After vortex mixing, perchloric acid was added to the samples, which were mixed and then kept on ice for 10 minutes prior to centrifugation at

6000 g for 5 minutes. The supernatant was removed and stored at -80C until analyzed by HPLC with fluorometric detection. Serotonin was determined with intra- and inter-assay coefficients of variation of less than 5 and 10%, respectively.

Synaptosome 5-HT Uptake

Synaptosomes were prepared as described previously. Briefly, 5-HT uptake was determined at 20nM and 100nM with tritiated 5-HT (Perkin Elmer). Serotonin uptake was conducted at 37° C for five minutes, with SERT-specific uptake determined by subtracting S-citalopram blocked non-specific uptake. Resulting uptake data were normalized to total protein.

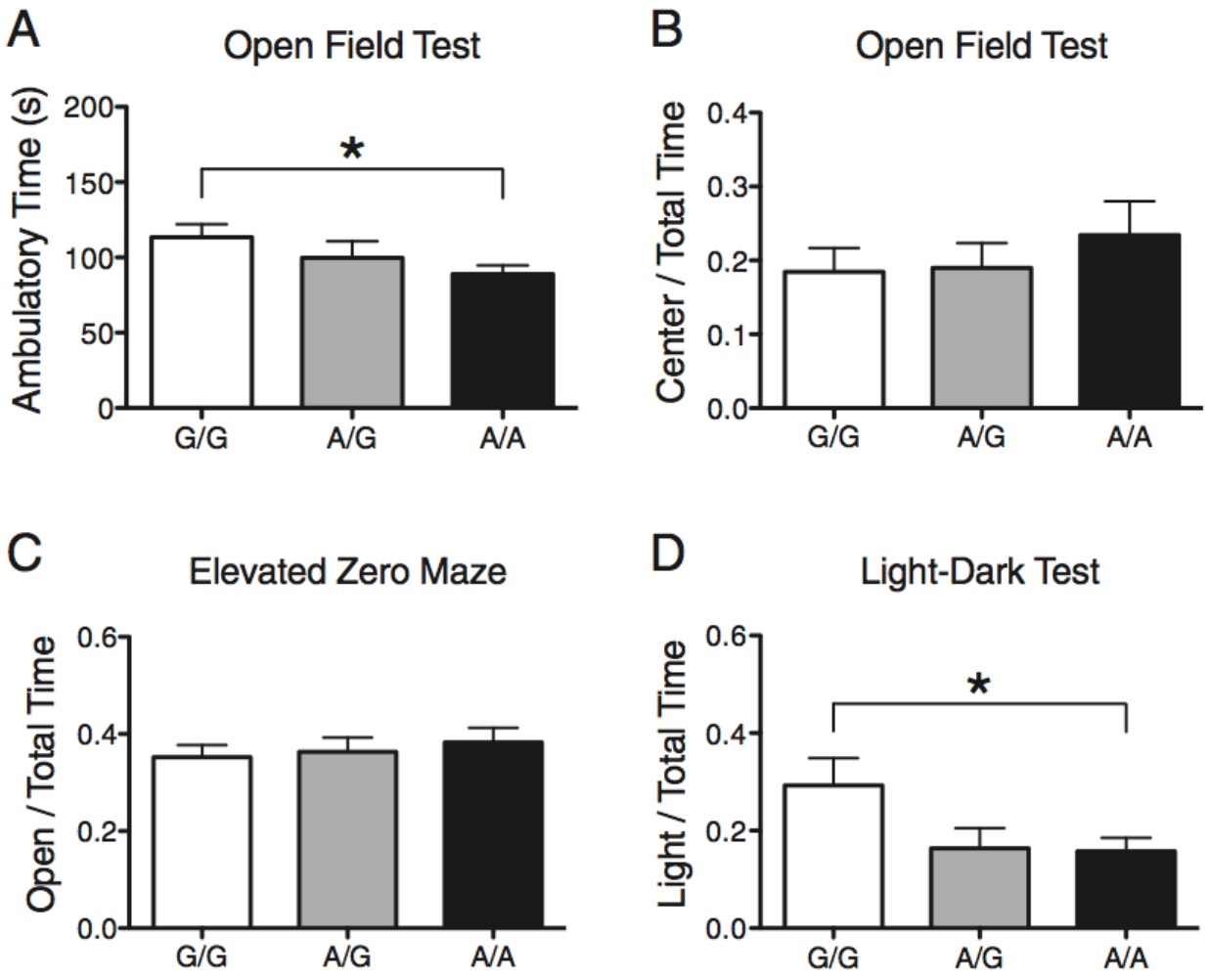

Appendix Figure 12. Activity and anxiety-like behavior in male C57 SERT Ala56 knock-in mice. A) Time (mean, standard error of the mean) spent ambulating during the first 5 minutes in the open field for wildtype littermate controls (G/G, n = 20), heterozygous (A/G, n = 16), and homozygous (A/A, n = 20) SERT Ala56 mice; **B**) Time spent in the center (>1 cM away from the side) of the open field divided by total time in the open field; **C**) Time spent in the open zone divided by total time in the elevated zero maze; **D**) Time spent in the light chamber divided by total time in the light-dark test. * P < 0.05

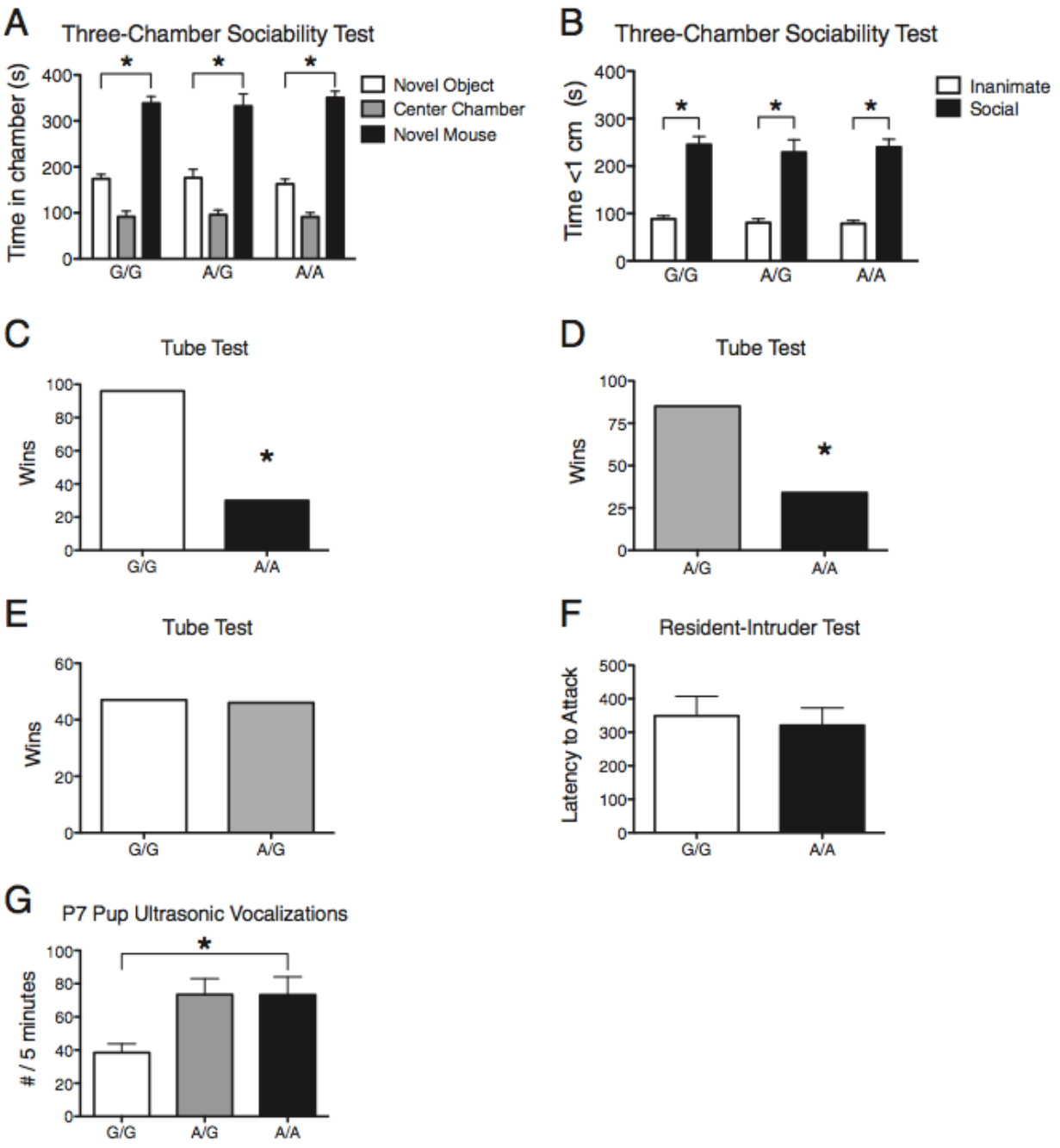

Appendix Figure 13. Social and communication behavior in male C57 SERT Ala56 knock-in mice. A) Time (mean, standard error of the mean) spent in the social stimulus chamber (novel mouse), center chamber, or inanimate stimulus chamber (novel object) in the three-chamber sociability test for wildtype littermate controls (G/G, n = 20), heterozygous (A/G, n = 16), and homozygous (A/A, n = 20) SERT Ala56 mice; **B**) Time spent within 1 cm of the social stimulus or inanimate stimulus in the three-chamber sociability test; **C**) Number of wins (frontward exit) for wildtype littermate controls (G/G) or SERT Ala56/Ala56 (A/A) mice when confronting the other genotype in the tube test; **D**) Number of wins for heterozygous (A/G) or homozygous SERT Ala56 (A/A) mice

when confronting the other genotype in the tube test; **E**) Number of wins for wildtype (G/G) or heterozygous SERT Ala56 (A/G) mice when confronting the other genotype in the tube test; **F**) Latency to attack a wildtype 129S4 mouse introduced into the cage of a subject animal who had been singly housed for 7 days (n = 16 per genotype); **G**) Pup vocalizations upon separation from the dam for 5 min at postnatal day 7 for wildtype littermate controls (G/G, n = 36), heterozygous (A/G, n = 65), and homozygous SERT Ala56 (A/A, n = 33) mouse pups. * $P < 0.05$

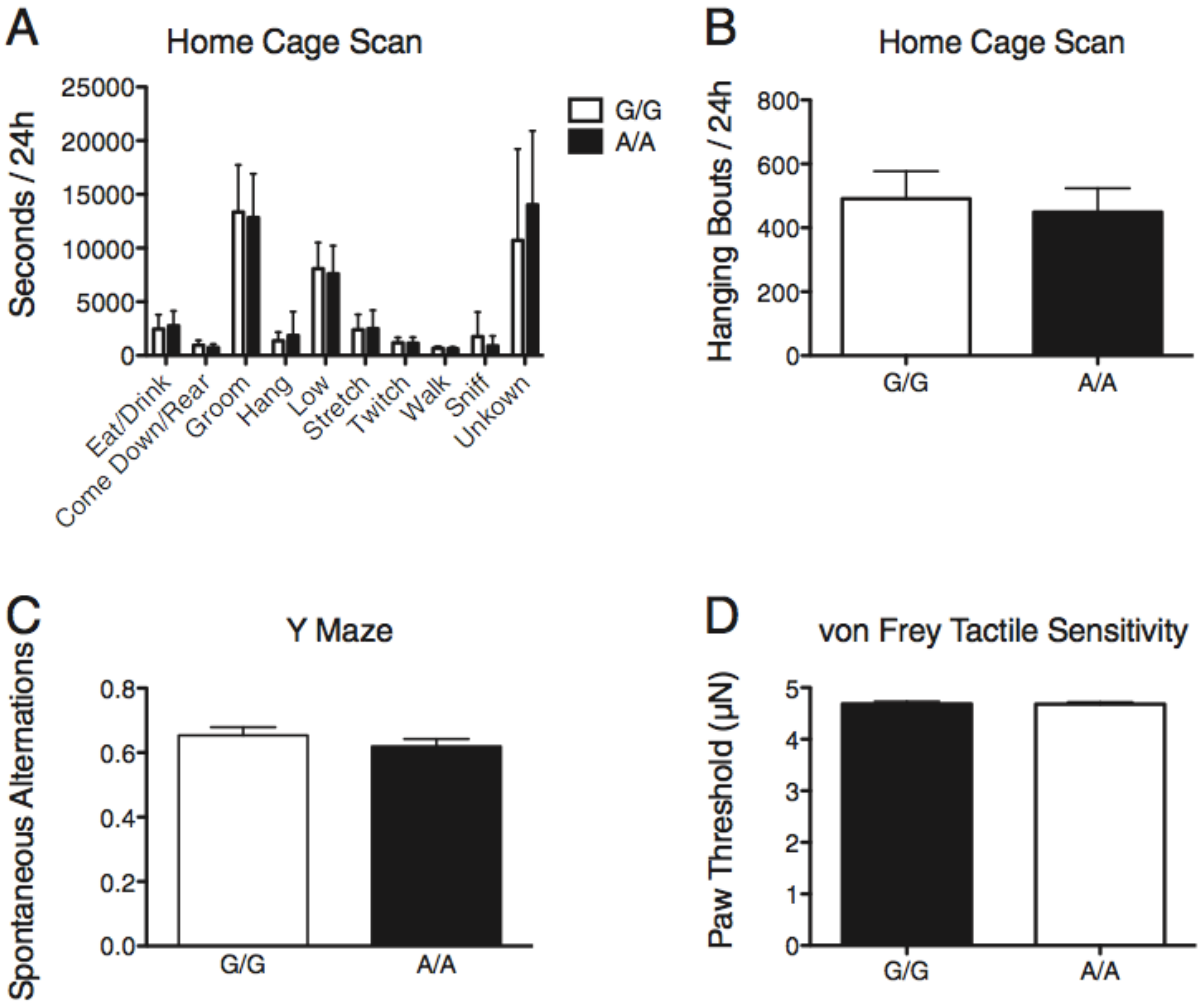

Appendix Figure 14. Home cage, exploratory, and sensory behavior in male C57 SERT Ala56 knock-in mice. A) Time (mean, standard error of the mean) spent performing individual non-sleep behaviors over 24 hours in the home cage in wildtype littermate controls (G/G, n = 12) and homozygous (A/A, n = 12) SERT Ala56 mice; **B**) Number of bouts of hanging behavior in 24 hours in the home cage; **C**) Ratio of spontaneous alternations, defined as entering a different arm than on the previous two entries, divided by total entries in the Y maze (n = 20 per genotype); **D**) Force threshold at which the paw is moved upon bending of the von Frey filaments (n = 20 per genotype).

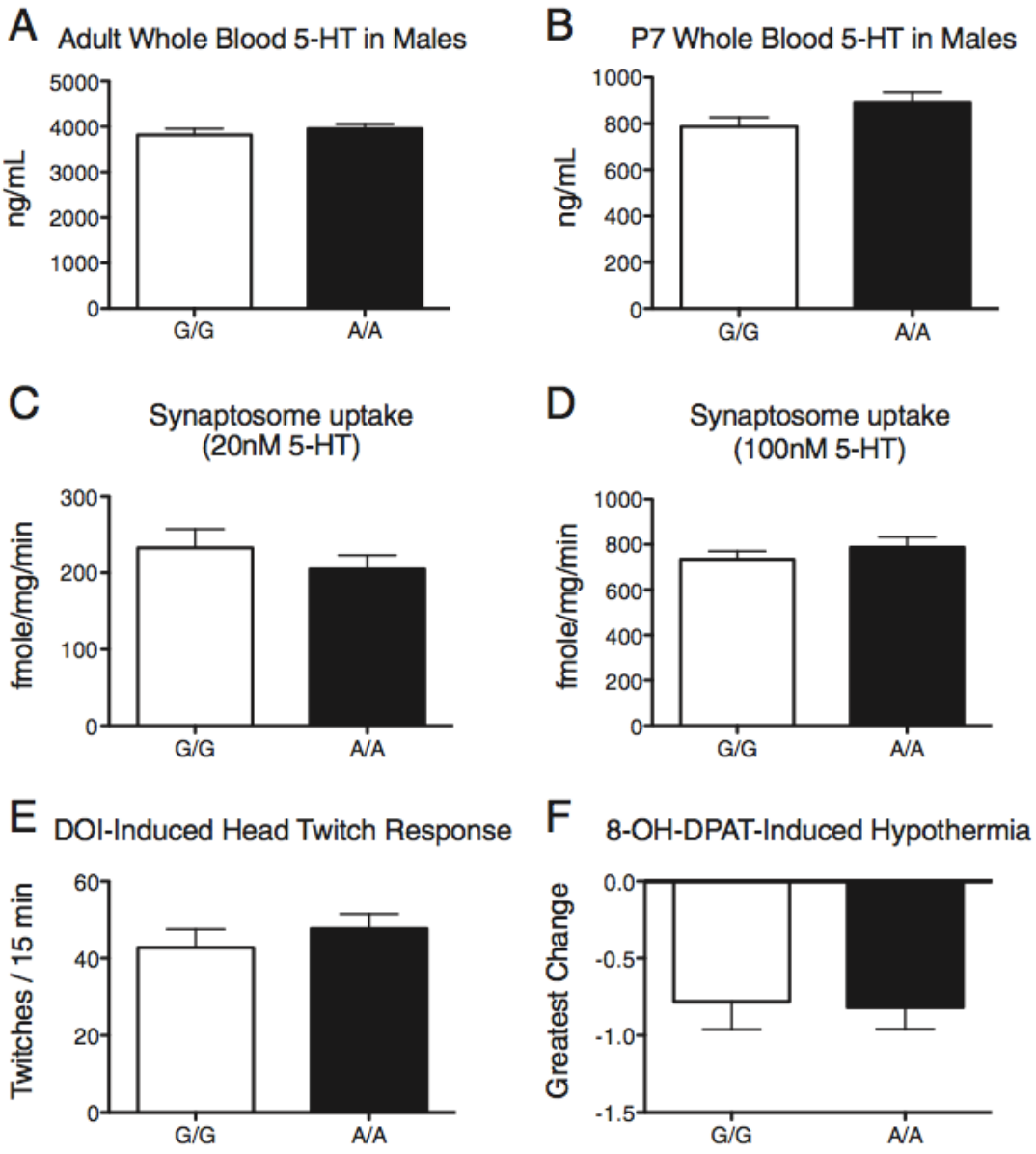

Appendix Figure 15. Assays of the serotonin system in C57 SERT Ala56 knock-in mice. **A**) Whole blood serotonin levels (mean, standard error of the mean) in male wildtype littermate control (G/G, n = 12) and homozygous SERT Ala56 (A/A, n = 12) pups at postnatal day 7; **B**) Whole blood serotonin levels in female pups at postnatal day 7 (n = 12 per genotype); **C**) Synaptosome uptake of 20 nM ^{3H}5-HT during a 5 minute assay at 37°C, (n = 6 per genotype, with 3 replicates for each subject); **D**) Synaptosome uptake of 100 nM ^{3H}5-HT during a 5 minute assay at 37°C (n = 6 per genotype, with 3 replicates for each subject); **E**) Head twitch response to injection of the 5-HT_2 agonist DOI during a 15 minute observation period (n = 12 per genotype); **F**) Decrease in rectal temperature from baseline in response to injection of the mixed 5-$HT_{1A/7}$ agonist 8-OH-DPAT (n = 10 per genotype).

REFERENCES

Abney, M., McPeek, M.S., and Ober, C. (2001). Broad and narrow heritabilities of quantitative traits in a founder population. American journal of human genetics *68*, 1302-1307.

Abrahams, B.S., and Geschwind, D.H. (2008). Advances in autism genetics: on the threshold of a new neurobiology. Nature reviews Genetics *9*, 341-355.

Abramson, R.K., Wright, H.H., Carpenter, R., Brennan, W., Lumpuy, O., Cole, E., and Young, S.R. (1989). Elevated blood serotonin in autistic probands and their first-degree relatives. Journal of autism and developmental disorders *19*, 397-407.

Adamsen, D., Meili, D., Blau, N., Thony, B., and Ramaekers, V. (2011). Autism associated with low 5-hydroxyindolacetic acid in CSF and the heterozygous SLC6A4 gene Gly56Ala plus 5-HTTLPR L/L promoter variants. Molecular genetics and metabolism *102*, 368-373.

Adkins, E.M., Barker, E.L., and Blakely, R.D. (2001). Interactions of tryptamine derivatives with serotonin transporter species variants implicate transmembrane domain I in substrate recognition. Molecular pharmacology *59*, 514-523.

Adolphs, R., Tranel, D., and Damasio, A.R. (1998). The human amygdala in social judgment. Nature *393*, 470-474.

Agmon, A., and Connors, B.W. (1991). Thalamocortical responses of mouse somatosensory (barrel) cortex in vitro. Neuroscience *41*, 365-379.

Ahern, G.P. (2011). 5-HT and the immune system. Current opinion in pharmacology *11*, 29-33.

Aluvihare, V.R., Kallikourdis, M., and Betz, A.G. (2004). Regulatory T cells mediate maternal tolerance to the fetus. Nature immunology *5*, 266-271.

Amireault, P., Sibon, D., and Cote, F. (2013). Life without peripheral serotonin: insights from tryptophan hydroxylase 1 knockout mice reveal the existence of paracrine/autocrine serotonergic networks. ACS chemical neuroscience *4*, 64-71.

Anders, S., Pyl, P.T., and Huber, W. (2014). HTSeq-a Python framework to work with high-throughput sequencing data. Bioinformatics.

Anderson, G.M., Feibel, F.C., and Cohen, D.J. (1987). Determination of serotonin in whole blood, platelet-rich plasma, platelet-poor plasma and plasma ultrafiltrate. Life sciences *40*, 1063-1070.

Anderson, G.M., Gutknecht, L., Cohen, D.J., Brailly-Tabard, S., Cohen, J.H., Ferrari, P., Roubertoux, P.L., and Tordjman, S. (2002). Serotonin transporter promoter variants in

autism: functional effects and relationship to platelet hyperserotonemia. Molecular psychiatry *7*, 831-836.

Anderson, G.M., Minderaa, R.B., van Benthem, P.P., Volkmar, F.R., and Cohen, D.J. (1984). Platelet imipramine binding in autistic subjects. Psychiatry research *11*, 133-141.

Ansorge, M.S., Zhou, M., Lira, A., Hen, R., and Gingrich, J.A. (2004). Early-life blockade of the 5-HT transporter alters emotional behavior in adult mice. Science *306*, 879-881.

Ashley, C.T., Jr., Wilkinson, K.D., Reines, D., and Warren, S.T. (1993a). FMR1 protein: conserved RNP family domains and selective RNA binding. Science *262*, 563-566.

Ashley, C.T., Sutcliffe, J.S., Kunst, C.B., Leiner, H.A., Eichler, E.E., Nelson, D.L., and Warren, S.T. (1993b). Human and murine FMR-1: alternative splicing and translational initiation downstream of the CGG-repeat. Nature genetics *4*, 244-251.

Auda, G.R., Kirk, S.H., Billett, M.A., and Billett, E.E. (1998). Localization of monoamine oxidase mRNA in human placenta. The journal of histochemistry and cytochemistry : official journal of the Histochemistry Society *46*, 1393-1400.

Baganz, N.L., and Blakely, R.D. (2013). A dialogue between the immune system and brain, spoken in the language of serotonin. ACS chemical neuroscience *4*, 48-63.

Bailey, A., Le Couteur, A., Gottesman, I., Bolton, P., Simonoff, E., Yuzda, E., and Rutter, M. (1995). Autism as a strongly genetic disorder: evidence from a British twin study. Psychological medicine *25*, 63-77.

Balkovetz, D.F., Tiruppathi, C., Leibach, F.H., Mahesh, V.B., and Ganapathy, V. (1989). Evidence for an imipramine-sensitive serotonin transporter in human placental brush-border membranes. The Journal of biological chemistry *264*, 2195-2198.

Barak, Y., Sadovsky, Y., and Shalom-Barak, T. (2008). PPAR Signaling in Placental Development and Function. PPAR research *2008*, 142082.

Baranek, G.T., David, F.J., Poe, M.D., Stone, W.L., and Watson, L.R. (2006). Sensory Experiences Questionnaire: discriminating sensory features in young children with autism, developmental delays, and typical development. Journal of child psychology and psychiatry, and allied disciplines *47*, 591-601.

Baranek, G.T., Foster, L.G., and Berkson, G. (1997). Tactile defensiveness and stereotyped behaviors. The American journal of occupational therapy : official publication of the American Occupational Therapy Association *51*, 91-95.

Bauman, A.L., Apparsundaram, S., Ramamoorthy, S., Wadzinski, B.E., Vaughan, R.A., and Blakely, R.D. (2000). Cocaine and antidepressant-sensitive biogenic amine transporters exist in regulated complexes with protein phosphatase 2A. The Journal of neuroscience : the official journal of the Society for Neuroscience *20*, 7571-7578.

Bazalakova, M.H., Wright, J., Schneble, E.J., McDonald, M.P., Heilman, C.J., Levey, A.I., and Blakely, R.D. (2007). Deficits in acetylcholine homeostasis, receptors and behaviors in choline transporter heterozygous mice. Genes, brain, and behavior *6*, 411-424.

Bear, M.F., Huber, K.M., and Warren, S.T. (2004). The mGluR theory of fragile X mental retardation. Trends in neurosciences *27*, 370-377.

Ben-Sasson, A., Hen, L., Fluss, R., Cermak, S.A., Engel-Yeger, B., and Gal, E. (2009). A meta-analysis of sensory modulation symptoms in individuals with autism spectrum disorders. Journal of autism and developmental disorders *39*, 1-11.

Bennett-Clarke, C.A., Chiaia, N.L., and Rhoades, R.W. (1996). Thalamocortical afferents in rat transiently express high-affinity serotonin uptake sites. Brain research *733*, 301-306.

Bennett-Clarke, C.A., Lane, R.D., and Rhoades, R.W. (1995). Fenfluramine depletes serotonin from the developing cortex and alters thalamocortical organization. Brain research *702*, 255-260.

Bennett-Clarke, C.A., Leslie, M.J., Chiaia, N.L., and Rhoades, R.W. (1993). Serotonin 1B receptors in the developing somatosensory and visual cortices are located on thalamocortical axons. Proceedings of the National Academy of Sciences of the United States of America *90*, 153-157.

Bennett-Clarke, C.A., Leslie, M.J., Lane, R.D., and Rhoades, R.W. (1994). Effect of serotonin depletion on vibrissa-related patterns of thalamic afferents in the rat's somatosensory cortex. The Journal of neuroscience : the official journal of the Society for Neuroscience *14*, 7594-7607.

Bernardet, M., and Crusio, W.E. (2006). Fmr1 KO mice as a possible model of autistic features. TheScientificWorldJournal *6*, 1164-1176.

Berry-Kravis, E., Hessl, D., Abbeduto, L., Reiss, A.L., Beckel-Mitchener, A., Urv, T.K., and Outcome Measures Working, G. (2013). Outcome measures for clinical trials in fragile X syndrome. Journal of developmental and behavioral pediatrics : JDBP *34*, 508-522.

Binda, F., Lute, B.J., Dipace, C., Blakely, R.D., and Galli, A. (2006). The N-terminus of the norepinephrine transporter regulates the magnitude and selectivity of the transporter-associated leak current. Neuropharmacology *50*, 354-361.

Blakely, R.D., Berson, H.E., Fremeau, R.T., Jr., Caron, M.G., Peek, M.M., Prince, H.K., and Bradley, C.C. (1991). Cloning and expression of a functional serotonin transporter from rat brain. Nature *354*, 66-70.

Blakely, R.D., Defelice, L.J., and Galli, A. (2005). Biogenic amine neurotransmitter transporters: just when you thought you knew them. Physiology *20*, 225-231.

Blakely, R.D., and Edwards, R.H. (2012). Vesicular and plasma membrane transporters for neurotransmitters. Cold Spring Harbor perspectives in biology *4*.

Blakemore, S.J., Tavassoli, T., Calo, S., Thomas, R.M., Catmur, C., Frith, U., and Haggard, P. (2006). Tactile sensitivity in Asperger syndrome. Brain and cognition *61*, 5-13.

Bonnin, A., Goeden, N., Chen, K., Wilson, M.L., King, J., Shih, J.C., Blakely, R.D., Deneris, E.S., and Levitt, P. (2011). A transient placental source of serotonin for the fetal forebrain. Nature *472*, 347-350.

Bonnin, A., Peng, W., Hewlett, W., and Levitt, P. (2006). Expression mapping of 5-HT1 serotonin receptor subtypes during fetal and early postnatal mouse forebrain development. Neuroscience *141*, 781-794.

Bonnin, A., Torii, M., Wang, L., Rakic, P., and Levitt, P. (2007). Serotonin modulates the response of embryonic thalamocortical axons to netrin-1. Nature neuroscience *10*, 588-597.

Boyce-Rustay, J.M., and Holmes, A. (2006). Genetic inactivation of the NMDA receptor NR2A subunit has anxiolytic- and antidepressant-like effects in mice. Neuropsychopharmacology : official publication of the American College of Neuropsychopharmacology *31*, 2405-2414.

Boyd, B.A., Baranek, G.T., Sideris, J., Poe, M.D., Watson, L.R., Patten, E., and Miller, H. (2010). Sensory features and repetitive behaviors in children with autism and developmental delays. Autism research : official journal of the International Society for Autism Research *3*, 78-87.

Braunschweig, D., Krakowiak, P., Duncanson, P., Boyce, R., Hansen, R.L., Ashwood, P., Hertz-Picciotto, I., Pessah, I.N., and Van de Water, J. (2013). Autism-specific maternal autoantibodies recognize critical proteins in developing brain. Translational psychiatry *3*, e277.

Bronson, S.L., and Bale, T.L. (2014). Prenatal stress-induced increases in placental inflammation and offspring hyperactivity are male-specific and ameliorated by maternal antiinflammatory treatment. Endocrinology *155*, 2635-2646.

Brune, C.W., Kim, S.J., Salt, J., Leventhal, B.L., Lord, C., and Cook, E.H., Jr. (2006). 5-HTTLPR Genotype-Specific Phenotype in Children and Adolescents With Autism. The American journal of psychiatry *163*, 2148-2156.

Buiting, K., Saitoh, S., Gross, S., Dittrich, B., Schwartz, S., Nicholls, R.D., and Horsthemke, B. (1995). Inherited microdeletions in the Angelman and Prader-Willi syndromes define an imprinting centre on human chromosome 15. Nature genetics *9*, 395-400.

Bulmer, J.N., Pace, D., and Ritson, A. (1988). Immunoregulatory cells in human decidua: morphology, immunohistochemistry and function. Reproduction, nutrition, development *28*, 1599-1613.

Burmeister, M., McInnis, M.G., and Zollner, S. (2008). Psychiatric genetics: progress amid controversy. Nature reviews Genetics *9*, 527-540.

Burns, C.M., Chu, H., Rueter, S.M., Hutchinson, L.K., Canton, H., Sanders-Bush, E., and Emeson, R.B. (1997). Regulation of serotonin-2C receptor G-protein coupling by RNA editing. Nature *387*, 303-308.

Canli, T., and Lesch, K.P. (2007). Long story short: the serotonin transporter in emotion regulation and social cognition. Nature neuroscience *10*, 1103-1109.

Carneiro, A.M., Airey, D.C., Thompson, B., Zhu, C.B., Lu, L., Chesler, E.J., Erikson, K.M., and Blakely, R.D. (2009). Functional coding variation in recombinant inbred mouse lines reveals multiple serotonin transporter-associated phenotypes. Proceedings of the National Academy of Sciences of the United States of America *106*, 2047-2052.

Carneiro, A.M., Cook, E.H., Murphy, D.L., and Blakely, R.D. (2008). Interactions between integrin alphaIIbbeta3 and the serotonin transporter regulate serotonin transport and platelet aggregation in mice and humans. The Journal of clinical investigation *118*, 1544-1552.

Cascio, C.J., McGlone, F., Folger, S., Tannan, V., Baranek, G., Pelphrey, K.A., and Essick, G. (2008). Tactile perception in adults with autism: a multidimensional psychophysical study. J Autism Dev Disord *38*, 127-137.

Cascio, C.J., Moana-Filho, E.J., Guest, S., Nebel, M.B., Weisner, J., Baranek, G.T., and Essick, G.K. (2012). Perceptual and neural response to affective tactile texture stimulation in adults with autism spectrum disorders. Autism research : official journal of the International Society for Autism Research *5*, 231-244.

Cases, O., Vitalis, T., Seif, I., De Maeyer, E., Sotelo, C., and Gaspar, P. (1996). Lack of barrels in the somatosensory cortex of monoamine oxidase A-deficient mice: role of a serotonin excess during the critical period. Neuron *16*, 297-307.

Chadman, K.K., Gong, S., Scattoni, M.L., Boltuck, S.E., Gandhy, S.U., Heintz, N., and Crawley, J.N. (2008). Minimal aberrant behavioral phenotypes of neuroligin-3 R451C knockin mice. Autism research : official journal of the International Society for Autism Research *1*, 147-158.

Chen, J.J., Li, Z., Pan, H., Murphy, D.L., Tamir, H., Koepsell, H., and Gershon, M.D. (2001). Maintenance of serotonin in the intestinal mucosa and ganglia of mice that lack the high-affinity serotonin transporter: Abnormal intestinal motility and the expression of cation transporters. The Journal of neuroscience : the official journal of the Society for Neuroscience *21*, 6348-6361.

Chen, Y.H., Rodgers, J., and McConachie, H. (2009). Restricted and repetitive behaviours, sensory processing and cognitive style in children with autism spectrum disorders. Journal of autism and developmental disorders *39*, 635-642.

Chugani, D.C., Muzik, O., Behen, M., Rothermel, R., Janisse, J.J., Lee, J., and Chugani, H.T. (1999). Developmental changes in brain serotonin synthesis capacity in autistic and nonautistic children. Annals of neurology *45*, 287-295.

Ciccone, M.A., Timmons, M., Phillips, A., and Quick, M.W. (2008). Calcium/calmodulin-dependent kinase II regulates the interaction between the serotonin transporter and syntaxin 1A. Neuropharmacology *55*, 763-770.

Coffee, B., Keith, K., Albizua, I., Malone, T., Mowrey, J., Sherman, S.L., and Warren, S.T. (2009). Incidence of fragile X syndrome by newborn screening for methylated FMR1 DNA. American journal of human genetics *85*, 503-514.

Conrad, L.C., Leonard, C.M., and Pfaff, D.W. (1974). Connections of the median and dorsal raphe nuclei in the rat: an autoradiographic and degeneration study. The Journal of comparative neurology *156*, 179-205.

Consortium, T.D.-B.F.X. (1994). Fmr1 knockout mice: a model to study fragile X mental retardation. Cell *78*, 23-33.

Cook, E.H., Jr., Arora, R.C., Anderson, G.M., Berry-Kravis, E.M., Yan, S.Y., Yeoh, H.C., Sklena, P.J., Charak, D.A., and Leventhal, B.L. (1993). Platelet serotonin studies in hyperserotonemic relatives of children with autistic disorder. Life sciences *52*, 2005-2015.

Cook, E.H., Jr., Leventhal, B.L., Heller, W., Metz, J., Wainwright, M., and Freedman, D.X. (1990). Autistic children and their first-degree relatives: relationships between serotonin and norepinephrine levels and intelligence. The Journal of neuropsychiatry and clinical neurosciences *2*, 268-274.

Cook, E.H., and Leventhal, B.L. (1996). The serotonin system in autism. Current opinion in pediatrics *8*, 348-354.

Coskun, M.A., Varghese, L., Reddoch, S., Castillo, E.M., Pearson, D.A., Loveland, K.A., Papanicolaou, A.C., and Sheth, B.R. (2009). How somatic cortical maps differ in autistic and typical brains. Neuroreport *20*, 175-179.

Cote, F., Fligny, C., Bayard, E., Launay, J.M., Gershon, M.D., Mallet, J., and Vodjdani, G. (2007). Maternal serotonin is crucial for murine embryonic development. Proceedings of the National Academy of Sciences of the United States of America *104*, 329-334.

Courchesne, E., Karns, C.M., Davis, H.R., Ziccardi, R., Carper, R.A., Tigue, Z.D., Chisum, H.J., Moses, P., Pierce, K., Lord, C.*, et al.* (2001). Unusual brain growth patterns in early life in patients with autistic disorder: an MRI study. Neurology *57*, 245-254.

Coutinho, A.M., Oliveira, G., Morgadinho, T., Fesel, C., Macedo, T.R., Bento, C., Marques, C., Ataide, A., Miguel, T., Borges, L.*, et al.* (2004). Variants of the serotonin transporter gene (SLC6A4) significantly contribute to hyperserotonemia in autism. Molecular psychiatry *9*, 264-271.

Coutinho, A.M., Sousa, I., Martins, M., Correia, C., Morgadinho, T., Bento, C., Marques, C., Ataide, A., Miguel, T.S., Moore, J.H.*, et al.* (2007). Evidence for epistasis between SLC6A4 and ITGB3 in autism etiology and in the determination of platelet serotonin levels. Human genetics *121*, 243-256.

Crane, L., Goddard, L., and Pring, L. (2009). Sensory processing in adults with autism spectrum disorders. Autism : the international journal of research and practice *13*, 215-228.

Cross, S., Kim, S.J., Weiss, L.A., Delahanty, R.J., Sutcliffe, J.S., Leventhal, B.L., Cook, E.H., Jr., and Veenstra-Vanderweele, J. (2008). Molecular genetics of the platelet serotonin system in first-degree relatives of patients with autism. Neuropsychopharmacology : official publication of the American College of Neuropsychopharmacology *33*, 353-360.

D'Amato, R.J., Blue, M.E., Largent, B.L., Lynch, D.R., Ledbetter, D.J., Molliver, M.E., and Snyder, S.H. (1987). Ontogeny of the serotonergic projection to rat neocortex: transient expression of a dense innervation to primary sensory areas. Proceedings of the National Academy of Sciences of the United States of America *84*, 4322-4326.

Dahlstroem, A., and Fuxe, K. (1964). Evidence for the Existence of Monoamine-Containing Neurons in the Central Nervous System. I. Demonstration of Monoamines in the Cell Bodies of Brain Stem Neurons. Acta physiologica Scandinavica Supplementum, SUPPL 232:231-255.

Daws, L.C., Toney, G.M., Davis, D.J., Gerhardt, G.A., and Frazer, A. (1997). In vivo chronoamperometric measurements of the clearance of exogenously applied serotonin in the rat dentate gyrus. Journal of neuroscience methods *78*, 139-150.

Dawson, N., Ferrington, L., Olverman, H.J., Harmar, A.J., and Kelly, P.A. (2009). Sex influences the effect of a lifelong increase in serotonin transporter function on cerebral metabolism. Journal of neuroscience research *87*, 2375-2385.

Developmental Disabilities Monitoring Network Surveillance Year Principal, I., Centers for Disease, C., and Prevention (2014). Prevalence of autism spectrum disorder among children aged 8 years - autism and developmental disabilities monitoring network, 11 sites, United States, 2010. Morbidity and mortality weekly report Surveillance summaries *63*, 1-21.

Devlin, B., Cook, E.H., Jr., Coon, H., Dawson, G., Grigorenko, E.L., McMahon, W., Minshew, N., Pauls, D., Smith, M., Spence, M.A.*, et al.* (2005). Autism and the serotonin transporter: the long and short of it. Molecular psychiatry *10*, 1110-1116.

Devlin, B., Melhem, N., and Roeder, K. (2011). Do common variants play a role in risk for autism? Evidence and theoretical musings. Brain research *1380*, 78-84.

Dickel, D.E., Veenstra-VanderWeele, J., Bivens, N.C., Wu, X., Fischer, D.J., Van Etten-Lee, M., Himle, J.A., Leventhal, B.L., Cook, E.H., Jr., and Hanna, G.L. (2007). Association studies of

serotonin system candidate genes in early-onset obsessive-compulsive disorder. Biological psychiatry *61*, 322-329.

Dolen, G., Carpenter, R.L., Ocain, T.D., and Bear, M.F. (2010). Mechanism-based approaches to treating fragile X. Pharmacology & therapeutics *127*, 78-93.

Dolen, G., Osterweil, E., Rao, B.S., Smith, G.B., Auerbach, B.D., Chattarji, S., and Bear, M.F. (2007). Correction of fragile X syndrome in mice. Neuron *56*, 955-962.

Dunn, W. (1999). The Sensory Profile Manual (San Antonio, TX: Psychological Corporation).

Duvall, J.A., Lu, A., Cantor, R.M., Todd, R.D., Constantino, J.N., and Geschwind, D.H. (2007). A quantitative trait locus analysis of social responsiveness in multiplex autism families. The American journal of psychiatry *164*, 656-662.

Erspamer, V., and Asero, B. (1952). Identification of enteramine, the specific hormone of the enterochromaffin cell system, as 5-hydroxytryptamine. Nature *169*, 800-801.

Erzurumlu, R.S., and Gaspar, P. (2012). Development and critical period plasticity of the barrel cortex. The European journal of neuroscience *35*, 1540-1553.

Esaki, T., Cook, M., Shimoji, K., Murphy, D.L., Sokoloff, L., and Holmes, A. (2005). Developmental disruption of serotonin transporter function impairs cerebral responses to whisker stimulation in mice. Proceedings of the National Academy of Sciences of the United States of America *102*, 5582-5587.

Etherton, M.R., Blaiss, C.A., Powell, C.M., and Sudhof, T.C. (2009). Mouse neurexin-1alpha deletion causes correlated electrophysiological and behavioral changes consistent with cognitive impairments. Proceedings of the National Academy of Sciences of the United States of America *106*, 17998-18003.

Evans, A.K., Reinders, N., Ashford, K.A., Christie, I.N., Wakerley, J.B., and Lowry, C.A. (2008). Evidence for serotonin synthesis-dependent regulation of in vitro neuronal firing rates in the midbrain raphe complex. European journal of pharmacology *590*, 136-149.

Foss-Feig, J.H., Heacock, J.L., and Cascio, C.J. (2012). Tactile Responsiveness Patterns and Their Association with Core Features in Autism Spectrum Disorders. Research in autism spectrum disorders *6*, 337-344.

Fox, M.A., Andrews, A.M., Wendland, J.R., Lesch, K.P., Holmes, A., and Murphy, D.L. (2007). A pharmacological analysis of mice with a targeted disruption of the serotonin transporter. Psychopharmacology *195*, 147-166.

Frederick, A.L., Saborido, T.P., and Stanwood, G.D. (2012). Neurobehavioral phenotyping of G(alphaq) knockout mice reveals impairments in motor functions and spatial working memory without changes in anxiety or behavioral despair. Frontiers in behavioral neuroscience *6*, 29.

Fujimiya, M., Kimura, H., and Maeda, T. (1986). Postnatal development of serotonin nerve fibers in the somatosensory cortex of mice studied by immunohistochemistry. The Journal of comparative neurology *246*, 191-201.

Fuller, R.W., Perry, K.W., and Molloy, B.B. (1974). Effect of an uptake inhibitor on serotonin metabolism in rat brain: studies with 3-(p-trifluoromethylphenoxy)-N-methyl-3-phenylpropylamine (Lilly 110140). Life sciences *15*, 1161-1171.

Gabriele, S., Sacco, R., and Persico, A.M. (2014). Blood serotonin levels in autism spectrum disorder: a systematic review and meta-analysis. European neuropsychopharmacology : the journal of the European College of Neuropsychopharmacology *24*, 919-929.

Gaspar, P., Cases, O., and Maroteaux, L. (2003). The developmental role of serotonin: news from mouse molecular genetics. Nature reviews Neuroscience *4*, 1002-1012.

Girgis, R.R., Slifstein, M., Xu, X., Frankle, W.G., Anagnostou, E., Wasserman, S., Pepa, L., Kolevzon, A., Abi-Dargham, A., Laruelle, M*., et al.* (2011). The 5-HT(2A) receptor and serotonin transporter in Asperger's disorder: A PET study with [(1)(1)C]MDL 100907 and [(1)(1)C]DASB. Psychiatry research *194*, 230-234.

Glatt, C.E., DeYoung, J.A., Delgado, S., Service, S.K., Giacomini, K.M., Edwards, R.H., Risch, N., and Freimer, N.B. (2001). Screening a large reference sample to identify very low frequency sequence variants: comparisons between two genes. Nature genetics *27*, 435-438.

Gleason, G., Liu, B., Bruening, S., Zupan, B., Auerbach, A., Mark, W., Oh, J.E., Gal-Toth, J., Lee, F., and Toth, M. (2010). The serotonin1A receptor gene as a genetic and prenatal maternal environmental factor in anxiety. Proceedings of the National Academy of Sciences of the United States of America *107*, 7592-7597.

Goeden, N., and Bonnin, A. (2013). Ex vivo perfusion of mid-to-late-gestation mouse placenta for maternal-fetal interaction studies during pregnancy. Nature protocols *8*, 66-74.

Goldberg, J., Anderson, G.M., Zwaigenbaum, L., Hall, G.B., Nahmias, C., Thompson, A., and Szatmari, P. (2009). Cortical serotonin type-2 receptor density in parents of children with autism spectrum disorders. Journal of autism and developmental disorders *39*, 97-104.

Gratten, J., Visscher, P.M., Mowry, B.J., and Wray, N.R. (2013). Interpreting the role of de novo protein-coding mutations in neuropsychiatric disease. Nature genetics *45*, 234-238.

Guy, J., Hendrich, B., Holmes, M., Martin, J.E., and Bird, A. (2001). A mouse Mecp2-null mutation causes neurological symptoms that mimic Rett syndrome. Nature genetics *27*, 322-326.

Hanley, H.G., Stahl, S.M., and Freedman, D.X. (1977). Hyperserotonemia and amine metabolites in autistic and retarded children. Archives of general psychiatry *34*, 521-531.

Hannon, J., and Hoyer, D. (2008). Molecular biology of 5-HT receptors. Behavioural brain research *195*, 198-213.

Happe, F., Ehlers, S., Fletcher, P., Frith, U., Johansson, M., Gillberg, C., Dolan, R., Frackowiak, R., and Frith, C. (1996). 'Theory of mind' in the brain. Evidence from a PET scan study of Asperger syndrome. Neuroreport *8*, 197-201.

Hardebo, J.E., and Owman, C. (1980). Barrier mechanisms for neurotransmitter monoamines and their precursors at the blood-brain interface. Annals of neurology *8*, 1-31.

Hariri, A.R., and Holmes, A. (2006). Genetics of emotional regulation: the role of the serotonin transporter in neural function. Trends in cognitive sciences *10*, 182-191.

Hariri, A.R., Mattay, V.S., Tessitore, A., Kolachana, B., Fera, F., Goldman, D., Egan, M.F., and Weinberger, D.R. (2002). Serotonin transporter genetic variation and the response of the human amygdala. Science *297*, 400-403.

Harris, S.W., Hessl, D., Goodlin-Jones, B., Ferranti, J., Bacalman, S., Barbato, I., Tassone, F., Hagerman, P.J., Herman, H., and Hagerman, R.J. (2008). Autism profiles of males with fragile X syndrome. American journal of mental retardation : AJMR *113*, 427-438.

Hay-Schmidt, A. (2000). The evolution of the serotonergic nervous system. Proceedings Biological sciences / The Royal Society *267*, 1071-1079.

Heils, A., Teufel, A., Petri, S., Stober, G., Riederer, P., Bengel, D., and Lesch, K.P. (1996). Allelic variation of human serotonin transporter gene expression. Journal of neurochemistry *66*, 2621-2624.

Hsiao, E.Y., and Patterson, P.H. (2012). Placental regulation of maternal-fetal interactions and brain development. Developmental neurobiology *72*, 1317-1326.

Hu, X., Oroszi, G., Chun, J., Smith, T.L., Goldman, D., and Schuckit, M.A. (2005). An expanded evaluation of the relationship of four alleles to the level of response to alcohol and the alcoholism risk. Alcoholism, clinical and experimental research *29*, 8-16.

Huber, K.M., Gallagher, S.M., Warren, S.T., and Bear, M.F. (2002). Altered synaptic plasticity in a mouse model of fragile X mental retardation. Proceedings of the National Academy of Sciences of the United States of America *99*, 7746-7750.

Jacobs, B.L., and Azmitia, E.C. (1992). Structure and function of the brain serotonin system. Physiological reviews *72*, 165-229.

Jamain, S., Radyushkin, K., Hammerschmidt, K., Granon, S., Boretius, S., Varoqueaux, F., Ramanantsoa, N., Gallego, J., Ronnenberg, A., Winter, D.*, et al.* (2008). Reduced social interaction and ultrasonic communication in a mouse model of monogenic heritable autism. Proceedings of the National Academy of Sciences of the United States of America *105*, 1710-1715.

Jennings, K.A., Sheward, W.J., Harmar, A.J., and Sharp, T. (2008). Evidence that genetic variation in 5-HT transporter expression is linked to changes in 5-HT2A receptor function. Neuropharmacology *54*, 776-783.

Jiang, Y.H., Pan, Y., Zhu, L., Landa, L., Yoo, J., Spencer, C., Lorenzo, I., Brilliant, M., Noebels, J., and Beaudet, A.L. (2010). Altered ultrasonic vocalization and impaired learning and memory in Angelman syndrome mouse model with a large maternal deletion from Ube3a to Gabrb3. PloS one *5*, e12278.

Jitsuki, S., Takemoto, K., Kawasaki, T., Tada, H., Takahashi, A., Becamel, C., Sano, A., Yuzaki, M., Zukin, R.S., Ziff, E.B.*, et al.* (2011). Serotonin mediates cross-modal reorganization of cortical circuits. Neuron *69*, 780-792.

Kaufman, A.S., and Kaufman, N.L. (2004). KBIT2: Kaufman Brief Intelligence Test - Second Edition (Circle Pines MN: AGS Publishing).

Kern, J.K., Trivedi, M.H., Garver, C.R., Grannemann, B.D., Andrews, A.A., Savla, J.S., Johnson, D.G., Mehta, J.A., and Schroeder, J.L. (2006). The pattern of sensory processing abnormalities in autism. Autism : the international journal of research and practice *10*, 480-494.

Kerr, T.M., Muller, C.L., Miah, M., Jetter, C.S., Pfeiffer, R., Shah, C., Baganz, N., Anderson, G.M., Crawley, J.N., Sutcliffe, J.S.*, et al.* (2013). Genetic background modulates phenotypes of serotonin transporter Ala56 knock-in mice. Molecular autism *4*, 35.

Kim, D., Pertea, G., Trapnell, C., Pimentel, H., Kelley, R., and Salzberg, S.L. (2013). TopHat2: accurate alignment of transcriptomes in the presence of insertions, deletions and gene fusions. Genome biology *14*, R36.

Kim, H., Toyofuku, Y., Lynn, F.C., Chak, E., Uchida, T., Mizukami, H., Fujitani, Y., Kawamori, R., Miyatsuka, T., Kosaka, Y.*, et al.* (2010). Serotonin regulates pancreatic beta cell mass during pregnancy. Nature medicine *16*, 804-808.

Kishore, S., and Stamm, S. (2006). The snoRNA HBII-52 regulates alternative splicing of the serotonin receptor 2C. Science *311*, 230-232.

Kistner-Griffin, E., Brune, C.W., Davis, L.K., Sutcliffe, J.S., Cox, N.J., and Cook, E.H., Jr. (2011). Parent-of-origin effects of the serotonin transporter gene associated with autism. American journal of medical genetics Part B, Neuropsychiatric genetics : the official publication of the International Society of Psychiatric Genetics *156*, 139-144.

Kobayashi, T., Minowa, O., Sugitani, Y., Takai, S., Mitani, H., Kobayashi, E., Noda, T., and Hino, O. (2001). A germ-line Tsc1 mutation causes tumor development and embryonic lethality that are similar, but not identical to, those caused by Tsc2 mutation in mice. Proceedings of the National Academy of Sciences of the United States of America *98*, 8762-8767.

Kolevzon, A., Newcorn, J.H., Kryzak, L., Chaplin, W., Watner, D., Hollander, E., Smith, C.J., Cook, E.H., Jr., and Silverman, J.M. (2010). Relationship between whole blood serotonin and repetitive behaviors in autism. Psychiatry research *175*, 274-276.

Kwon, C.H., Luikart, B.W., Powell, C.M., Zhou, J., Matheny, S.A., Zhang, W., Li, Y., Baker, S.J., and Parada, L.F. (2006). Pten regulates neuronal arborization and social interaction in mice. Neuron *50*, 377-388.

Lam, K.S., and Aman, M.G. (2007). The Repetitive Behavior Scale-Revised: independent validation in individuals with autism spectrum disorders. J Autism Dev Disord *37*, 855-866.

Landa, R.J., Holman, K.C., and Garrett-Mayer, E. (2007). Social and communication development in toddlers with early and later diagnosis of autism spectrum disorders. Archives of general psychiatry *64*, 853-864.

Lauder, J.M. (1993). Neurotransmitters as growth regulatory signals: role of receptors and second messengers. Trends in neurosciences *16*, 233-240.

Laurent, A., Goaillard, J.M., Cases, O., Lebrand, C., Gaspar, P., and Ropert, N. (2002). Activity-dependent presynaptic effect of serotonin 1B receptors on the somatosensory thalamocortical transmission in neonatal mice. The Journal of neuroscience : the official journal of the Society for Neuroscience *22*, 886-900.

Lebrand, C., Cases, O., Adelbrecht, C., Doye, A., Alvarez, C., El Mestikawy, S., Seif, I., and Gaspar, P. (1996). Transient uptake and storage of serotonin in developing thalamic neurons. Neuron *17*, 823-835.

Leekam, S.R., Nieto, C., Libby, S.J., Wing, L., and Gould, J. (2007). Describing the sensory abnormalities of children and adults with autism. J Autism Dev Disord *37*, 894-910.

Lesch, K.P., Bengel, D., Heils, A., Sabol, S.Z., Greenberg, B.D., Petri, S., Benjamin, J., Muller, C.R., Hamer, D.H., and Murphy, D.L. (1996). Association of anxiety-related traits with a polymorphism in the serotonin transporter gene regulatory region. Science *274*, 1527-1531.

Li, H., Handsaker, B., Wysoker, A., Fennell, T., Ruan, J., Homer, N., Marth, G., Abecasis, G., Durbin, R., and Genome Project Data Processing, S. (2009). The Sequence Alignment/Map format and SAMtools. Bioinformatics *25*, 2078-2079.

Lidow, M.S., and Rakic, P. (1992). Scheduling of monoaminergic neurotransmitter receptor expression in the primate neocortex during postnatal development. Cerebral cortex *2*, 401-416.

Little, L.M., Freuler, A.C., Houser, M.B., Guckian, L., Carbine, K., David, F.J., and Baranek, G.T. (2011). Psychometric validation of the Sensory Experiences Questionnaire. The American journal of occupational therapy : official publication of the American Occupational Therapy Association *65*, 207-210.

Lord, C., Risi, S., Lambrecht, L., Cook, E.H., Jr., Leventhal, B.L., DiLavore, P.C., Pickles, A., and Rutter, M. (2000). The autism diagnostic observation schedule-generic: a standard measure of social and communication deficits associated with the spectrum of autism. J Autism Dev Disord *30*, 205-223.

Lord, C., Rutter, M., and Le Couteur, A. (1994). Autism Diagnostic Interview-Revised: a revised version of a diagnostic interview for caregivers of individuals with possible pervasive developmental disorders. J Autism Dev Disord *24*, 659-685.

Lovenberg, W., Jequier, E., and Sjoerdsma, A. (1967). Tryptophan hydroxylation: measurement in pineal gland, brainstem, and carcinoid tumor. Science *155*, 217-219.

Lucki, I., Dalvi, A., and Mayorga, A.J. (2001). Sensitivity to the effects of pharmacologically selective antidepressants in different strains of mice. Psychopharmacology *155*, 315-322.

Lyall, K., Pauls, D.L., Spiegelman, D., Ascherio, A., and Santangelo, S.L. (2012). Pregnancy complications and obstetric suboptimality in association with autism spectrum disorders in children of the Nurses' Health Study II. Autism research : official journal of the International Society for Autism Research *5*, 21-30.

Ma, D.Q., Rabionet, R., Konidari, I., Jaworski, J., Cukier, H.N., Wright, H.H., Abramson, R.K., Gilbert, J.R., Cuccaro, M.L., Pericak-Vance, M.A*., et al.* (2010). Association and gene-gene interaction of SLC6A4 and ITGB3 in autism. American journal of medical genetics Part B, Neuropsychiatric genetics : the official publication of the International Society of Psychiatric Genetics *153B*, 477-483.

Ma, P.M., and Woolsey, T.A. (1984). Cytoarchitectonic correlates of the vibrissae in the medullary trigeminal complex of the mouse. Brain research *306*, 374-379.

Makkonen, I., Riikonen, R., Kokki, H., Airaksinen, M.M., and Kuikka, J.T. (2008). Serotonin and dopamine transporter binding in children with autism determined by SPECT. Developmental medicine and child neurology *50*, 593-597.

Malkova, N.V., Yu, C.Z., Hsiao, E.Y., Moore, M.J., and Patterson, P.H. (2012). Maternal immune activation yields offspring displaying mouse versions of the three core symptoms of autism. Brain, behavior, and immunity *26*, 607-616.

Manolio, T.A., Collins, F.S., Cox, N.J., Goldstein, D.B., Hindorff, L.A., Hunter, D.J., McCarthy, M.I., Ramos, E.M., Cardon, L.R., Chakravarti, A*., et al.* (2009). Finding the missing heritability of complex diseases. Nature *461*, 747-753.

Marco, E.J., Khatibi, K., Hill, S.S., Siegel, B., Arroyo, M.S., Dowling, A.F., Neuhaus, J.M., Sherr, E.H., Hinkley, L.N., and Nagarajan, S.S. (2012). Children with autism show reduced somatosensory response: an MEG study. Autism research : official journal of the International Society for Autism Research *5*, 340-351.

McBride, P.A., Anderson, G.M., Hertzig, M.E., Snow, M.E., Thompson, S.M., Khait, V.D., Shapiro, T., and Cohen, D.J. (1998). Effects of diagnosis, race, and puberty on platelet serotonin levels in autism and mental retardation. Journal of the American Academy of Child and Adolescent Psychiatry *37*, 767-776.

McCarthy, D.J., Chen, Y., and Smyth, G.K. (2012). Differential expression analysis of multifactor RNA-Seq experiments with respect to biological variation. Nucleic acids research *40*, 4288-4297.

McCauley, J.L., Olson, L.M., Dowd, M., Amin, T., Steele, A., Blakely, R.D., Folstein, S.E., Haines, J.L., and Sutcliffe, J.S. (2004). Linkage and association analysis at the serotonin transporter (SLC6A4) locus in a rigid-compulsive subset of autism. American journal of medical genetics Part B, Neuropsychiatric genetics : the official publication of the International Society of Psychiatric Genetics *127B*, 104-112.

McNaughton, C.H., Moon, J., Strawderman, M.S., Maclean, K.N., Evans, J., and Strupp, B.J. (2008). Evidence for social anxiety and impaired social cognition in a mouse model of fragile X syndrome. Behavioral neuroscience *122*, 293-300.

Meltzer, H.Y., and Arora, R.C. (1988). Genetic control of serotonin uptake in blood platelets: a twin study. Psychiatry research *24*, 263-269.

Michalon, A., Sidorov, M., Ballard, T.M., Ozmen, L., Spooren, W., Wettstein, J.G., Jaeschke, G., Bear, M.F., and Lindemann, L. (2012). Chronic pharmacological mGlu5 inhibition corrects fragile X in adult mice. Neuron *74*, 49-56.

Millan, M.J., Marin, P., Bockaert, J., and Mannoury la Cour, C. (2008). Signaling at G-protein-coupled serotonin receptors: recent advances and future research directions. Trends in pharmacological sciences *29*, 454-464.

Mineur, Y.S., Sluyter, F., de Wit, S., Oostra, B.A., and Crusio, W.E. (2002). Behavioral and neuroanatomical characterization of the Fmr1 knockout mouse. Hippocampus *12*, 39-46.

Miyakawa, T., Yamada, M., Duttaroy, A., and Wess, J. (2001). Hyperactivity and intact hippocampus-dependent learning in mice lacking the M1 muscarinic acetylcholine receptor. The Journal of neuroscience : the official journal of the Society for Neuroscience *21*, 5239-5250.

Molloy, C.A., and Manning-Courtney, P. (2003). Prevalence of chronic gastrointestinal symptoms in children with autism and autistic spectrum disorders. Autism : the international journal of research and practice *7*, 165-171.

Mor, G., and Cardenas, I. (2010). The immune system in pregnancy: a unique complexity. American journal of reproductive immunology *63*, 425-433.

Moretti, P., Bouwknecht, J.A., Teague, R., Paylor, R., and Zoghbi, H.Y. (2005). Abnormalities of social interactions and home-cage behavior in a mouse model of Rett syndrome. Human molecular genetics *14*, 205-220.

Moy, S.S., Nadler, J.J., Perez, A., Barbaro, R.P., Johns, J.M., Magnuson, T.R., Piven, J., and Crawley, J.N. (2004). Sociability and preference for social novelty in five inbred strains: an approach to assess autistic-like behavior in mice. Genes, brain, and behavior *3*, 287-302.

Moy, S.S., Nadler, J.J., Young, N.B., Nonneman, R.J., Grossman, A.W., Murphy, D.L., D'Ercole, A.J., Crawley, J.N., Magnuson, T.R., and Lauder, J.M. (2009). Social approach in genetically engineered mouse lines relevant to autism. Genes, brain, and behavior *8*, 129-142.

Moy, S.S., Nadler, J.J., Young, N.B., Perez, A., Holloway, L.P., Barbaro, R.P., Barbaro, J.R., Wilson, L.M., Threadgill, D.W., Lauder, J.M.*, et al.* (2007). Mouse behavioral tasks relevant to autism: phenotypes of 10 inbred strains. Behavioural brain research *176*, 4-20.

Mulder, E.J., Anderson, G.M., Kema, I.P., de Bildt, A., van Lang, N.D., den Boer, J.A., and Minderaa, R.B. (2004). Platelet serotonin levels in pervasive developmental disorders and mental retardation: diagnostic group differences, within-group distribution, and behavioral correlates. Journal of the American Academy of Child and Adolescent Psychiatry *43*, 491-499.

Mullen, E. (1995). Mullen scales of early learning (Circle Pines, MN: American Guidance Service).

Muller, H.K., Wiborg, O., and Haase, J. (2006). Subcellular redistribution of the serotonin transporter by secretory carrier membrane protein 2. The Journal of biological chemistry *281*, 28901-28909.

Munn, D.H., Zhou, M., Attwood, J.T., Bondarev, I., Conway, S.J., Marshall, B., Brown, C., and Mellor, A.L. (1998). Prevention of allogeneic fetal rejection by tryptophan catabolism. Science *281*, 1191-1193.

Myers, R.E., Swett, C., and Miller, M. (1973). Loss of social group affinity following prefrontal lesions in free-ranging macaques. Brain research *64*, 257-269.

Nadler, J.J., Moy, S.S., Dold, G., Trang, D., Simmons, N., Perez, A., Young, N.B., Barbaro, R.P., Piven, J., Magnuson, T.R.*, et al.* (2004). Automated apparatus for quantitation of social approach behaviors in mice. Genes, brain, and behavior *3*, 303-314.

Nakamura, K., Sekine, Y., Ouchi, Y., Tsujii, M., Yoshikawa, E., Futatsubashi, M., Tsuchiya, K.J., Sugihara, G., Iwata, Y., Suzuki, K.*, et al.* (2010). Brain serotonin and dopamine transporter bindings in adults with high-functioning autism. Archives of general psychiatry *67*, 59-68.

Napolioni, V., Lombardi, F., Sacco, R., Curatolo, P., Manzi, B., Alessandrelli, R., Militerni, R., Bravaccio, C., Lenti, C., Saccani, M.*, et al.* (2011). Family-based association study of ITGB3 in

autism spectrum disorder and its endophenotypes. European journal of human genetics : EJHG *19*, 353-359.

Nicholson, C., and Sykova, E. (1998). Extracellular space structure revealed by diffusion analysis. Trends in neurosciences *21*, 207-215.

Nunemaker, C.S., DeFazio, R.A., and Moenter, S.M. (2003). A targeted extracellular approach for recording long-term firing patterns of excitable cells: a practical guide. Biological procedures online *5*, 53-62.

O'Hearn, E., and Molliver, M.E. (1984). Organization of raphe-cortical projections in rat: a quantitative retrograde study. Brain research bulletin *13*, 709-726.

O'Riordan, M., and Passetti, F. (2006). Discrimination in autism within different sensory modalities. J Autism Dev Disord *36*, 665-675.

Oberle, I., Rousseau, F., Heitz, D., Kretz, C., Devys, D., Hanauer, A., Boue, J., Bertheas, M.F., and Mandel, J.L. (1991). Instability of a 550-base pair DNA segment and abnormal methylation in fragile X syndrome. Science *252*, 1097-1102.

Ozaki, N., Goldman, D., Kaye, W.H., Plotnicov, K., Greenberg, B.D., Lappalainen, J., Rudnick, G., and Murphy, D.L. (2003). Serotonin transporter missense mutation associated with a complex neuropsychiatric phenotype. Molecular psychiatry *8*, 933-936.

Partington, M.W., Tu, J.B., and Wong, C.Y. (1973). Blood serotonin levels in severe mental retardation. Developmental medicine and child neurology *15*, 616-627.

Patten, E., Ausderau, K.K., Watson, L.R., and Baranek, G.T. (2013). Sensory Response Patterns in Nonverbal Children with ASD. Autism research and treatment *2013*, 436286.

Peca, J., Feliciano, C., Ting, J.T., Wang, W., Wells, M.F., Venkatraman, T.N., Lascola, C.D., Fu, Z., and Feng, G. (2011). Shank3 mutant mice display autistic-like behaviours and striatal dysfunction. Nature *472*, 437-442.

Penagarikano, O., Abrahams, B.S., Herman, E.I., Winden, K.D., Gdalyahu, A., Dong, H., Sonnenblick, L.I., Gruver, R., Almajano, J., Bragin, A.*, et al.* (2011). Absence of CNTNAP2 leads to epilepsy, neuronal migration abnormalities, and core autism-related deficits. Cell *147*, 235-246.

Perry, W., Minassian, A., Lopez, B., Maron, L., and Lincoln, A. (2007). Sensorimotor gating deficits in adults with autism. Biological psychiatry *61*, 482-486.

Persico, A.M., Altamura, C., Calia, E., Puglisi-Allegra, S., Ventura, R., Lucchese, F., and Keller, F. (2000). Serotonin depletion and barrel cortex development: impact of growth impairment vs. serotonin effects on thalamocortical endings. Cerebral cortex *10*, 181-191.

Philofsky, A., Hepburn, S.L., Hayes, A., Hagerman, R., and Rogers, S.J. (2004). Linguistic and cognitive functioning and autism symptoms in young children with fragile X syndrome. American journal of mental retardation : AJMR *109*, 208-218.

Pietropaolo, S., Guilleminot, A., Martin, B., D'Amato, F.R., and Crusio, W.E. (2011). Genetic-background modulation of core and variable autistic-like symptoms in Fmr1 knock-out mice. PloS one *6*, e17073.

Piven, J., Tsai, G.C., Nehme, E., Coyle, J.T., Chase, G.A., and Folstein, S.E. (1991). Platelet serotonin, a possible marker for familial autism. Journal of autism and developmental disorders *21*, 51-59.

Prasad, H.C., Steiner, J.A., Sutcliffe, J.S., and Blakely, R.D. (2009). Enhanced activity of human serotonin transporter variants associated with autism. Philosophical transactions of the Royal Society of London Series B, Biological sciences *364*, 163-173.

Prasad, H.C., Zhu, C.B., McCauley, J.L., Samuvel, D.J., Ramamoorthy, S., Shelton, R.C., Hewlett, W.A., Sutcliffe, J.S., and Blakely, R.D. (2005). Human serotonin transporter variants display altered sensitivity to protein kinase G and p38 mitogen-activated protein kinase. Proceedings of the National Academy of Sciences of the United States of America *102*, 11545-11550.

Prasad, P.D., Hoffmans, B.J., Moe, A.J., Smith, C.H., Leibach, F.H., and Ganapathy, V. (1996). Functional expression of the plasma membrane serotonin transporter but not the vesicular monoamine transporter in human placental trophoblasts and choriocarcinoma cells. Placenta *17*, 201-207.

Qian, Y., Melikian, H.E., Rye, D.B., Levey, A.I., and Blakely, R.D. (1995). Identification and characterization of antidepressant-sensitive serotonin transporter proteins using site-specific antibodies. The Journal of neuroscience : the official journal of the Society for Neuroscience *15*, 1261-1274.

Ramamoorthy, S., Bauman, A.L., Moore, K.R., Han, H., Yang-Feng, T., Chang, A.S., Ganapathy, V., and Blakely, R.D. (1993). Antidepressant- and cocaine-sensitive human serotonin transporter: molecular cloning, expression, and chromosomal localization. Proceedings of the National Academy of Sciences of the United States of America *90*, 2542-2546.

Ramamoorthy, S., Samuvel, D.J., Buck, E.R., Rudnick, G., and Jayanthi, L.D. (2007). Phosphorylation of threonine residue 276 is required for acute regulation of serotonin transporter by cyclic GMP. The Journal of biological chemistry *282*, 11639-11647.

Rapport, M.M., Green, A.A., and Page, I.H. (1948). Serum vasoconstrictor, serotonin; isolation and characterization. The Journal of biological chemistry *176*, 1243-1251.

Raznahan, A., Pugliese, L., Barker, G.J., Daly, E., Powell, J., Bolton, P.F., and Murphy, D.G. (2009). Serotonin transporter genotype and neuroanatomy in autism spectrum disorders. Psychiatric genetics *19*, 147-150.

Rhoades, R.W., Bennett-Clarke, C.A., Shi, M.Y., and Mooney, R.D. (1994). Effects of 5-HT on thalamocortical synaptic transmission in the developing rat. Journal of neurophysiology *72*, 2438-2450.

Rogers, S.J., Hepburn, S., and Wehner, E. (2003). Parent reports of sensory symptoms in toddlers with autism and those with other developmental disorders. J Autism Dev Disord *33*, 631-642.

Rogers, S.J., and Ozonoff, S. (2005). Annotation: what do we know about sensory dysfunction in autism? A critical review of the empirical evidence. Journal of child psychology and psychiatry, and allied disciplines *46*, 1255-1268.

Rossant, J., and Cross, J.C. (2001). Placental development: lessons from mouse mutants. Nature reviews Genetics *2*, 538-548.

Rusyniak, D.E., Zaretskaia, M.V., Zaretsky, D.V., and DiMicco, J.A. (2007). 3,4-Methylenedioxymethamphetamine- and 8-hydroxy-2-di-n-propylamino-tetralin-induced hypothermia: role and location of 5-hydroxytryptamine 1A receptors. The Journal of pharmacology and experimental therapeutics *323*, 477-487.

Rutter, M., Bailey, A., and Lord, C. (2003). The social communication questionnaire (Los Angeles: Western Psychological Services).

Sacco, R., Curatolo, P., Manzi, B., Militerni, R., Bravaccio, C., Frolli, A., Lenti, C., Saccani, M., Elia, M., Reichelt, K.L.*, et al.* (2010). Principal pathogenetic components and biological endophenotypes in autism spectrum disorders. Autism research : official journal of the International Society for Autism Research *3*, 237-252.

Sakurai, T., Reichert, J., Hoffman, E.J., Cai, G., Jones, H.B., Faham, M., and Buxbaum, J.D. (2008). A large-scale screen for coding variants in SERT/SLC6A4 in autism spectrum disorders. Autism research : official journal of the International Society for Autism Research *1*, 251-257.

Salichon, N., Gaspar, P., Upton, A.L., Picaud, S., Hanoun, N., Hamon, M., De Maeyer, E., Murphy, D.L., Mossner, R., Lesch, K.P.*, et al.* (2001). Excessive activation of serotonin (5-HT) 1B receptors disrupts the formation of sensory maps in monoamine oxidase a and 5-ht transporter knock-out mice. The Journal of neuroscience : the official journal of the Society for Neuroscience *21*, 884-896.

Samuvel, D.J., Jayanthi, L.D., Bhat, N.R., and Ramamoorthy, S. (2005). A role for p38 mitogen-activated protein kinase in the regulation of the serotonin transporter: evidence for distinct cellular mechanisms involved in transporter surface expression. The Journal of neuroscience : the official journal of the Society for Neuroscience *25*, 29-41.

Schain, R.J., and Freedman, D.X. (1961). Studies on 5-hydroxyindole metabolism in autistic and other mentally retarded children. The Journal of pediatrics *58*, 315-320.

Schwartzer, J.J., Careaga, M., Onore, C.E., Rushakoff, J.A., Berman, R.F., and Ashwood, P. (2013). Maternal immune activation and strain specific interactions in the development of autism-like behaviors in mice. Translational psychiatry *3*, e240.

Scott, M.M., Wylie, C.J., Lerch, J.K., Murphy, R., Lobur, K., Herlitze, S., Jiang, W., Conlon, R.A., Strowbridge, B.W., and Deneris, E.S. (2005). A genetic approach to access serotonin neurons for in vivo and in vitro studies. Proceedings of the National Academy of Sciences of the United States of America *102*, 16472-16477.

Shoaf, S.E., Carson, R.E., Hommer, D., Williams, W.A., Higley, J.D., Schmall, B., Herscovitch, P., Eckelman, W.C., and Linnoila, M. (2000). The suitability of [11C]-alpha-methyl-L-tryptophan as a tracer for serotonin synthesis: studies with dual administration of [11C] and [14C] labeled tracer. Journal of cerebral blood flow and metabolism : official journal of the International Society of Cerebral Blood Flow and Metabolism *20*, 244-252.

Silverman, J.L., Yang, M., Lord, C., and Crawley, J.N. (2010). Behavioural phenotyping assays for mouse models of autism. Nature reviews Neuroscience *11*, 490-502.

Snyder, S.H. (1970). Putative neurotransmitters in the brain: selective neuronal uptake, subcellular localization, and interactions with centrally acting drugs. Biological psychiatry *2*, 367-389.

Spencer, C.M., Alekseyenko, O., Hamilton, S.M., Thomas, A.M., Serysheva, E., Yuva-Paylor, L.A., and Paylor, R. (2011). Modifying behavioral phenotypes in Fmr1KO mice: genetic background differences reveal autistic-like responses. Autism research : official journal of the International Society for Autism Research *4*, 40-56.

Spencer, C.M., Alekseyenko, O., Serysheva, E., Yuva-Paylor, L.A., and Paylor, R. (2005). Altered anxiety-related and social behaviors in the Fmr1 knockout mouse model of fragile X syndrome. Genes, brain, and behavior *4*, 420-430.

State, M.W., and Levitt, P. (2011). The conundrums of understanding genetic risks for autism spectrum disorders. Nature neuroscience *14*, 1499-1506.

Steele, A.D., Jackson, W.S., King, O.D., and Lindquist, S. (2007). The power of automated high-resolution behavior analysis revealed by its application to mouse models of Huntington's and prion diseases. Proceedings of the National Academy of Sciences of the United States of America *104*, 1983-1988.

Steiner, J.A., Carneiro, A.M., and Blakely, R.D. (2008). Going with the flow: trafficking-dependent and -independent regulation of serotonin transport. Traffic *9*, 1393-1402.

Steiner, J.A., Carneiro, A.M., Wright, J., Matthies, H.J., Prasad, H.C., Nicki, C.K., Dostmann, W.R., Buchanan, C.C., Corbin, J.D., Francis, S.H.*, et al.* (2009). cGMP-dependent protein kinase Ialpha associates with the antidepressant-sensitive serotonin transporter and dictates rapid modulation of serotonin uptake. Molecular brain *2*, 26.

Stone, J.L., Merriman, B., Cantor, R.M., Yonan, A.L., Gilliam, T.C., Geschwind, D.H., and Nelson, S.F. (2004). Evidence for sex-specific risk alleles in autism spectrum disorder. American journal of human genetics *75*, 1117-1123.

Sutcliffe, J.S., Delahanty, R.J., Prasad, H.C., McCauley, J.L., Han, Q., Jiang, L., Li, C., Folstein, S.E., and Blakely, R.D. (2005). Allelic heterogeneity at the serotonin transporter locus (SLC6A4) confers susceptibility to autism and rigid-compulsive behaviors. American journal of human genetics *77*, 265-279.

Tabuchi, K., Blundell, J., Etherton, M.R., Hammer, R.E., Liu, X., Powell, C.M., and Sudhof, T.C. (2007). A neuroligin-3 mutation implicated in autism increases inhibitory synaptic transmission in mice. Science *318*, 71-76.

Tavassoli, T., Hoekstra, R.A., and Baron-Cohen, S. (2014). The Sensory Perception Quotient (SPQ): development and validation of a new sensory questionnaire for adults with and without autism. Molecular autism *5*, 29.

Tomchek, S.D., and Dunn, W. (2007). Sensory processing in children with and without autism: a comparative study using the short sensory profile. The American journal of occupational therapy : official publication of the American Occupational Therapy Association *61*, 190-200.

Tommerdahl, M., Tannan, V., Cascio, C.J., Baranek, G.T., and Whitsel, B.L. (2007). Vibrotactile adaptation fails to enhance spatial localization in adults with autism. Brain research *1154*, 116-123.

Tordjman, S., Gutknecht, L., Carlier, M., Spitz, E., Antoine, C., Slama, F., Carsalade, V., Cohen, D.J., Ferrari, P., Roubertoux, P.L.*, et al.* (2001). Role of the serotonin transporter gene in the behavioral expression of autism. Molecular psychiatry *6*, 434-439.

Toth, M. (2014). Mechanisms of Non-Genetic Inheritance and Psychiatric Disorders. Neuropsychopharmacology : official publication of the American College of Neuropsychopharmacology.

Tsang, K.M., Croen, L.A., Torres, A.R., Kharrazi, M., Delorenze, G.N., Windham, G.C., Yoshida, C.K., Zerbo, O., and Weiss, L.A. (2013). A genome-wide survey of transgenerational genetic effects in autism. PloS one *8*, e76978.

Van Der Loos, H. (1976). Barreloids in mouse somatosensory thalamus. Neuroscience letters *2*, 1-6.

van Kleef, E.S., Gaspar, P., and Bonnin, A. (2012). Insights into the complex influence of 5-HT signaling on thalamocortical axonal system development. The European journal of neuroscience *35*, 1563-1572.

Vaswani, M., Linda, F.K., and Ramesh, S. (2003). Role of selective serotonin reuptake inhibitors in psychiatric disorders: a comprehensive review. Progress in neuro-psychopharmacology & biological psychiatry *27*, 85-102.

Veenstra-Vanderweele, J., Jessen, T.N., Thompson, B.J., Carter, M., Prasad, H.C., Steiner, J.A., Sutcliffe, J.S., and Blakely, R.D. (2009). Modeling rare gene variation to gain insight into the oldest biomarker in autism: construction of the serotonin transporter Gly56Ala knock-in mouse. Journal of neurodevelopmental disorders *1*, 158-171.

Veenstra-VanderWeele, J., Muller, C.L., Iwamoto, H., Sauer, J.E., Owens, W.A., Shah, C.R., Cohen, J., Mannangatti, P., Jessen, T., Thompson, B.J.*, et al.* (2012). Autism gene variant causes hyperserotonemia, serotonin receptor hypersensitivity, social impairment and repetitive behavior. Proceedings of the National Academy of Sciences of the United States of America *109*, 5469-5474.

Veenstra-VanderWeele, J., and Warren, Z. (2014). Intervention in the Context of Development: Pathways Toward New Treatments. Neuropsychopharmacology : official publication of the American College of Neuropsychopharmacology.

Verkerk, A.J., Pieretti, M., Sutcliffe, J.S., Fu, Y.H., Kuhl, D.P., Pizzuti, A., Reiner, O., Richards, S., Victoria, M.F., Zhang, F.P.*, et al.* (1991). Identification of a gene (FMR-1) containing a CGG repeat coincident with a breakpoint cluster region exhibiting length variation in fragile X syndrome. Cell *65*, 905-914.

Volkmar, F.R., and Nelson, D.S. (1990). Seizure disorders in autism. Journal of the American Academy of Child and Adolescent Psychiatry *29*, 127-129.

Walker, C.K., Anderson, K.W., Milano, K.M., Ye, S., Tancredi, D.J., Pessah, I.N., Hertz-Picciotto, I., and Kliman, H.J. (2013). Trophoblast inclusions are significantly increased in the placentas of children in families at risk for autism. Biological psychiatry *74*, 204-211.

Walther, D.J., Peter, J.U., Bashammakh, S., Hortnagl, H., Voits, M., Fink, H., and Bader, M. (2003). Synthesis of serotonin by a second tryptophan hydroxylase isoform. Science *299*, 76.

Wang, F., Zhu, J., Zhu, H., Zhang, Q., Lin, Z., and Hu, H. (2011). Bidirectional control of social hierarchy by synaptic efficacy in medial prefrontal cortex. Science *334*, 693-697.

Wassink, T.H., Hazlett, H.C., Epping, E.A., Arndt, S., Dager, S.R., Schellenberg, G.D., Dawson, G., and Piven, J. (2007). Cerebral cortical gray matter overgrowth and functional variation of the serotonin transporter gene in autism. Archives of general psychiatry *64*, 709-717.

Watson, L.R., Patten, E., Baranek, G.T., Poe, M., Boyd, B.A., Freuler, A., and Lorenzi, J. (2011). Differential associations between sensory response patterns and language, social, and communication measures in children with autism or other developmental disabilities. Journal of speech, language, and hearing research : JSLHR *54*, 1562-1576.

Weiler, I.J., and Greenough, W.T. (1999). Synaptic synthesis of the Fragile X protein: possible involvement in synapse maturation and elimination. American journal of medical genetics *83*, 248-252.

Weiss, L.A., Abney, M., Cook, E.H., Jr., and Ober, C. (2005). Sex-specific genetic architecture of whole blood serotonin levels. American journal of human genetics *76*, 33-41.

Weiss, L.A., Ober, C., and Cook, E.H., Jr. (2006). ITGB3 shows genetic and expression interaction with SLC6A4. Human genetics *120*, 93-100.

Weiss, L.A., Veenstra-Vanderweele, J., Newman, D.L., Kim, S.J., Dytch, H., McPeek, M.S., Cheng, S., Ober, C., Cook, E.H., Jr., and Abney, M. (2004). Genome-wide association study identifies ITGB3 as a QTL for whole blood serotonin. European journal of human genetics : EJHG *12*, 949-954.

Welch, J.M., Lu, J., Rodriguiz, R.M., Trotta, N.C., Peca, J., Ding, J.D., Feliciano, C., Chen, M., Adams, J.P., Luo, J.*, et al.* (2007). Cortico-striatal synaptic defects and OCD-like behaviours in Sapap3-mutant mice. Nature *448*, 894-900.

Welker, C. (1971). Microelectrode delineation of fine grain somatotopic organization of (SmI) cerebral neocortex in albino rat. Brain research *26*, 259-275.

Werling, D.M., Lowe, J.K., Luo, R., Cantor, R.M., and Geschwind, D.H. (2014). Replication of linkage at chromosome 20p13 and identification of suggestive sex-differential risk loci for autism spectrum disorder. Molecular autism *5*, 13.

Weschsler, D. (1999). WASI: Wechsler Abbreviated Scale of Intelligence (San Antonio, TX: Harcourt Assessment, Inc.).

Whyte, A., Jessen, T., Varney, S., and Carneiro, A.M. (2014). Serotonin transporter and integrin beta 3 genes interact to modulate serotonin uptake in mouse brain. Neurochemistry international *73*, 122-126.

Wiggins, J.L., Peltier, S.J., Bedoyan, J.K., Carrasco, M., Welsh, R.C., Martin, D.M., Lord, C., and Monk, C.S. (2012). The impact of serotonin transporter genotype on default network connectivity in children and adolescents with autism spectrum disorders. NeuroImage Clinical *2*, 17-24.

Wiggins, J.L., Swartz, J.R., Martin, D.M., Lord, C., and Monk, C.S. (2014). Serotonin transporter genotype impacts amygdala habituation in youth with autism spectrum disorders. Social cognitive and affective neuroscience *9*, 832-838.

Wiggins, L.D., Robins, D.L., Bakeman, R., and Adamson, L.B. (2009). Brief report: sensory abnormalities as distinguishing symptoms of autism spectrum disorders in young children. J Autism Dev Disord *39*, 1087-1091.

Willins, D.L., and Meltzer, H.Y. (1997). Direct injection of 5-HT2A receptor agonists into the medial prefrontal cortex produces a head-twitch response in rats. The Journal of pharmacology and experimental therapeutics *282*, 699-706.

Winslow, J.T., Hearn, E.F., Ferguson, J., Young, L.J., Matzuk, M.M., and Insel, T.R. (2000). Infant vocalization, adult aggression, and fear behavior of an oxytocin null mutant mouse. Hormones and behavior *37*, 145-155.

Wischmeyer, E., and Karschin, A. (1996). Receptor stimulation causes slow inhibition of IRK1 inwardly rectifying K+ channels by direct protein kinase A-mediated phosphorylation. Proceedings of the National Academy of Sciences of the United States of America *93*, 5819-5823.

Woolsey, T.A., and Van der Loos, H. (1970). The structural organization of layer IV in the somatosensory region (SI) of mouse cerebral cortex. The description of a cortical field composed of discrete cytoarchitectonic units. Brain research *17*, 205-242.

Xu, G., Jing, J., Bowers, K., Liu, B., and Bao, W. (2014). Maternal diabetes and the risk of autism spectrum disorders in the offspring: a systematic review and meta-analysis. Journal of autism and developmental disorders *44*, 766-775.

Yamashita, A., Singh, S.K., Kawate, T., Jin, Y., and Gouaux, E. (2005). Crystal structure of a bacterial homologue of Na+/Cl--dependent neurotransmitter transporters. Nature *437*, 215-223.

Yan, Q.J., Asafo-Adjei, P.K., Arnold, H.M., Brown, R.E., and Bauchwitz, R.P. (2004). A phenotypic and molecular characterization of the fmr1-tm1Cgr fragile X mouse. Genes, brain, and behavior *3*, 337-359.

Yang, M., Clarke, A.M., and Crawley, J.N. (2009). Postnatal lesion evidence against a primary role for the corpus callosum in mouse sociability. The European journal of neuroscience *29*, 1663-1677.

Yavarone, M.S., Shuey, D.L., Sadler, T.W., and Lauder, J.M. (1993). Serotonin uptake in the ectoplacental cone and placenta of the mouse. Placenta *14*, 149-161.

Ye, R., Carneiro, A.M., Airey, D., Sanders-Bush, E., Williams, R.W., Lu, L., Wang, J., Zhang, B., and Blakely, R.D. (2014). Evaluation of heritable determinants of blood and brain serotonin homeostasis using recombinant inbred mice. Genes, brain, and behavior *13*, 247-260.

Yonan, A.L., Alarcon, M., Cheng, R., Magnusson, P.K., Spence, S.J., Palmer, A.A., Grunn, A., Juo, S.H., Terwilliger, J.D., Liu, J.*, et al.* (2003). A genomewide screen of 345 families for autism-susceptibility loci. American journal of human genetics *73*, 886-897.

Young, D.M., Schenk, A.K., Yang, S.B., Jan, Y.N., and Jan, L.Y. (2010). Altered ultrasonic vocalizations in a tuberous sclerosis mouse model of autism. Proceedings of the National Academy of Sciences of the United States of America *107*, 11074-11079.

Yuan, H., and Dougherty, J.D. (2014). Investigation of maternal genotype effects in autism by genome-wide association. Autism research : official journal of the International Society for Autism Research *7*, 245-253.

Zhang, B., Kirov, S., and Snoddy, J. (2005). WebGestalt: an integrated system for exploring gene sets in various biological contexts. Nucleic acids research *33*, W741-748.

Zhu, C.B., Hewlett, W.A., Feoktistov, I., Biaggioni, I., and Blakely, R.D. (2004). Adenosine receptor, protein kinase G, and p38 mitogen-activated protein kinase-dependent up-regulation of serotonin transporters involves both transporter trafficking and activation. Molecular pharmacology *65*, 1462-1474.